

LOCATING AN UNDERWATER SITE OF A  
NUCLEAR EXPLOSION DETECTED BY  
A HYDROACOUSTIC NETWORK

THOMAS J. HUGHES

LIBRARY  
U.S. NAVAL POSTGRADUATE SCHOOL  
MONTEREY, CALIFORNIA









LOCATING AN UNDERWATER SITE  
OF A NUCLEAR EXPLOSION DETECTED  
BY A HYDROACOUSTIC NETWORK

\* \* \* \* \*

Thomas J. Hughes





LOCATING AN UNDERWATER SITE  
OF A NUCLEAR EXPLOSION DETECTED  
BY A HYDROACOUSTIC NETWORK

by

Thomas J. Hughes

Lieutenant Commander, United States Navy

Submitted in partial fulfillment of  
the requirements for the degree of

MASTER OF SCIENCE

United States Naval Postgraduate School  
Monterey, California

1 9 6 2

H86

LOCATING AN UNDERWATER SITE  
OF A NUCLEAR EXPLOSION DETECTED  
BY A HYDROACOUSTIC NETWORK

by

Thomas J. Hughes

This work is accepted as fulfilling  
the thesis requirements for the degree of  
MASTER OF SCIENCE



## ABSTRACT

There is a need for this country to be able to assure itself that an international ban on nuclear testing can be made effective. This thesis studies one small portion of that problem - to wit, the procedure for classifying an underwater detonation which has vented and which has been detected by a hydroacoustic network.

A MEASURE OF EFFECTIVENESS is developed, and after a study of some parameters such as height of search, search spacing, search width and current movements optimizing search plans are deduced.

One of the major difficulties in such a quantitative analysis is the non-deterministic nature of many of the parameters. The ideal search spacing was found to depend directly on the surface radioactive pool diameter. In order to develop plans this essential factor must be known. Unfortunately this depends on many variables over which the searcher has no control or knowledge. An averaging procedure is adopted and a factor established to compare spacings and determine which meets the criterion dictated by the MEASURE OF EFFECTIVENESS.

The writer wishes to express his appreciation for the assistance given him by Professor H. E. Handler, Professor R. Read and Professor E. M. Ward; for the assistance and encouragement given him by Professor W. P. Cunningham; and particularly to Professor E. J. Stewart for the kind and charitable way in which he made his time and advice available. Lastly, the writer wishes to thank Mrs. Martha Olson of U. S. Naval Radiological Defense Laboratory for making available hydrographic information compiled by her.



## TABLE OF CONTENTS

Section	Title	Page
1.	Introduction	1
2.	Statement of the problem	3
3.	Means of identification	3
4.	Detection capability	5
5.	Alternative courses of action	10
6.	Measure of effectiveness	12
7.	List of variables considered	13
8.	Hydroacoustic fix distribution	14
9.	Navigation error	14
10.	Search patterns	15
11.	Search width	16
12.	Aircraft capabilities	28
13.	Search procedure	28
14.	Conclusions	29
15.	Bibliography	32
Appendix		
I.	Height of surveying aircraft	33
II.	Search theory	42
III.	Search width	56
IV.	Effect of ocean currents	68
V.	Search plan for small fix deviation	88
VI.	Search plan for large fix deviation	94





## LIST OF ILLUSTRATIONS

Figure	Page
1. Effect of temperature changes with depth on sound ray path	7
2. Sound channels	7,8
3. Probability of detection for various pool sizes for a given spacing	20
4. Probability of detection for various spacings for a given radioactive pool diameter of minimum uniform surface intensity	21
5. Comparison of search patterns	24
6. Dimensions of search area on second pass (small location error)	27
7. Parameters of integration	34
8. Variation of intensity with height	41
9. Target's relative track	42
10. Detection at fixed speed and course	44
11. Parallel sweeps	45
12. Probabilities with parallel sweeps	50
13. Square of uniform coverage	51
14. Meter geometry (side view)	57
15. Surface geometry	57
16. System time constant effect	58
17. Geometry of detector view of high intensities	60
18. Graphic solutions for equations (7) and (8)	63
19. Identification of symbols for previous tables	67
20.-27. Direction of current for various areas	72-9
28. Current persistency	80
29. Frequency distribution of current speed	83
30. Pattern for retiring search	89



# LIST OF ILLUSTRATIONS (Cont'd)

Figure	Page
31. Search plan for small fix deviation	93
32. Search plan for large fix deviation	96

## Table

1. Analysis of probability of detection for given search spacings	17-9
2. Comparison of spacings using the MEASURE OF EFFECTIVENESS (LARGE LOCATION ERROR)	22
3. Comparison of spacings using the MEASURE OF EFFECTIVENESS (SMALL LOCATION ERROR)	25
4. Uniform square coverage probabilities	59
5. Data for graphical solution to transcendental equations	61-2
6. Search widths for various intensities	66
7. A measure of current persistency in five selected areas	81-2
8. Means and standard deviations of current speed in selected quadrangles	84-7



## 1. Introduction.

In October 1960 a technical symposium was held by the Advanced Research Projects Agency (ARPA) acting in behalf of the Department of Defense for the purpose of informing those in attendance of the scope, status and planning underway for Project VELA. Project VELA consists of research and development that is aimed at the improvement of our capability of detecting and identifying nuclear detonations that are contained below the surface of the earth, or underwater or that occur in space above the atmosphere.

It is well recognized that it is possible for a clever and determined nation to conduct subsurface and high altitude nuclear weapons tests without a significant risk of being detected. Detection of nuclear detonations on the surface or within the atmosphere is considered well in hand and not included in VELA. Ever since the Conference of Experts held in 1958 in Geneva, international groups have been attempting to establish methods and networks which would assure the participating nations that agreements to ban nuclear testing could be effectively enforced and thereby be the first step in solving one of the most important problems of our time - ARMS CONTROL.

The hope of Project VELA is to improve our detection and classification capability by at least one order of magnitude, and perhaps by as much as three, over a three year span. Such a quantum jump is considered feasible if sufficient independent scientific interest can be aroused while assigning a high priority to the investigation in as many of the government laboratories which have some measure to contribute.

The Project was subdivided into three major categories:



VELA HOTEL - Detection of very high altitude nuclear detonations by means of detectors mounted in satellites;

VELA SIERRA - Development of techniques and equipment to detect and identify high altitude nuclear detonations by ground based instrumentation;

VELA UNIFORM - Improve, markedly, equipment and techniques for detecting and identifying subsurface nuclear explosions from a distance as well as to develop rapid, economical techniques for conducting on-site inspections to determine whether a suspicious event was actually a nuclear explosion or not.

Project VELA UNIFORM includes a study of underwater detonations as part of its "subsurface" objective. The Naval Electronics Laboratory (NEL) at San Diego was assigned the task of investigating the detection of underwater explosions and the Naval Radiological Defense Laboratory (NRDL) was contracted to devise a searching procedure for obtaining samples to classify explosions detected by a network devised by NEL.

In a CONFIDENTIAL report /6/ NEL outlined a distribution of hydroacoustic stations which would be capable of detecting underwater blasts in most areas of the world. However, this network has practically no ability to classify explosions as nuclear or non-nuclear.

NRDL has pursued the problem of classifying a reported detonation by locating the scene by means of an appropriate search based on the fix information received from hydroacoustic and/or other correlated equipment, obtaining samples if possible and analyzing pertinent characteristics of the area.

The classification problem splits into two distinct categories re-





flecting two completely different physical characteristics of the scene. In the first case, the underwater nuclear explosion vents to the surface and scatters the attendant radioactive debris on the surface and probably into the air. In the second case the radiation is contained below the surface due to a combination of depth of explosion and yield of the device. This thesis is devoted to analyzing the first of these two categories.

## 2. Statement of the problem.

The objective of this study is to determine the optimum searching procedure for locating the site of an underwater explosion which has vented, in order to classify it as nuclear or non-nuclear.

## 3. Means of identification.

The most positive means of confirming that an explosion is nuclear is by a radiochemical analysis of a sample of the affected area.

After an explosion has been detected and a radiating sample obtained, it remains to distinguish the origin of the radiation. In spite of a radioactive sample a nuclear detonation could be disclaimed and the activity attributed to one of the following:

- a. Residue from previous explosions,
- b. Waste dumping,
- c. Reactor discharge,
- d. Accident.

Radiochemistry can detect fission fragments and normally determine the time of detonation by extrapolating back from ratios of certain isotopes present in the sample. This information correlated with seismic, hydroacoustic, air acoustic, and/or electromagnetic information of time



and location of detonation can readily refute a claim of residue from previous explosions or waste dumping as the source.

Normal reactor discharge does not contain fission fragments and would easily be repudiated as a cause for contamination. However, leakage from a reactor primary system could be a source of deceiving activity in the sample, but would not explain the detected explosion at the location.

An explosion of a reactor in water would have attendant debris, but with the burden of proof to counter such a claim upon the investigator, failure to find debris is unlikely to be satisfactorily conclusive that such an explosion did not take place.

Any surface sample is subject to prior masking by the dumping of fission fragments to confuse analysis. A determined effort to make radiochemical analysis of surface samples inconclusive is almost bound to be successful in a water contaminated area if the deceiver is willing to invest enough effort. Contaminated air samples from venting of underwater bubbles are less vulnerable.

Underwater pulsing of the bubble on its route to the surface leaves a trail of discrete thin laminas of radioactive material. To reduce the possibility of confusion of the surface sample by a masking attempt a further effort should be made to sample some of these lower strata.

Sampling procedures should recognize biological phenomena which can corroborate other evidence. Certain algae have a known affinity for Iodine 131 which has a short half life and can be identified as a fission fragment. Plankton can also produce evidence of an event. If there are land and shallow water in the vicinity, molluscs and tropical plant sam-



ples could produce valuable information.

Of course, specifically, well equipped search vehicles could arrive at reliable conclusions at the scene with pulse height analysis equipment, air drop water probes and well schooled personnel. However, it is not realistic to imagine planes particularly outfitted for this searching chore. Our forces must be more flexible for the large variety of missions they may be called on to perform. It is envisioned that patrol craft could be rigged with the detector described in USNRDL-TR-525/1/ or that bases from which these planes operate could have these meters available. However the more sophisticated equipment is not likely to be as well distributed.

Actual meter readings would be of some assistance in correlating with the time of the explosion by determining decay rates; however, continued dilution due to wind and sea movements will make analysis of this data much less reliable than water samples.

#### 4. Detection capability.

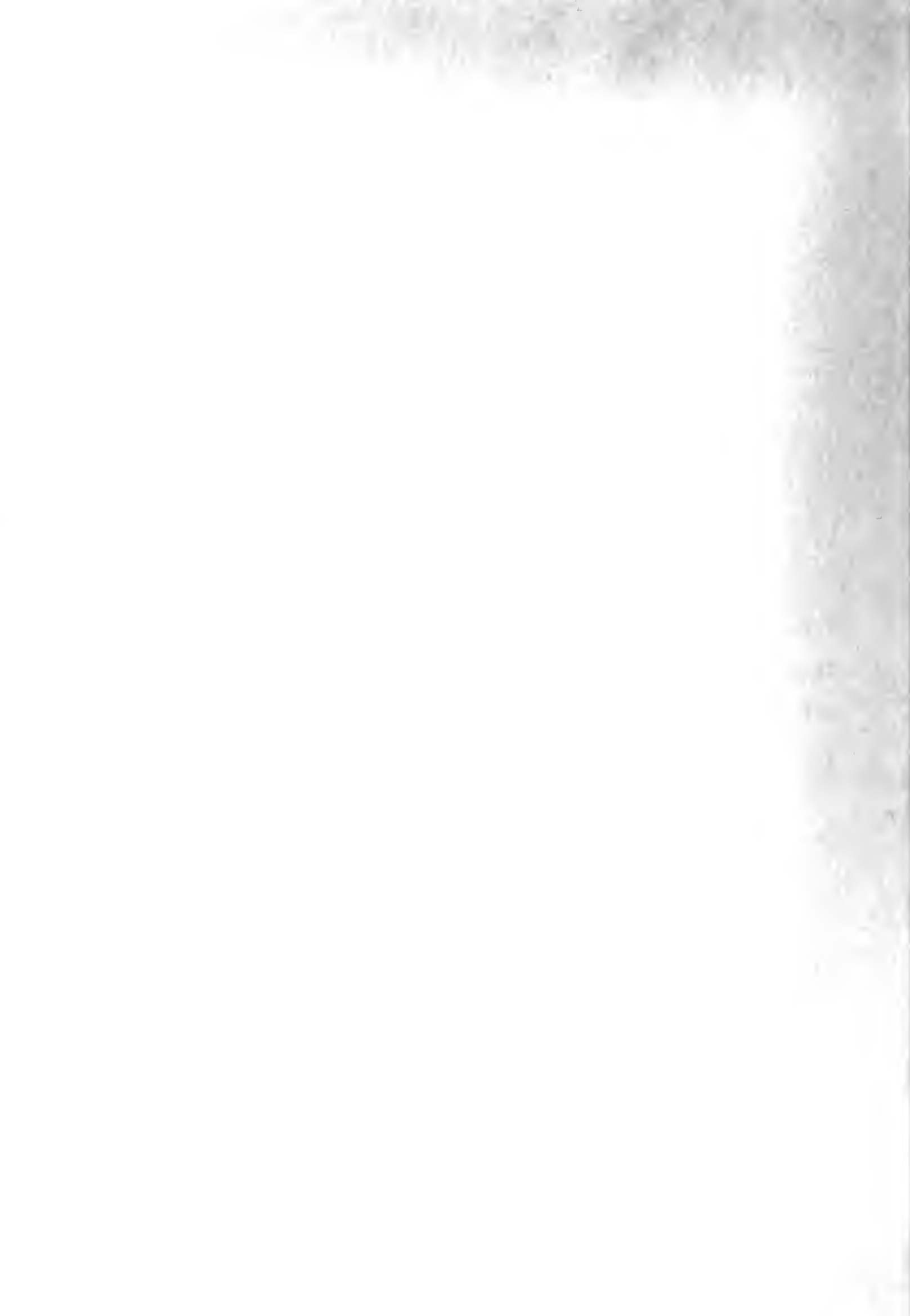
It is worthwhile to consider some of the major factors involved in the transmission of sound waves in water.

The sound reaching a receiver experiences three kinds of degradation:

a. Divergence - For a point source in a homogeneous medium the energy is dispersed in a sphere as it is radiated out so that a receiver perceives only an amount of energy proportional to the percent of area of the expanding sphere that it can observe.

b. Attenuation - There is a damping of the energy because the pressure is not in phase with the condensation due to viscosity, heat conduction and molecular absorption (due to magnesium sulphate).

c. Anomalies - There are many anomalies which contribute to the



peculiarities of underwater sound transmission but the principal ones are reflection and refraction.

$$\text{The velocity of sound in a fluid (C)} = \sqrt{\frac{B}{P}}$$

where B = Bulk Modulus

P = Density

As Temperature goes up P decreases;

As Salinity goes up B increases;

As Pressure increases P increases but B increases more.

Therefore the velocity increases as temperature, salinity and pressure increase.

Pressure increases with depth but temperature normally decreases, and temperature reductions have an overriding effect on the velocity. In the Atlantic a temperature of 2°C is reached at about 4000 feet and remains fairly constant from then on. Salinity remains relatively constant and velocity of sound increases with depth due to the pressure increase. In the Pacific the same conditions obtain at about 2000 feet. Near the equator this condition of constancy is reached at a lesser depth.

Near the surface radical temperature changes are not at all infrequent. Surface disturbances of storms mix the water for a considerable depth and sometimes send warm water down while the colder water is brought to the surface. This produces temperature inversions which have a drastic effect on sound transmission. This will be discussed in more detail below.

As the velocity increases the ray (perpendicular to the wave front) curves downward. Conversely, if the velocity decreases the ray curves upward.





Consider the following ray diagrams where the left depicts the temperature changes with depth and the right shows the ray path ( $\theta_0$  is original direction of propagation).

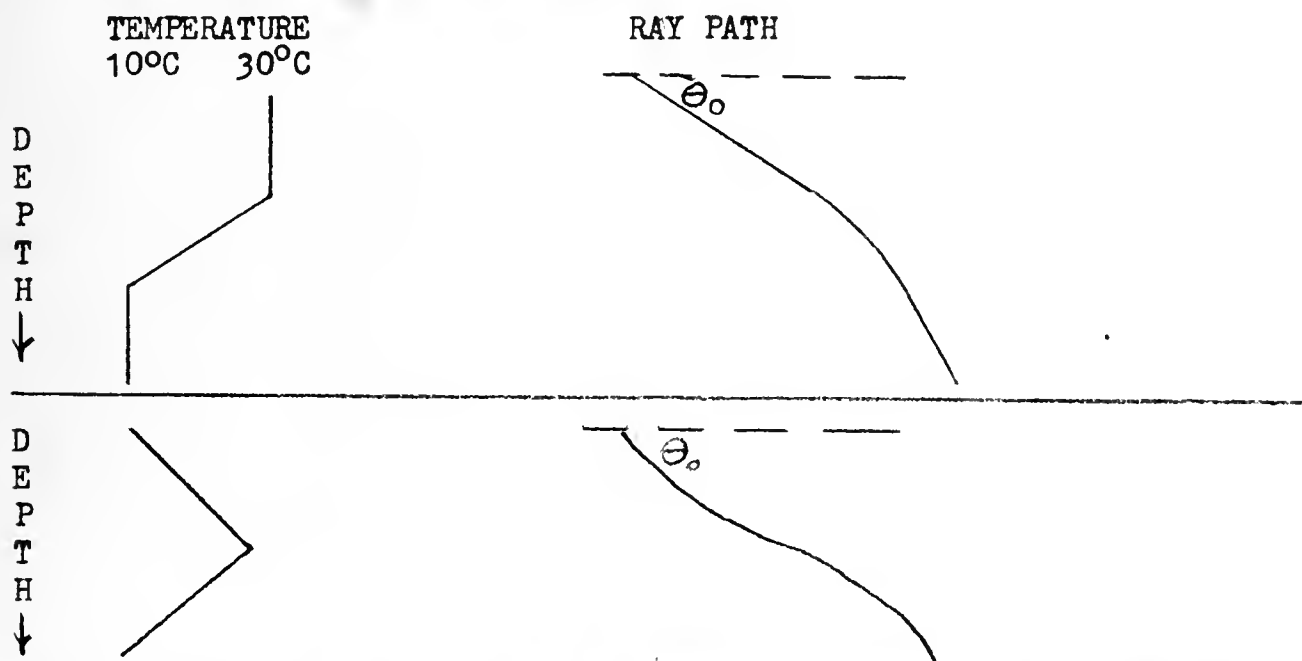
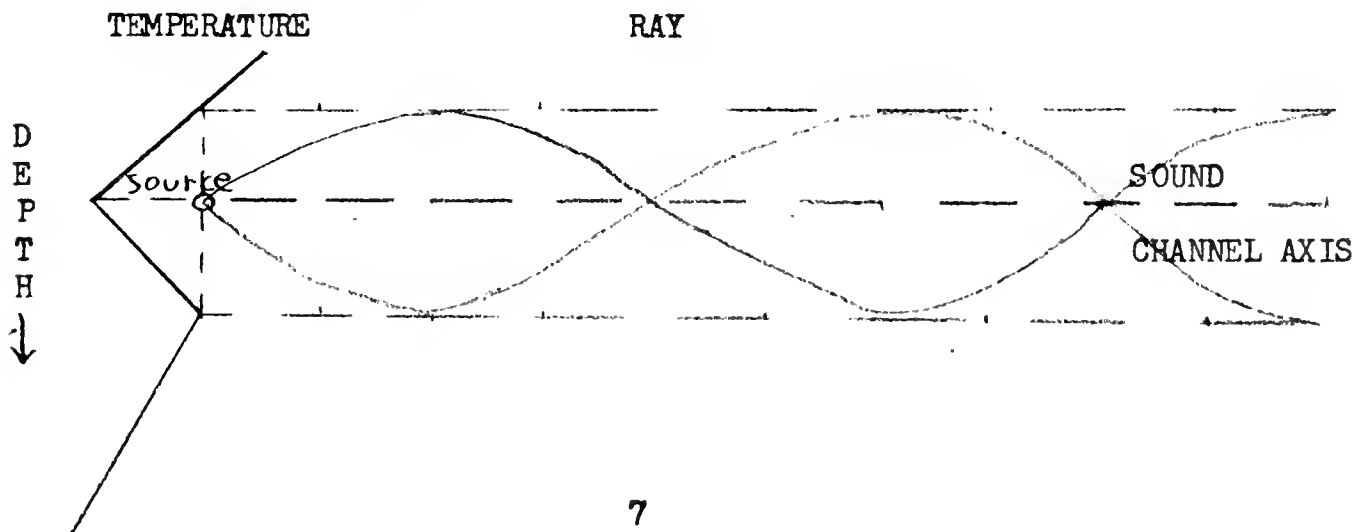


Fig. 1. Effect of temperature changes with depth on sound ray path.

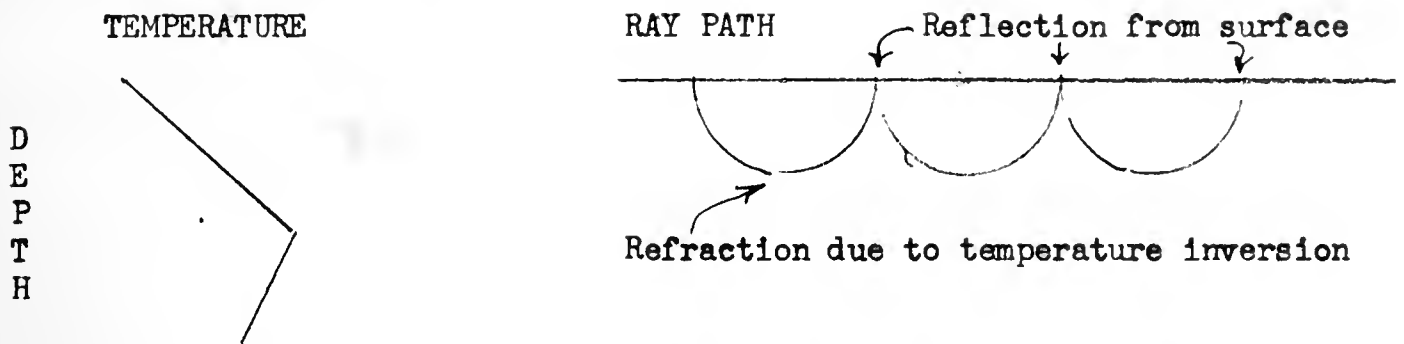
Sound channels occur when there is a minimum velocity at some depth with higher velocities above and below. The region of minimum velocity is called the axis. Sound originated on the axis and propagated along the axis will not diverge spherically but only cylindrically which means that the losses are cut down. Additionally, there is no major anomaly to degrade the wave.

#### a. Normal Sound Channel





b. Pseudo Sound Channel



c. At depth of 4000 feet in Atlantic and 2000 feet in Pacific:

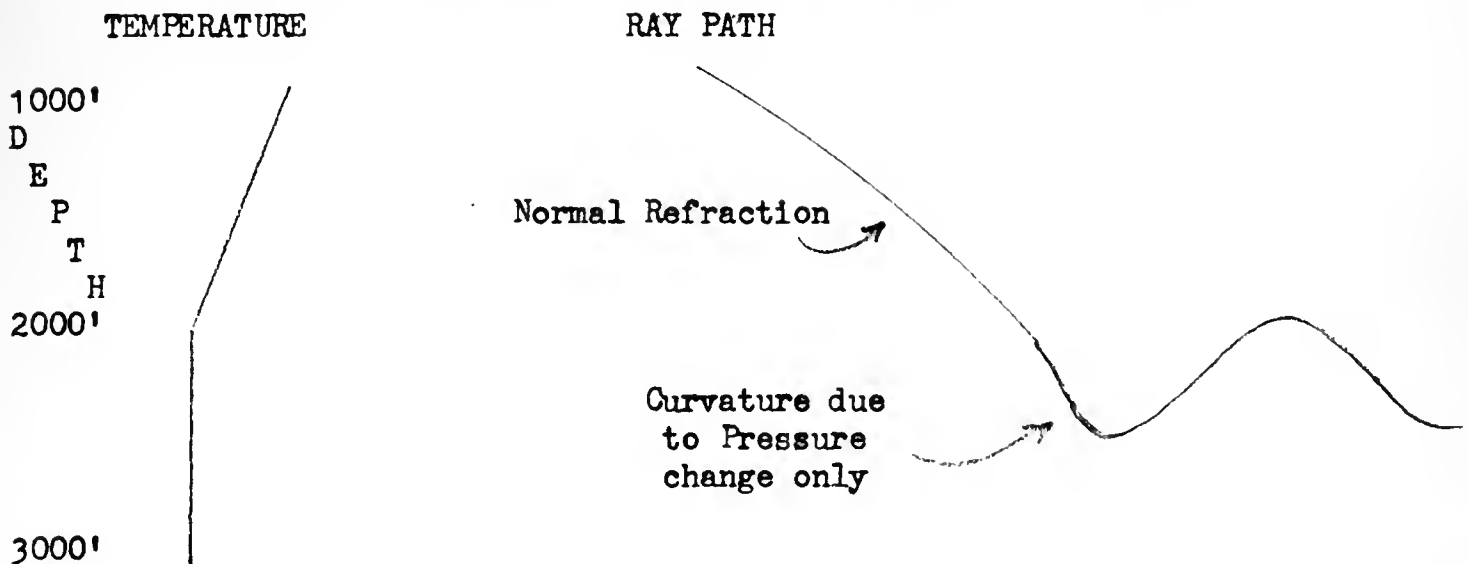


Fig. 2. Sound channels.

Sound sources do not have to be in the sound channel in order for sound to be propagated along the channel. Rays entering sound channels at small enough angles (usually less than  $15^\circ$ ) with the horizontal may be entrapped and then act as if they originated on the axis.

These few facts may help the reader to appreciate the following comment paraphrased from the preliminary NEL report /7/:

Historically it is apparent that even small explosions under ideal conditions can be detected at ranges of many thousands of miles<sup>1</sup>, whereas, the most powerful explosions under other conditions may

<sup>1</sup> MILES will be NAUTICAL MILES (6087 feet) throughout this thesis.



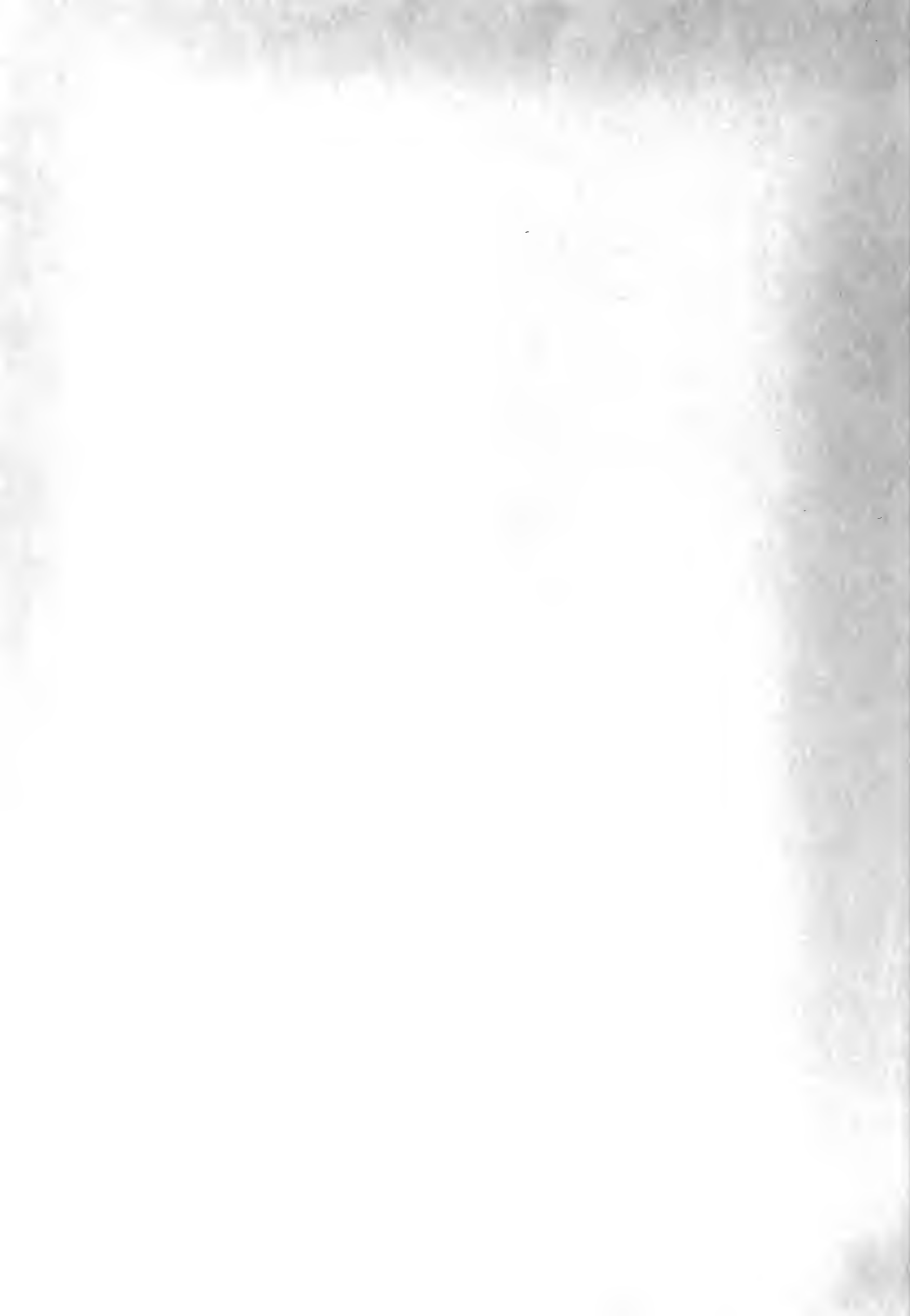
go undetected. For example; one pound of TNT exploded on the sound axis in the open ocean would be expected to produce a stronger signal than a 100 Megaton explosion under other extreme conditions. Obviously, then, the hydroacoustic detection of a nuclear burst is a complex problem and a generalized statement of the capability of such a system is not possible.

The interfaces between the air and the water or the land and the water provide a poor match for transmission of sound waves (high coefficient of reflection). As a result surface bursts or underground bursts are not well detected through hydroacoustic means just as underwater bursts are not well detected by seismic devices. For this same reason stations are not able to monitor inland seas and locations in lagoons or with seamounts between the event and the receiver.

The velocity of sound in water is about 4800 feet a second and it is possible that some stations will receive a signal as long as one hour after detonation (less than 3000 miles). It will take at least two more hours to correlate station information, evaluate, and call an alert.

There are many sources of confusion in detecting. Hydroacoustic stations will be unable to distinguish between chemical explosions and atomic explosions. Earthquakes and underwater volcanic disruptions when detected will be a concern and frequently non-discernible from man made explosions. The splash of missiles in deep water, ship propulsion noises and environmental sounds characteristic of the ocean can be distinguished.

In the Joint Committee Hearings /8/ Dr. H. Brown of Lawrence Radiation Laboratory estimated that there were 5000 continental earthquakes per year that could be suspected of being nuclear explosions of between one and five kilotons and that only a few percent could be identified as earthquakes by present criteria. About 100 disturbances would be suspected of being nuclear explosions of five kilotons or more. Since most



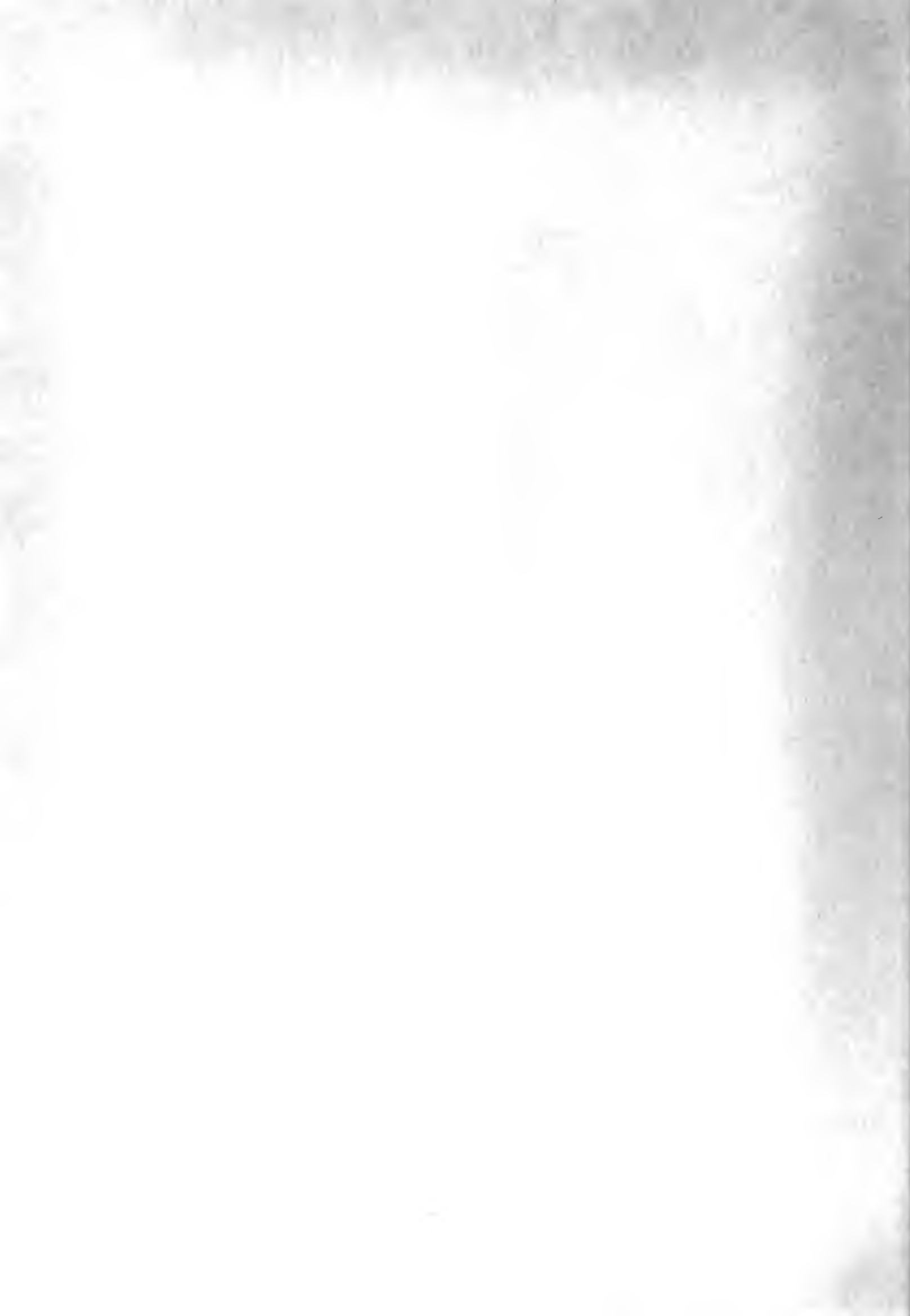
of the continental seismic false alarms are caused by these earthquakes it seems unlikely that the number of hydroacoustic false alarms due to natural causes would be this order of magnitude. Earthquake disturbances are not likely to be transmitted with too much energy through the interface with the water. Volcanic disruptions below the water may be misleading, but these are not near as numerous as continental earthquakes. The principal cause of false alarm in the hydroacoustic network is most likely to be chemical explosions transmitted by the Sound Channel mechanism.

#### 5. Alternative courses of action.

With our objective clear in mind - to determine whether a reported explosion was nuclear or non-nuclear - our problem is reduced to searching the area in question to determine if there is evidence of nuclear activity. Only by not obtaining evidence of nuclear activity can we assume that the disturbance was non-nuclear (ignoring the possibility of non-venting nuclear explosions for this study), and even then the conclusion is not absolute. The certainty with which a conclusion can be reached depends on the thoroughness of the search.

The courses of action that are open revolve about the approach to the development of a search plan.

a. Should the plan be based upon a random search approach, considering the target to be equally likely in some large area prescribed by hydroacoustic fix information? This would permit parallel sweeps through the area in an orderly fashion by several aircraft with no danger of interfering with each other. It would assure a thorough coverage of the area because navigation is simple and reliable.





b. Should the plan attempt to optimize search effort with respect to time? This would permit target distribution to be any shape that the physical situation dictates. The pattern would be formed to search the areas of greatest probability continuously with the distribution of the fix being the "a priori" function and an "a posteriori" function formed after each search. This approach would be best for the following considerations:

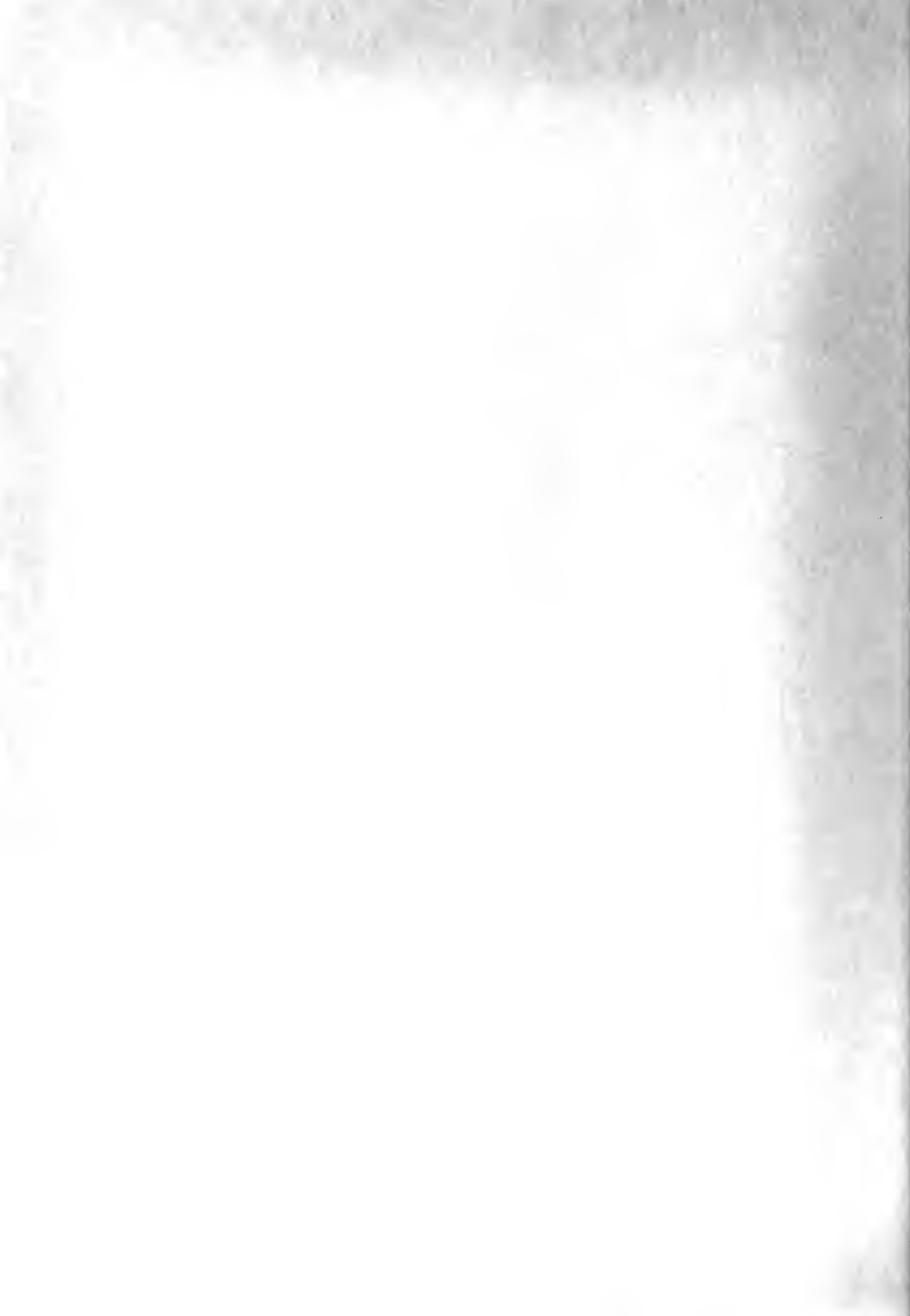
(1) Search craft may have to be recalled prior to completion of the plan or there may be a cost or utility consideration.

(2) International ground rules may limit time to search a given area or it may be desired to spend as little time as possible in a given area due to political or other considerations.

(3) There is the ever present marginal case where just enough radioactivity is present at one time in sufficient intensity (because of yield, depth of detonation, and/or dispersion) to be detected, but which will not be there at some later time.

A disadvantage to this approach to the search plan is that, unless target location distribution is in fact uniform, the navigation problems reduce the reliability of conforming to a given pattern, and holidays are left in the coverage. The probability of detection may in fact be less than a random pattern, although the same coverage effort is invested, because of those holidays. Secondly, there is a peculiarity in the radioactive pool contour under many conditions which reduces the probability of detection at certain times. The character of many pools is as follows:

Upon initial venting a high intensity area is established for a



certain distance around "ground zero." After some time passes many of the fission fragments sink, and fringe area activity is diluted beyond recognition. This decreases the contour of a given low isodose line. Then the particles that are suspended near the center spread out with water and wind movements and the low isodose contours spread out again, even beyond the original area.

It is impossible to fill in details of "how much?" or "how long?" or "what intensity?" because all answers depend on the physical conditions of venting and water movement. The point of mentioning it here is to acknowledge that it could affect the capability of our searching effort.

#### 6. Measure of effectiveness.

This situation is different from many military operations where the accomplishment of the objective is imperative, regardless of the cost. The search would be conducted during peacetime and there may be concern for the expense involved, particularly if many false alarms are encountered.

There is always a possibility of search vehicles having to be recalled because of more urgent commitments, logistic considerations or forbidding weather. As previously mentioned, international agreements may limit searching time.

Finally, there is a matter of using consistent logic in approaching the problem. As presented so far, and as the physical situation dictates, the problem admits the probabilistic nature of the fix information. Again ignoring the non-venting situation, there can never be an absolute assurance that the explosion was non-nuclear, but the probability of this fact approaches unity as the search effort approaches an extremely large value.



Therefore, the search will terminate, if a pool is not located, at some time before the evidence is absolutely conclusive that no pool exists. This will always be the case and the amount of search effort, or synonymously - time, is inherent in the problem and cannot be ignored.

Under these considerations the MEASURE OF EFFECTIVENESS is to maximize the probability of detection per time of search effort.

#### 7. List of variables to be considered.

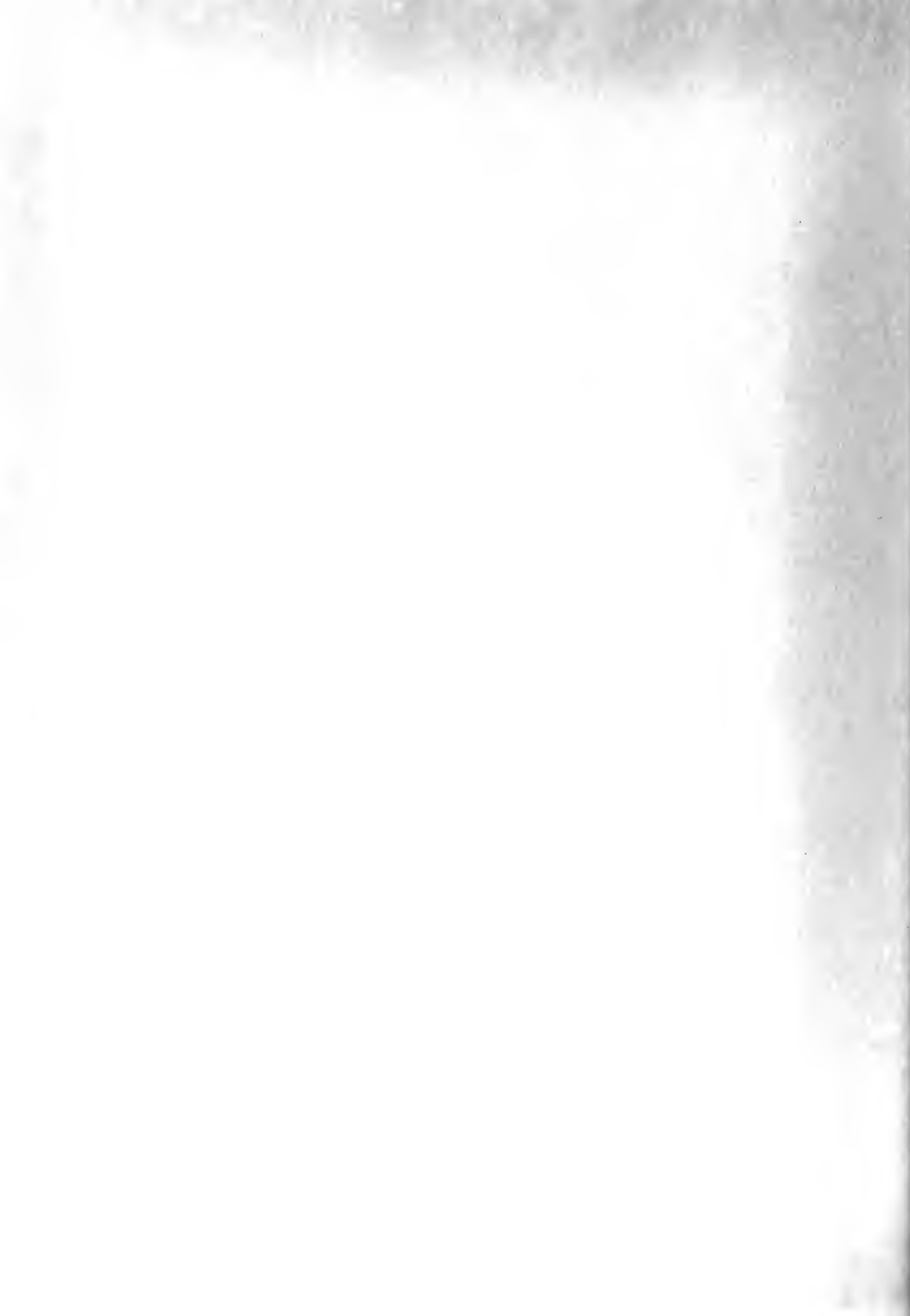
a. Height of search. This is discussed in detail in Appendix I. The conclusion is to fly as low as operationally feasible. A plot of intensity versus height in Appendix I shows the loss of intensity for altitudes from 0 to 40,000 feet.

b. Detector sensitivity. Appendix III is based on a detector which is capable of distinguishing 0.2 microroentgens at the meter. In order to meet this requirement the meter envisioned will be collimated to reduce the effect of cosmic radiation.

c. Search spacing. In Appendix II the search theory involved is discussed, and it is generally concluded that the spacing depends upon the search width (which is the effective visibility in the definite range law) and the standard deviation of the location errors.

d. Search width. The radioactive pool on the surface of the water coupled with the width of the detector view determine the search width. This is covered in detail in Appendix III.

e. Target motion. The movement of the radioactive pool, which is the object of the search, will depend principally on currents. Appendix IV investigates the variability of the water movement and concludes that the speed of movement is predictable but the direction is random.



f. Fix distribution.

g. Probability of detection. In Appendix III the probability of detection is computed for the ideal spacing - given the search width. Since the search width is not known in a realistic situation an averaging procedure must be resorted to. This is developed in paragraph 11 below.

h. Search aircraft characteristics.

i. Navigation errors in locating the center of the fix.

j. Time late at the scene.

#### 8. Hydroacoustic fix distribution.

The location of an explosion will be estimated by correlation between hydroacoustic detection stations. Their estimates will depend on physical conditions prevailing, but for this study the errors have been classed as having a standard deviation of 2.5 miles or 25 miles. The purpose of assuming deviations an order of magnitude apart is to see if the search plan is sensitive to such extremes. The distribution is assumed normal and the probability is represented by:

$$f(x,y) = f(r) = \frac{1}{2\pi\sigma^2} \exp\left(-\frac{r^2}{2\sigma^2}\right)$$

On the basis of this assumption Appendix II develops the ideal search spacing as  $0.75 (E\sigma)^{\frac{1}{2}}$  where E is the Effective Visibility and  $\sigma$  is the standard deviation.

#### 9. Navigation error.

Where there are no visual navigational aids available an aircraft can expect to arrive at a given location in accordance with some probability distribution. According to Bowditch /4/ celestial errors in air navigation of five to ten miles are considered normal for favorable con-





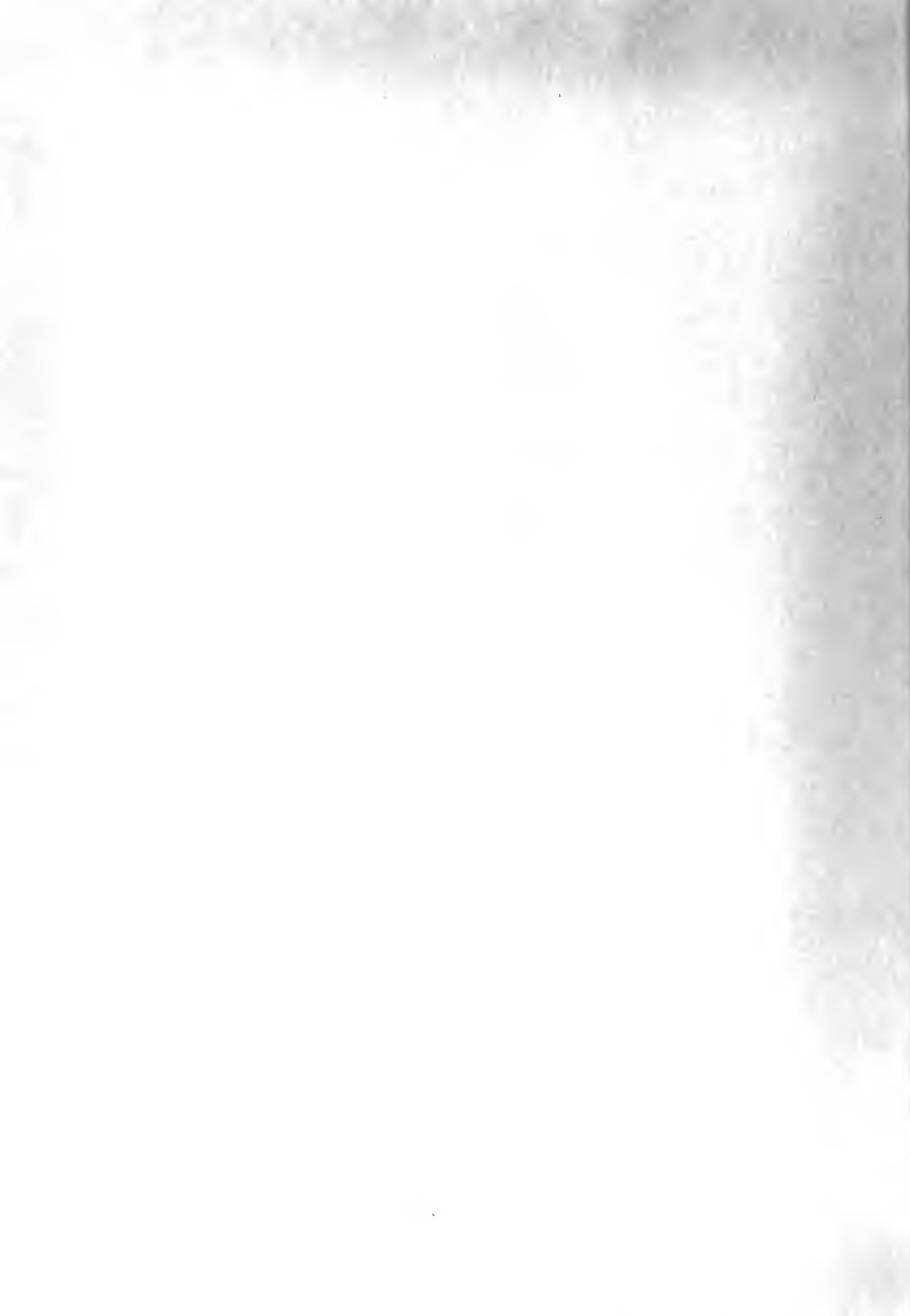
ditions (pg 676 paragraph 2806). Electronic navigational aids, where available, yield more accurate positioning. In this model it is assumed that the error due to navigation is normally distributed with a standard deviation of five miles. The variance is additive to the hydroacoustic fix variance since they are both normal and independent. When the fix standard deviation is 2.5 miles the total location standard deviation is 5.6 miles. When the fix deviation is 25 miles the location deviation is 25.5 miles.

These figures demonstrate that the navigation error has a substantial effect on the problem when the fix error is small, but it is rather inconsequential when the fix error is large.

#### 10. Search patterns.

Appendix IV discusses currents in detail and for this study the set is considered equally likely in any direction at a given location and time. The drift, on the other hand, can be predicted reasonably well. Koopman /2/ in sections 1.6 and 7.3 discusses a non-uniform distribution of targets. When the fix deviation is 2.5 miles the situation falls closely into the category of a circular distribution of the target with movement at a known speed in a random direction. The theory is to search on the peak of the distribution, then outside, then inside, ... etc. This pattern will give the maximum probability of detection per unit time for locating a moving target whose initial fix is not definite. See Appendix V for details of this plan.

When the location deviation is of the order of 25 miles or more and the time late is less than two days the target can be treated as stationary and the search pattern that applies is described by Koopman /2/ in paragraph 7.3.2. A set of expanding squares - squares of uniform cover-



age - are superimposed in the search pattern. See Appendix VI for details of this plan.

#### 11. Search width.

This one parameter remains to be determined. Appendix III discusses the geometry for determining the search width and it concludes that it is the width of a uniform pool of minimum intensity minus the detector view. Unfortunately, there is no way to determine the pool size. There are really not enough statistical data available to generally characterize pool contours for various depths, yields, sea and wind conditions and as a function of time.

##### a. Large location error.

As a matter of interest the following tables have been computed to consider the effect of using a search width for one size pool when the pool is actually some other size. These calculations are based on the estimated probability of detection given by Koopman /2/.

$$P = 1 - \left( \frac{1+nw}{s} \right) \exp \frac{-nw}{s}$$

n = Number of searches made (one for this table).

w = Search width.

s = Spacing of pattern.

As concluded in Appendix II the spacing is  $.75(E\sigma)^{\frac{1}{2}}$  and for this problem  $W = E$ . The standard deviation considered is 25.5 miles.

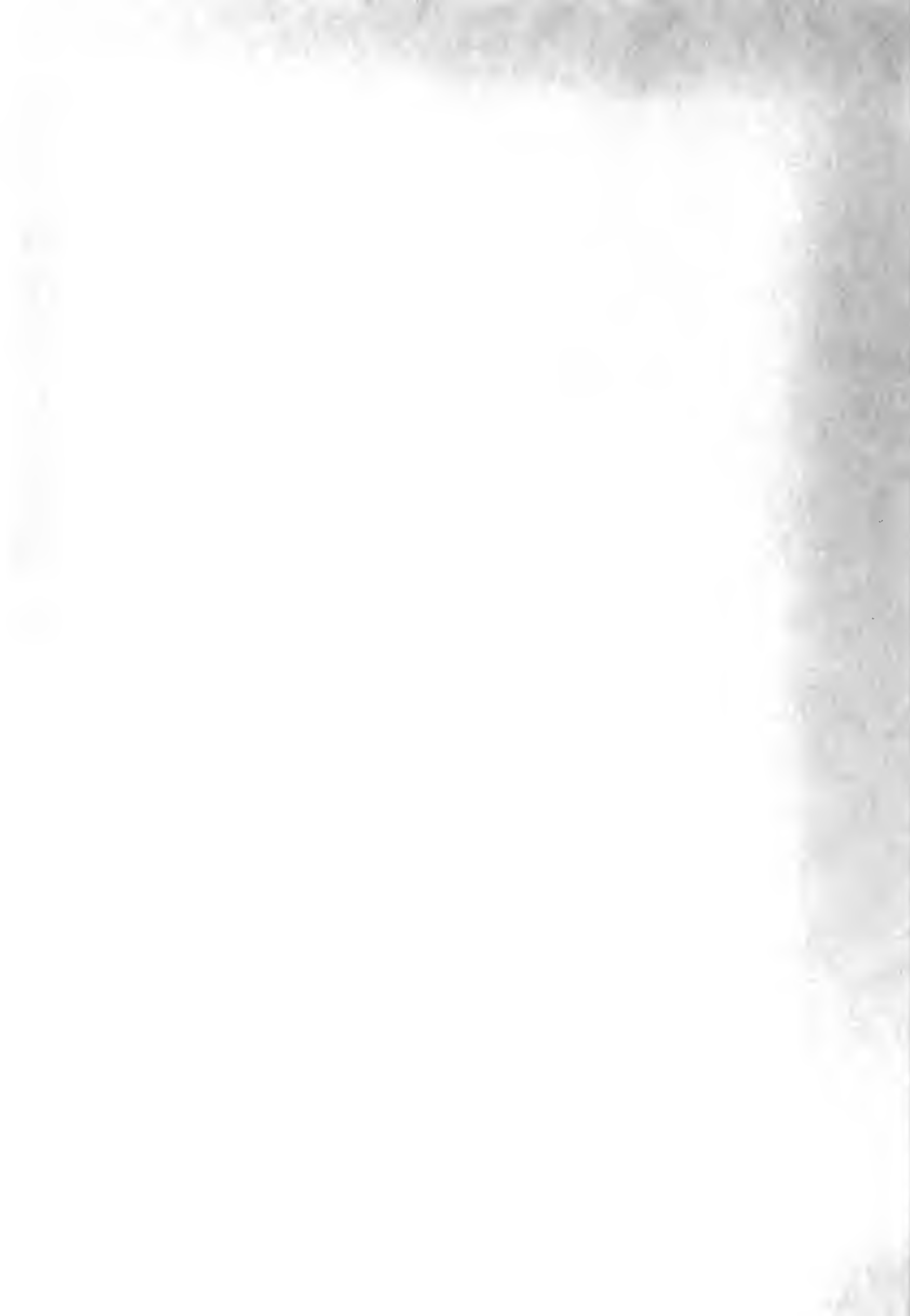


TABLE 1. Analysis of probability of detection for given search spacings.

Search spacing (S) = 4.31 miles - Computed for a 2 mile diameter pool

Pool Diameter (Pool of uniform minimum intensity)	Search Width (W = E)	$\frac{W}{S}$	Probability of Detection
2	1.3	.302	0.036
4	3.3	.766	.18
6	5.3	1.23	.348
8	7.3	1.692	.505
10	9.3	2.16	.634
20	19.3	4.48	.939
30	29.3	6.8	.991

Search spacing (S) = 6.86 - Computed for a 4 mile diameter pool

2	1.3	.1896	.015
4	3.3	.481	.085
6	5.3	.7725	.18
8	7.3	1.062	.287
10	9.3	1.352	.394
20	19.3	2.813	.7714
30	29.3	4.27	.9262

Search spacing (S) = 8.7 - Computed for a 6 mile diameter pool

2	1.3	.1495	.01
4	3.3	.3795	.055
6	5.3	.609	.125
8	7.3	.839	.205
10	9.3	1.068	.289
20	19.3	2.22	.652
30	29.3	3.375	.8513



Search spacing (S) = 10.2 - Computed for an 8 mile diameter pool

Pool Diameter	Search Width	$\frac{W}{S}$	Probability of Detection
2	1.3	.1273	.0075
4	3.3	.324	.04
6	5.3	.52	.095
8	7.3	.715	.161
10	9.3	.912	.23
20	19.3	1.893	.564
30	29.3	2.875	.78

Search spacing (S) = 11.5 - Computed for a 10 mile diameter pool

2	1.3	.113	.008
4	3.3	.287	.034
6	5.3	.461	.076
8	7.3	.634	.132
10	9.3	.808	.191
20	19.3	1.678	.5
30	29.3	2.55	.723

Search spacing (S) = 16.6 - Computed for a 20 mile diameter pool

2	1.3	.0783	.005
4	3.3	.1987	.0175
6	5.3	.319	.04
8	7.3	.44	.073
10	9.3	.56	.107
20	19.3	1.163	.325
30	29.3	1.764	.525





Search spacing (S) = 20.4 - Computed for a 30 mile diameter pool

Pool Diameter	Search Width	$\frac{W}{S}$	Probability of Detection
2	1.3	.0637	.002
4	3.3	.1618	.01
6	5.3	.26	.029
8	7.3	.358	.05
10	9.3	.456	.078
20	19.3	.946	.243
30	29.3	1.436	.421

Figure 3 is a plot of the probability of detection for each of the search spacings under considerations against the widths of the pools. A plot against search widths would be the same shape displaced to the left 0.7 miles. Figure 4 utilizes the same data but uses SPACING vice POOL DIAMETER as the abscissa.

In order to consider this nebulous problem more quantitatively, assume that any search width from 0 to 30 miles is equally likely and investigate the mean probability of detection for each search spacing over the span of search widths.

$$\begin{aligned}\bar{P} &= \int_0^{30} p(w)f(w)dw = \int_0^{30} \left[1 - \left(1 + \frac{W}{S}\right) \exp\left(-\frac{W}{S}\right)\right] \frac{dw}{30} \\ \bar{P} &= \frac{1}{30} \int_0^{30} \left[1 - \exp\left(-\frac{W}{S}\right) - \frac{W}{S} \exp\left(-\frac{W}{S}\right)\right] dw \\ \bar{P} &= \frac{1}{30} \left[ W + S \exp\left(-\frac{W}{S}\right) + S \exp\left(-\frac{W}{S}\right) \left(\frac{W+1}{S}\right) \right]_0^{30} \\ \bar{P} &= \frac{1}{30} \left[ 30 + S \exp\left(-\frac{30}{S}\right) + S \exp\left(-\frac{30}{S}\right) \left(\frac{30+1}{S}\right) - 2S \right]\end{aligned}$$

The Measure of Effectiveness is again called upon to decide which



Fig. 3. Probability of detection for various pool sizes for given spacings  $S(S)$ .

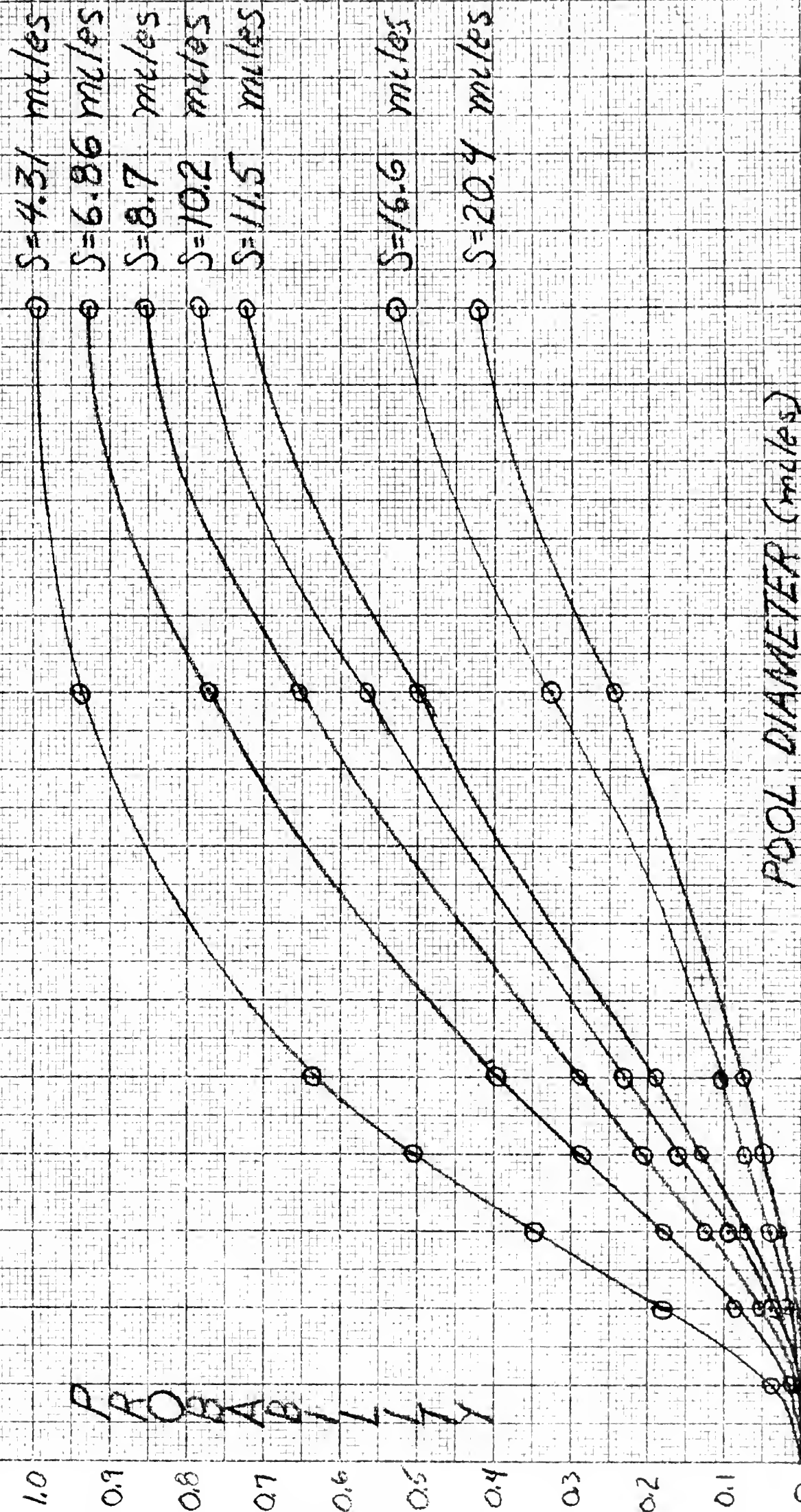
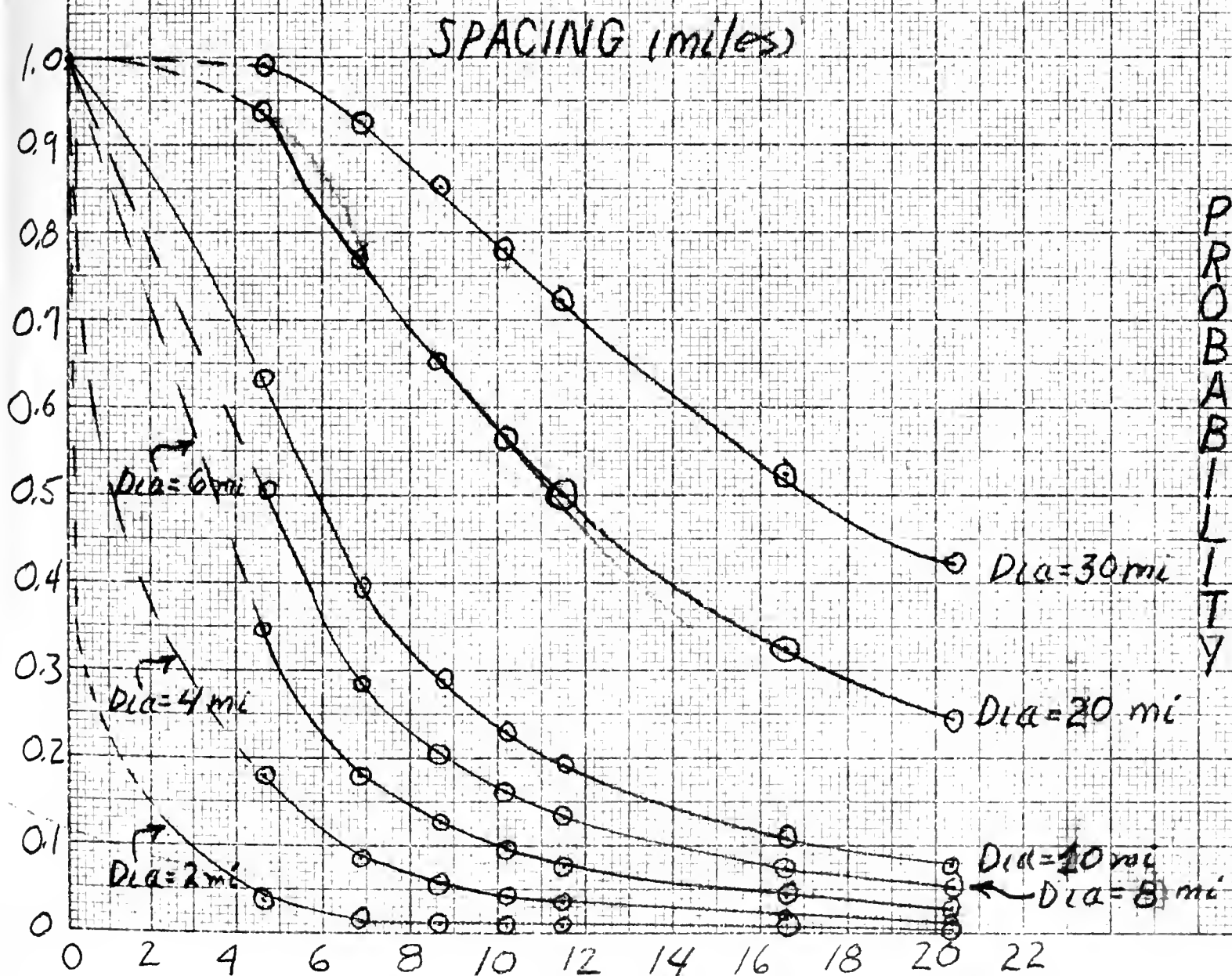




Fig 4. Probability of detection for various spacings for a radioactive pool diameter specified and of minimum uniform surface intensity.





spacing affords the best approach. It is desired to select the spacing which yields the maximum probability per unit time of search effort. The spacing (S) is inversely proportional to the time of search effort. Hence, by maximizing  $\bar{p}S$  the criterion previously established will be satisfied.

TABLE 2. Comparison of spacings using the MEASURE OF EFFECTIVENESS (LARGE LOCATION ERROR.

<u>Associated Pool Diameter</u>	<u>Spacing (S)</u>	<u>Ave. Prob. of Detect. (<math>\bar{p}</math>)</u>	<u>Measure of Effectiveness (<math>\bar{p}S</math>)</u>
2	4.31	.71355	3.07
4	6.86	.561145	3.855
6	8.7	.47058	4.10
8	10.2	.409	4.17
10	11.5	.3633	4.175
20	16.6	.239	3.965
30	20.4	.183	3.73

From the above table it can be seen that  $\bar{p}S$  is maximized around a spacing of 11.5 miles.

By differentiating the expression for  $\bar{p}S$  with respect to S and solving for the maximum the following is obtained:

$$\frac{d(\bar{p}S)}{dS} = \frac{d}{dS} \left[ S + \frac{S^2}{30} \exp\left(-\frac{30}{S}\right) + \frac{S^2}{30} \exp\left(-\frac{30}{S}\right) \left(\frac{30+1}{S}\right) - \frac{S^2}{15} \right]$$

$$\frac{d(\bar{p}S)}{dS} = 0 = 1 + \exp\left(-\frac{30}{S}\right) + \frac{1}{15} S \exp\left(-\frac{30}{S}\right) + \frac{30}{S} \exp\left(-\frac{30}{S}\right) + 2 \exp\left(-\frac{30}{S}\right) + \frac{S}{15} \exp\left(-\frac{30}{S}\right) - \frac{2S}{15}$$

The following transcendental results:

$$S \ln \left( \frac{2S^2 + 45S + 450}{2S^2 - 15S} \right) = 30$$





S = 11 satisfies this expression.

Substituting S = 11 into the expression for ( $\bar{p}$ S)

$$\bar{p}S = 4.18 \quad (\bar{p} = 0.38)$$

As a result of the above - based on the very stringent assumption that search widths will vary uniformly from 0 to 30 miles (implying pools from 0 to 30.7 miles in diameter) - it is concluded that a search spacing of 11 miles maximizes the ratio of probability of detection to time of search effort. This corresponds to anticipating an average search width of 8.44 miles and a pool diameter of 9.14 miles of uniform minimum intensity.

If the assumption had been that pool widths varied uniformly from 0 to 50 miles in diameter the conclusion would have been that a spacing of 25 miles is ideal. It is apparent that the conclusion is very sensitive to this assumption. Statistical data are required to provide a firmer base for this conclusion, but until data becomes available the assumption as stated is considered reasonable.

b. Small Location Error.

When the standard deviation of the location error is only 5.6 miles the effect of the current is relatively significant. After a delay of 24 hours the peak of the distribution would have moved out to a circle of 12 miles radius (assuming a drift of 0.5 knots). The search path is along the peak at the time of arrival (modifying spiral to an expanding square). After the first path the "a posteriori" probability becomes bimodal with a circular peak inside and one outside. The pattern continues to search these maxima.

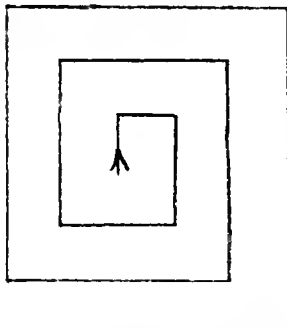
It is beyond the scope of this thesis to develop a probability of



detection statement for this situation, but it is worth considering the tendency of the "a posteriori" distribution. As each peak is searched the surface of probability becomes flatter until after one pass of the area the distribution approaches a uniform one. As the first search is being made, however, the situation is not much different from that developed in the case of the larger deviation. In the latter case the probability peak was continuously being pushed outward. In the situation of the moving target the circular peak is being split into two concentric rings enclosing the original peak. Each resulting ring is searched, and the peak is pushed both inward and outward as the search progresses.

In order to get some feel for the problem (which is more difficult mathematically than physically) the same expression for the probability of detection is used as a foundation for investigating the search width.

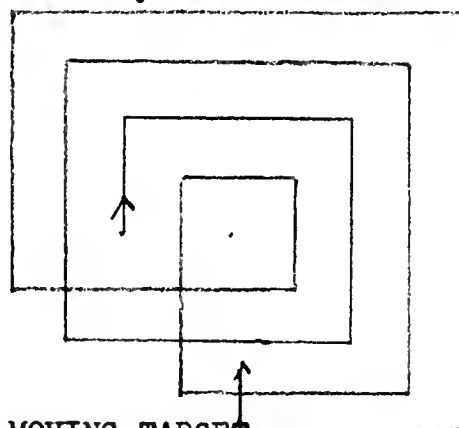
From a geometry standpoint, after an area of a given peripheral size is searched, 0.75 would receive the same intensity of search in the current problem as was received in the stationary, large deviation problem. The remaining quarter would be only half covered but with twice the effort.



STATIONARY TARGET,  
LARGE DEVIATION

$$P = 1 - \left(1 + \frac{nW}{S}\right) \exp\left(-\frac{nW}{S}\right)$$

$$n = 1$$



MOVING TARGET,  
SMALL DEVIATION

$$P \approx 0.75 \left[ 1 - \left(1 + \frac{W}{S}\right) \exp\left(-\frac{W}{S}\right) \right] + 0.125 \left[ 1 - \left(1 + \frac{2W}{S}\right) \exp\left(-\frac{2W}{S}\right) \right]$$

Fig. 5 Comparison of search patterns.



Under these very rough approximations and the assumptions of the previous discussion a table similar to Table 2 can be computed.

<u>Associated Pool Diameter</u>	<u>Spacing (S)</u>	<u>Average Prob. of Detection (<math>\bar{p}</math>)</u>	<u>Measure of Effectiveness (<math>\bar{p}S</math>)</u>
2	2.02	.767	1.55
4	3.22	.70	2.25
6	4.08	.654	2.67
8	4.79	.615	2.95
10	5.41	.582	3.15
20	7.79	.472	3.68
30	9.61	.409	3.93

TABLE 3. Comparison of spacings using the MEASURE OF EFFECTIVENESS (SMALL LOCATION ERROR).

This indicates that the largest spacing would maximize the approximate probability of detection per time of search effort provided the actual probability of detection is at least proportional to the above estimation and that pool sizes are equally likely in size from 0 to 30 miles.

After one pass of the area using the doubly expanding square and a spacing of 9.61 miles the target location distribution approaches a UNIFORM one. It is obviously not UNIFORM, but the peaks have been flattened and multiplied and the continued movement of the current throughout the search builds up the probability of the target being in a path already swept. The end result is that the unit mass is best considered to be evenly spread over the area.

As a result of this reasoning a parallel sweep search will maximize the probability of detection per time of search effort after the first



pass. The expression for probability of detection then becomes:

$$P = \frac{W}{S} \text{ for } S > W; \quad P = 1 \text{ for } S \leq W.$$

Following the same approach as in subparagraph 11.a. it is desired to determine the spacing that meets the established measure of effectiveness - again under the assumption of equally likely search widths (pool diameters) over the range of 0 to 30 miles.

$$\begin{aligned} \bar{p} &= \frac{1}{30} \int_0^{30} \frac{W}{S} dw \quad \text{for } S > W \\ &= \frac{1}{30} \left[ \frac{W^2}{2S} \right]_0^{30} = \frac{15}{S} \end{aligned}$$

We are interested in  $\bar{p}S$ . Since  $\bar{p}$  cannot exceed 1 there is no sense in making  $S$  smaller than 15 because  $\bar{p}$  would remain constant as  $S$  was made smaller and  $\bar{p}S$  would therefore decrease. Obviously the maximum is reached when  $S = W$ . Therefore this search should be conducted at a spacing of 15 miles.

For the second pass the search area should be a square whose dimensions are dictated by:

a. Three times the location standard deviation to provide an almost certainty that the pool was included in this circle at the time of the fix, plus,

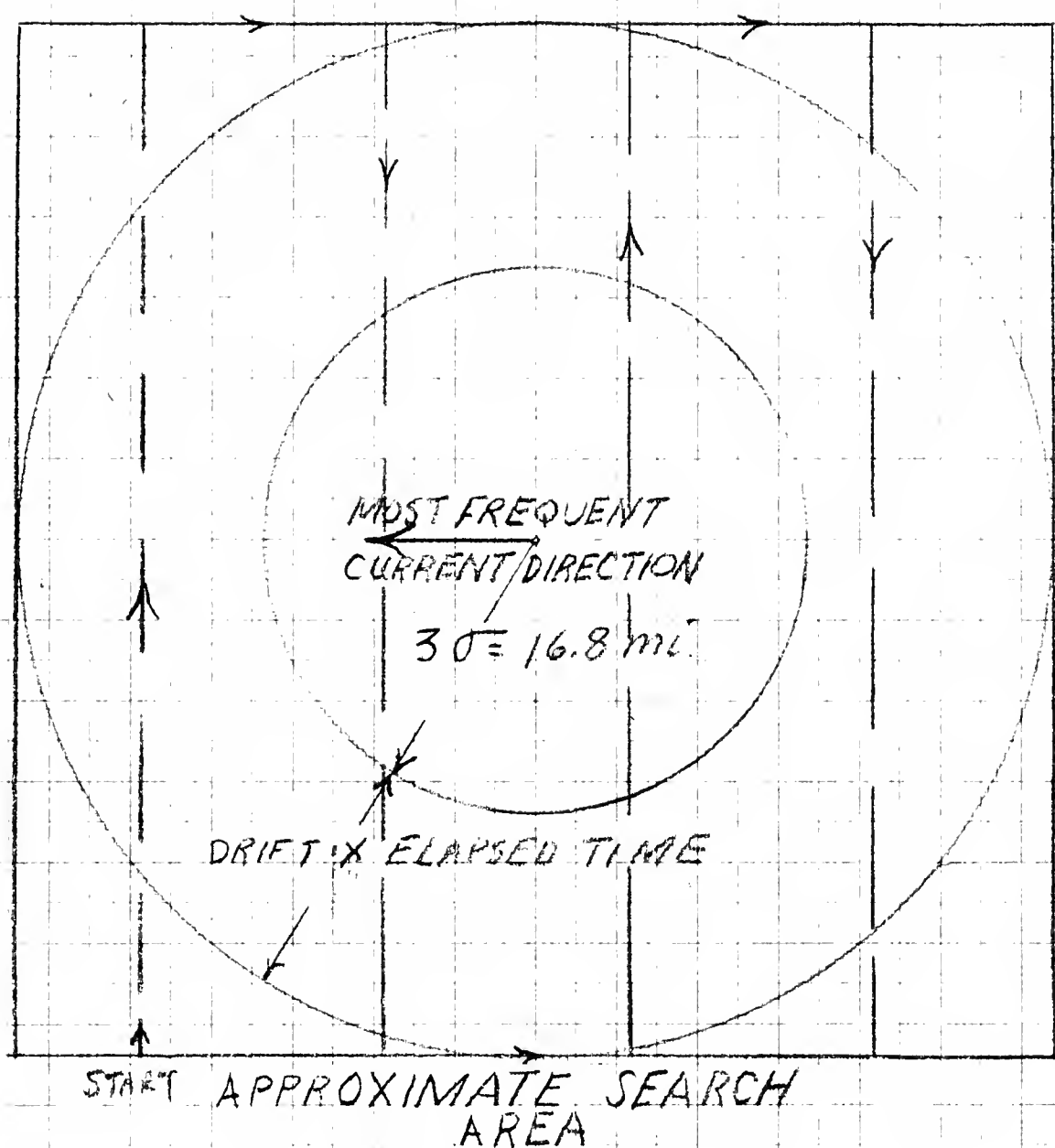
b. the product of the drift and the time that would elapse between the time of the fix and the time of completion of sweep of the area on this second pass.

The sweeps should start along the side perpendicular to the most frequent direction of the current at 15 mile spacing.





1 Small box =  $\frac{1}{2}$  mi x  $\frac{1}{2}$  mi



The above pattern is for 30 hours  
time late and drift of 0.5 Knots.

Dimension of square =  $2[(0.5 \times 30) + 16.8] = 63.6 \text{ mi}$

Length of search =  $\frac{45 + (4 \times 63.6)}{130} = 1 \text{ hr } 40 \text{ min}$   
(300 mi.)

Spacing = 15 mi.

Fig. 6 Dimensions of Search Area on 2<sup>nd</sup> pass.



## 12. Aircraft capabilities.

It is assumed that an aircraft will be available for the search equipped with the proper survey meter and water sample floats capable of the following:

- a. Maximum range to scene 1000 miles with minimum of 3 hours on station available.
- b. Search speed 180 knots.

## 13. Search procedure.

This problem deals with an underwater burst which vents to the atmosphere. All of the effort of the study has been devoted to an analysis of activity at the scene, but the study has presupposed that an air sampling barrier would be established downwind from the blast. Any samples obtained from this endeavor would not be subject to masking and quite informative about the circumstances of the origin of the blast.

As previously mentioned, correlation of hydroacoustic information may take several hours. It is reasonable to assume that as much as 24 hours may pass before search craft could arrive at the scene. The appropriate search plan should be followed depending on the physical situation. If a pool or suspected pool is located an attempt should be made to locate the area of highest intensity (with due regard for safety of the crew). Intensity readings should be taken and correlated with position and time as accurate as possible. Relative positions within the pool are more important than exact geographical locations. At the point of highest intensity water sampling floats should be dropped for later recovery by surface craft or helicopters.

The search aircraft should remain in the area as long as safety and



operational requirements permit so it can direct other searching activity for recovering water sample floats.

Frequent intensity readings may provide sufficient information to establish decay curves to extrapolate back to the time of detonation. Great accuracy would be necessary in correlating the movement of the pool, height of aircraft, location of aircraft over some relative point of the pool, etc. to permit much of an estimate of the decay rate. The best procedure would be to keep recording the intensity of the area of highest intensity to provide some semblance of a reference. This would corroborate hydroacoustic information.

Normal search procedures should be followed in marking datum and search area, and making reports.

#### 14. Conclusions.

The problem was to determine the optimal searching procedure for locating the site of an underwater explosion which had vented, in order to classify it as nuclear or non-nuclear.

A hydroacoustic network is anticipated to be the detecting agent. Such a network has no ability to distinguish an underwater nuclear explosion from a non-nuclear one. Classification must be accomplished by a thorough investigation of the scene for evidence of nuclear activity. If no such evidence is found a probability statement can be made of the nature of the explosion, and upon this information a decision to terminate or continue the search can be reached.

A MEASURE OF EFFECTIVENESS was established to be:

Maximize the probability of detection per time of search effort.

Several parameters were investigated to appreciate their effect on the problem.



a. Height.

It was determined that the maximum intensity reading at the meter occurs on the surface. As altitude is increased the intensity decreases up to an altitude above 20,000 feet. After that the increase is gradual and almost negligible. Of course at such a height the interest is only academic since very few waves have sufficient energy to survive that thickness of air.

b. Search Spacing.

The development for search spacing as presented by Koopman /2/ was expanded and adopted for this study.

c. Search Width.

The effective search width was determined to depend on the radioactive pool diameter which was an unknown quantity. Pool diameters depend on yield, depth of detonation, and physical characteristics of the water and the exploded device. In order to discuss the problem quantitatively an averaging procedure was used, assuming any pool diameter to be equally likely between 0 and 30 miles. This is a very brash assumption, and the results of the study depend heavily on this weighting function. Unfortunately, little statistical data are available which might indicate the distribution of this function. This assumed UNIFORM distribution of weights provides an unexpected conclusion when the criterion is the MEASURE OF EFFECTIVENESS mentioned above. If the weight function favored some particular pool diameter it would be reasonable to adopt the most effective spacing for that diameter; however if there is no bias toward a particular width the conclusion is not so evident. Various spacings were concluded to be optimum depending on the standard deviation of the distributions considered.





d. Location Error.

There are two categories of location error considered. Large errors with standard deviations above 25 miles dictated a search plan that ignored current drift. For smaller deviations the drift had to be reckoned with in designing the search plan. The location error considered the effect of both the initial hydroacoustic fix error and navigational errors of aircraft arriving at a given spot in the open ocean.

When current movement was considered (with small standard deviations of location) the direction was assumed to be random, but the drift can be predicted within an acceptable margin.

e. Search Plans.

When the standard deviation of the location distribution is large the squares of uniform coverage maximize the probability of detection per time of search effort. On the other hand if the deviation is small, a retiring search maximizes this criterion for the first pass. For subsequent passes of the small deviation problem the "a posteriori" rippled distribution approaches a UNIFORM, and a parallel sweep search is considered best.

Finally, although this comment is beyond the scope of the stated problem, it seems worth mentioning in passing that very little special equipment is required to perform this function of classifying detected disturbances. Water sample floats which can be dropped from an aircraft, sample the water and seal themselves - to be recovered by surface craft or helicopters, and the survey meters described by NRDL /1/ are the only non-standard items needed. These items can be based ashore and on carriers and need not be on aircraft until a plane is assigned a particular task of classifying.



## BIBLIOGRAPHY

1. Radiation Instrumentation for the Classification of Nuclear Explosions at Sea. USNRDL-TR-525 of 7 September 1961 by E. J. Wesley of U. S. Naval Radiological Defense Laboratory, San Francisco 24, California.
2. Search and Screening. OEG Report No. 56 by B. O. Koopman of Office of Chief of Naval Operations.
3. Marine Geology by P. H. Kuener; Wiley.
4. American Practical Navigator Bowditch; U. S. Navy Hydrographic Office (HO Pub No. 9, 1958).
5. Atlas of Surface Currents. Northwestern Pacific Ocean. HO Pub No. 569; Reprinted 1953.
6. Hydroacoustic Detection of Nuclear Explosions (U), U. S. Naval Electronics Laboratory CONFIDENTIAL Report 1061 of 2 August 1961.
7. Preliminary Draft "The Feasibility of Hydroacoustic Detection of Nuclear Explosions Detonated in Violation of a Possible Test Moratorium (CONFIDENTIAL); ARPA Order No. 192-61; Project Code No. 8100, 4-28-61.
8. Hearings Before the Special Subcommittee on Radiation - Joint Committee on Atomic Energy, Congress of the United States, 86th Congress; 2nd Section; 9-22 April 1960.



## APPENDIX I

### HEIGHT OF SURVEYING AIRCRAFT

In order to determine an appropriate search plan the search height must be determined. According to reference /1/ the meter will be constructed with a shield forming a cone about the axis to prevent excessive interference from cosmic radiation. This shielding forms a central angle of  $150^\circ$ .

As the search craft increases its height the area seen by the meter will increase and one would expect this to increase the intensity at the instrument. However, the attenuation due to the atmosphere will decrease the intensity at the meter.

#### Model assumptions:

1. The pool is UNIFORM and INFINITE in diameter.
2. Gamma energy at the surface is 1 MEV and the "build-up" factor is not considered.
3. Absorption is linear varying at a constant rate with distance from the source.
4. Height of meter is much greater than the diameter of the meter opening.

$I$  = Intensity of radiation at the meter.

$A$  = Area of meter opening.

$I_0$  = Intensity of point sources at the surface.

$h$  = Height of instrument.

$u$  = Linear coefficient of absorption in air ( $2.265 \times 10^{-3}/\text{FT}$ ).

$x$  = Distance of meter from radiating source.

$r$  = Distance of source along water from point on surface directly below aircraft.



$\theta$  = Angle of rotation of "r" on surface.

$\phi$  = Angle that point radiating source makes with meter.

$w$  = Solid angle subtended by meter opening at radiating source.

The portion of the radiation that arrives at the meter from each point source is equal to the ratio of the solid angle ( $w$ ) subtended divided by 4 .

$$\frac{W}{4} = \frac{A \cos \phi}{x^2 4}$$

This assumes that  $h$  is much greater than the diameter of  $A$ ; therefore the projection of the area of the meter opening on a plane tangent to a sphere expanded about the point source is approximately equal to the projection onto the sphere.

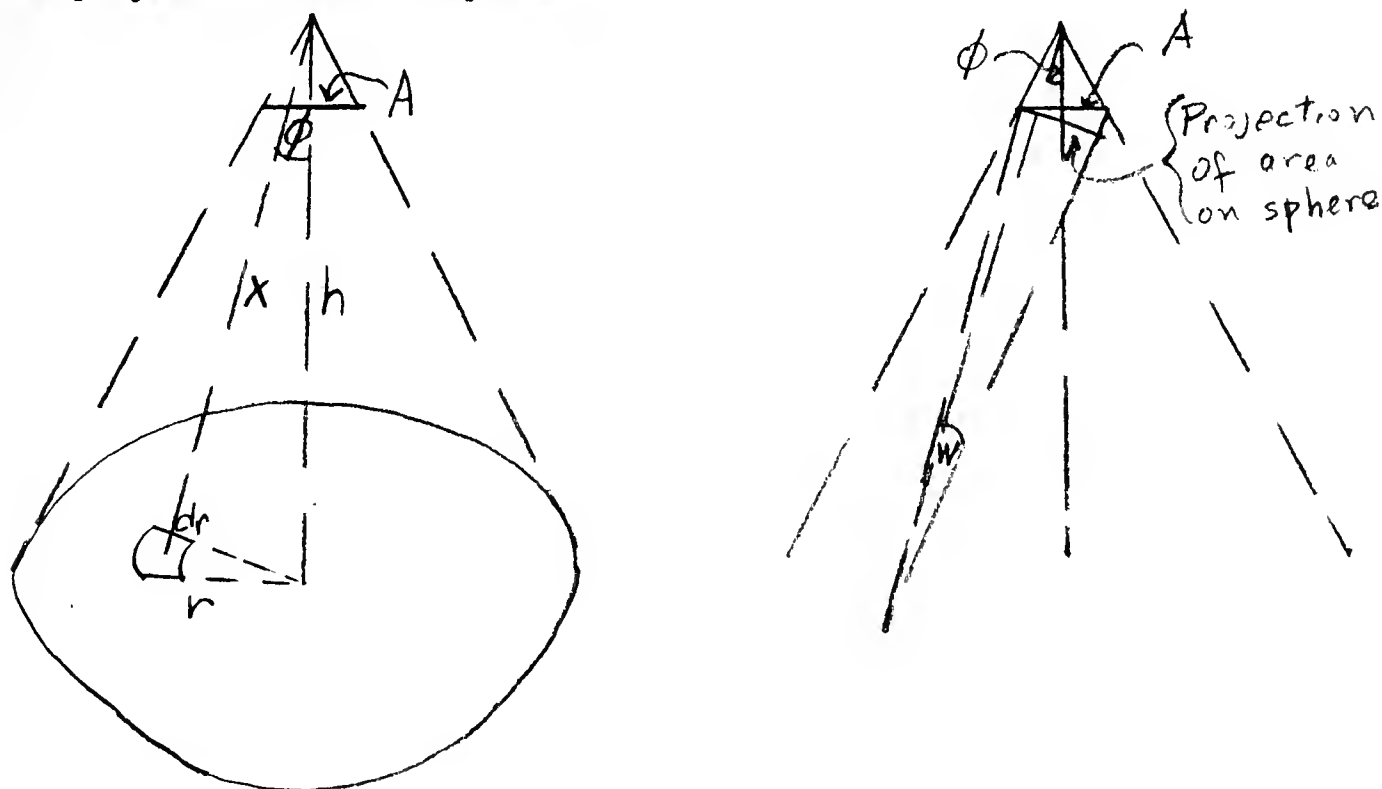


Fig. 7 Parameters of integration.

$$I = \int_0^{h \tan \phi} \int_0^{2\pi} \frac{I_0 A \cos \phi}{4\pi x^2} \exp[-ux] r dr d\theta$$





$$\cos \phi = \frac{h}{x}$$

$$r = (x^2 - h^2)^{\frac{1}{2}}$$

$$dr = \frac{x}{(x^2 - h^2)^{\frac{1}{2}}}$$

$$(1) \quad I = \int_h^{h \sec \phi} \frac{I_0 A h}{2} \frac{\exp[-ux]}{x^2} dx$$

It would be of interest to find a height which would maximize the intensity at the meter if such exists.

The integrand in (1) is continuous except at 0 and the derivative can be investigated by applying Leibnitz's Rule:

$$(2) \quad \frac{dI}{dh} = \frac{I_0 A}{2} \left[ \frac{h \exp(-u h \sec \phi)}{h^2 \sec^2 \phi} \sec \phi - \frac{h \exp(-u h)}{h^2} + \int_h^{h \sec \phi} \frac{\exp(-ux) dx}{x^2} \right]$$

Consider the last integral in (2).

$$\begin{aligned} \int_h^{h \sec \phi} \frac{\exp(-ux) dx}{x^2} &= \left[ \frac{-\exp(-ux)}{x} - u \int \frac{\exp(-ux) dx}{x} \right]_h^{h \sec \phi} \\ &= \left[ \frac{-\exp(-ux)}{x} - u (\ln x - ux + \frac{u^2 x^2}{2 \cdot 2!} - \frac{u^3 x^3}{3 \cdot 3!} + \frac{u^4 x^4}{4 \cdot 4!} \dots) \right]_h^{h \sec \phi} \end{aligned}$$

This term by term integration is justified by virtue of uniform convergence of the infinite series expansion.

Substituting this in (2):

$$(3) \quad \frac{dI}{dh} = -\ln \sec \phi + u h (\sec \phi - 1) - \frac{u^2 h^2}{4} (\sec^2 \phi - 1) + \frac{u^3 h^3}{18} (\sec^3 \phi - 1) - \frac{u^4 h^4}{96} (\sec^4 \phi - 1) \dots$$

$$\sec \phi = 3.8637$$



$\frac{dI}{dh}$  was programmed on the 1604 computer for a large number of values

of  $h$ . The results showed that the derivative was always negative, becoming smaller in absolute value as height increased. This indicates that a plot of the intensity would be an exponential decay with its maximum value at  $h = 0$ .

Assumption 3 in the previous model is not realistic because the attenuation varies with density. Since air density varies with height the coefficient of absorption must also vary with height. The mass coefficient of absorption is equal to the linear coefficient divided by the density and it does not vary with the chemical or physical condition of the medium. For air this quantity is  $0.0274 \text{ cm}^2/\text{gm}$ .

According to the Barometer equation derived in STATISTICAL MECHANICS:

$$P = P_0 \exp\left(\frac{-mgh}{KT}\right)$$

$P$  = Density at height of instrument.

$m$  = Mass of a molecule of the medium.

$g$  = Acceleration due to gravity.

$h$  = Height of the instrument.

$K$  = Boltzman's constant.

$T$  = Temperature (degrees KELVIN).

$P_0$  = Atmospheric density at sea level.

$u'$  = Mass coefficient of absorption.

$x$  = Slant range from radiating source to meter.

$\emptyset$  = Limit of shielding ( $75^\circ$ ).

Returning to equation (1) and substituting:



$$\exp[-ux] = \exp[-u'Px] = \exp\left[-u'xP_0 \exp\left(-\frac{mgh}{KT}\right)\right]$$

$$I = \int_h^{h \sec \phi} \frac{I_0 A h \exp\left[-u'xP_0 \exp\left(-\frac{mgh}{KT}\right)\right]}{2 x^2} dx$$

$$(4) \quad \frac{1}{B} \frac{dI}{dh} = \frac{\exp\left[-u'P_0 \exp\left(-\frac{mgh}{KT}\right) h \sec \phi\right]}{h \sec \phi} - \frac{\exp\left[-u'P_0 \exp\left(-\frac{mgh}{KT}\right) h\right]}{h} \\ + \int_h^{h \sec \phi} h \frac{mg}{KT} \exp\left(-\frac{mgh}{KT}\right) u'P_0 \frac{\exp\left[-u'P_0 \exp\left(-\frac{mgh}{KT}\right) x\right]}{x} dx \\ + \int_h^{h \sec \phi} \frac{\exp\left[-u'P_0 \exp\left(-\frac{mgh}{KT}\right) x\right]}{x^2} dx \quad B = \frac{I_0 A}{2}$$

The last integral of equation (4) becomes:

$$(5) \quad \left[ -\frac{\exp(-ax)}{x} \right]_h^{h \sec \phi} - a \int_h^{h \sec \phi} \frac{\exp(-ax)}{x} dx \quad \text{Where } a = u'P_0 \exp\left(-\frac{mgh}{KT}\right)$$

The first part of (5) balances the first two terms of (4).

$$(6) \quad \frac{1}{B} \frac{dI}{dh} = a \left( h \frac{mg}{KT} - 1 \right) \int_h^{h \sec \phi} \frac{\exp(-ax)}{x} dx \\ = a \left( h \frac{mg}{KT} - 1 \right) \left[ \ln \sec \phi - ah(\sec \phi - 1) + \frac{a^2 h^2}{2 \cdot 2!} (\sec^2 \phi - 1) \dots \right]$$

Consider the following:

"a" is positive for all values of h;

The infinite series is always positive;

$$h \frac{mg}{KT} - 1 \text{ is 0 when } h = \frac{KT}{mg}$$

Therefore there is a maximum or minimum or flex at  $h = \frac{KT}{mg}$

$$\frac{d^2 I}{dh^2} \bigg|_{h = \frac{KT}{mg}} = Ba \left[ \ln \sec \phi - ah(\sec \phi - 1) + \frac{a^2 h^2}{2 \cdot 2!} (\sec^2 \phi - 1) \dots \right]$$



Again "a", B and the series are positive. The conclusion is that  $h = \frac{KT}{mg}$  is a minimum point.

Equation (6) was programmed out to 30 terms for values of height from -100 to 40,000 feet and several sensitivity checks were made.

The temperature is recognized as a variable over the range investigated and it was varied from 300°K (81°F) to 273°K (32°F). The values varied slightly but the structure of the curve remained the same. A few points were checked with the temperature at 243°K (-40°F) and again the height of the minimum decreased slightly but the structure of the curve remained the same. This covered the range that average temperatures could reach and the minimum varied from 21100 feet to 26070 feet.

Variations in surface air density ( $P_0$ ) were looked at but their effect were even less significant.

Variations in "g" were not looked at, but they are obviously of no concern.

Lastly, the evaluation was made for 10 terms of the series and then for 30 terms of the series. In both cases the values were the same out to eight significant figures.

As a final investigation the expression for the intensity was programmed and curves obtained are presented in figure 8. It is satisfying that the same MINIMUM points were reached by two independent approaches and two different programs.

The development was as follows:

$$I = \int_h^{h \sec \phi} \frac{I_0 A}{2} \frac{h \exp(-ax)}{x^2} dx$$





$$\begin{aligned}
&= \frac{I_0 A h}{2} \left[ \frac{-\exp(-ax)}{x} \right]_{h \sec \phi}^{h \sec \phi - a} - a \int_{h \sec \phi}^{h \sec \phi - a} \frac{\exp(-ax)}{x} dx \\
&= -\frac{I_0 A h}{2} \left[ \frac{\exp(-h \sec \phi a)}{h \sec \phi} - \frac{\exp(-ha)}{h} \right] + a \left[ \ln \sec \phi - a h (\sec \phi - 1) \dots \right] \\
&= \frac{I_0 A}{2} \left[ \left(1 - \frac{1}{\sec \phi}\right) + ha \left( \ln \sec \phi + \left(1 - \frac{1}{2!}\right) ha (\sec \phi - 1) \right. \right. \\
&\quad \left. \left. + \left( \frac{-1}{2 \cdot 2!} \right) h^2 a^2 (\sec^2 \phi - 1) \dots + \left( \frac{1}{-n \cdot n!} + \frac{1}{(n+1)!} \right) h^n a^n (\sec^n \phi - 1) \dots \right] \\
I &= \frac{I_0 A}{2} \left[ .741 + ha \left( -\ln \sec \phi + \left(1 - \frac{1}{2!}\right) ha (\sec \phi - 1) \dots \right) \right]
\end{aligned}$$

In fig. 8 the bracketed quantity is plotted as  $f(h)$  - the "Intensity factor".

### CONCLUSIONS

1. The greatest intensity at the meter will be experienced when the height is zero.

2. The minimum point of intensity is little more than academic interest since the assumption of a UNIFORM source of diameter at least equal to the field of the meter becomes a stringent condition at 25,000 feet. The pool would have to be 30 miles in diameter. More directly, this problem is interested in maximum intensities.

3. Operational conditions will dictate the height of search with the aim of flying as low as feasible on a prolonged mission. Figure 8 demonstrates the degradation of intensity at the meter (and therefore the decrease in search width) for the height of search selected. It is not possible to predict the decrease in probability of detection which will be experienced as height increases because the physical conditions of the pool of radiation are not known. Since the meter has a threshold intensity which must be reached before a signal can be recognized, flying

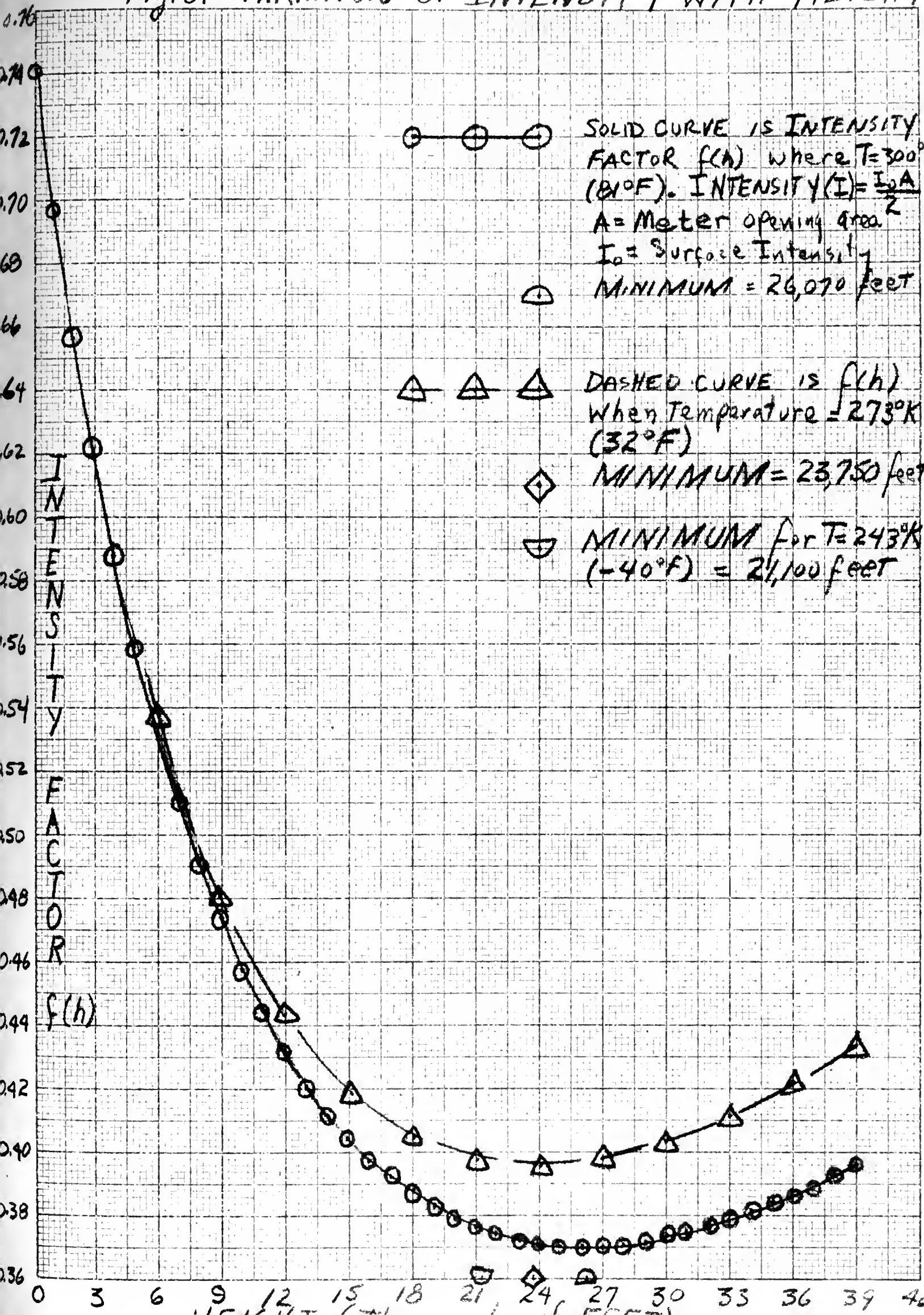


at a greater altitude than operationally necessary may degenerate the intensity at the meter so that the threshold is not reached - whereas it may have been reached at the lower level.

4. At the altitudes that are operationally feasible the curve will give a reliable indication of Intensity factor ( $f(h)$ ) for any atmospheric conditions (neglecting the build-up factor effects) since it is insensitive to temperature changes below 3000 feet.



Fig. 8. VARIATION OF INTENSITY WITH HEIGHT





## APPENDIX II

### SEARCH THEORY

This appendix is based on Koopman's Search and Screening (OEG Report No. 56) /2/. An attempt is made to present his development in more detail as it applies to this thesis.

A. Development of probability of detection of a target of lateral range  $X$  from a straight aircraft track:

$$(1) \quad p(X) = 1 - \exp\left[-0.092\left(\frac{E}{X}\right)^2\right]$$

1. Consider the case of "continuous looking" where "s" is the instantaneous probability density of detecting a target. If s remains constant throughout a search  $p(t) = 1 - \exp(-st)$  where  $p(t)$  is the probability of detection during time  $t$ .

If  $s$  is a changing density because of relative movement with respect to the observer, and is time - dependent, the expression is more complicated. The instantaneous density  $s$  is inherently dependent on range and the fact that it varies with time is conveyed by the symbol  $s_t$ .

$$p(t) = 1 - \exp\left[-\int_0^t s_t dt\right]$$

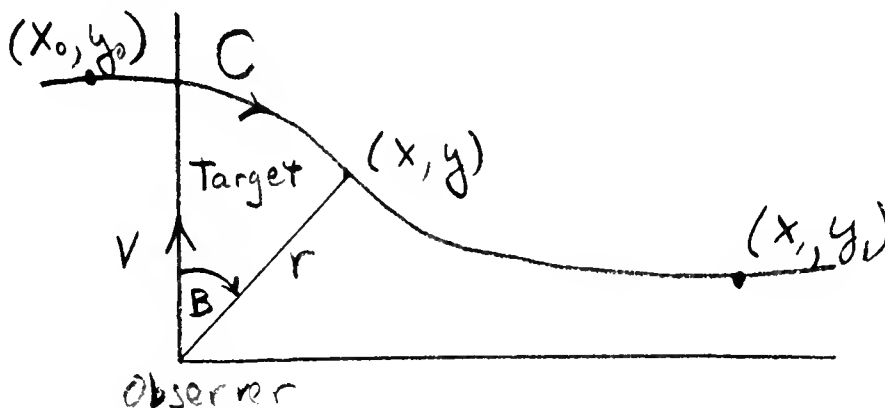


Fig. 9 Target's relative track.

The target is at  $(x, y)$  at time  $t$  and  $x = x(t)$ ,  $y = y(t)$ . Let the





initial position at  $t = t'$  be  $X_0 = X(t')$ ,  $y_0 = y(t')$ , and the final position at  $t = t''$  is  $X_1 = X(t'')$ ,  $y_1 = y(t'')$  with the target tracing a track along  $C$  in figure 9 above.

$$s = s \left[ (x^2(t) + y^2(t))^{\frac{1}{2}} \right] = s_t$$

The probability of detection along path  $C$  is:

$$p_c = 1 - \exp \left[ - \int_{t'}^{t''} s \left( [x^2(t) + y^2(t)]^{\frac{1}{2}} \right) dt \right]$$

The integral is a line integral along  $C$ ; if " $w$ " is the relative speed and " $l$ " is the arc length along  $C$  from  $X_0$ ,  $Y_0$ , then

$$p_c = 1 - \exp \left[ - \int_C s \left( [x^2(t) + y^2(t)]^{\frac{1}{2}} \right) \frac{dl}{w} \right] \quad dt = \frac{dl}{w}$$

Following Koopman's notation the exponent is called the sighting potential  $F[C]$ . This quantity possesses the property of additivity so that where  $C = C_1 + C_2$ , then  $F[C] = F[C_1] + F[C_2]$

In the case where  $X$  is the lateral range,  $X$  is constant and  $y = wt$  ( $w$  is a constant).

$$F[C] = \int_{t'}^{t''} s \left( [x^2 + w^2 t^2]^{\frac{1}{2}} \right) dt = \frac{1}{w} \int_{y'}^{y''} s \left( [x^2 + y^2]^{\frac{1}{2}} \right) dy$$

According to the inverse cube law of sighting where  $h \ll r$

$$(2) \quad s = \frac{k h}{r^3}$$

$$F[C] = \frac{k h}{w} \int_{y'}^{y''} \frac{dy}{(x^2 + y^2)^{3/2}}$$

$$= \frac{k h}{w} \left[ \frac{y}{x^2 (x^2 + y^2)^{\frac{1}{2}}} \right]_{y'}^{y''}$$

$$= \frac{k h}{w} \left[ \frac{y''}{x^2 (x^2 + y^2)^{\frac{1}{2}}} - \frac{y'}{x^2 (x^2 + y^2)^{\frac{1}{2}}} \right]$$



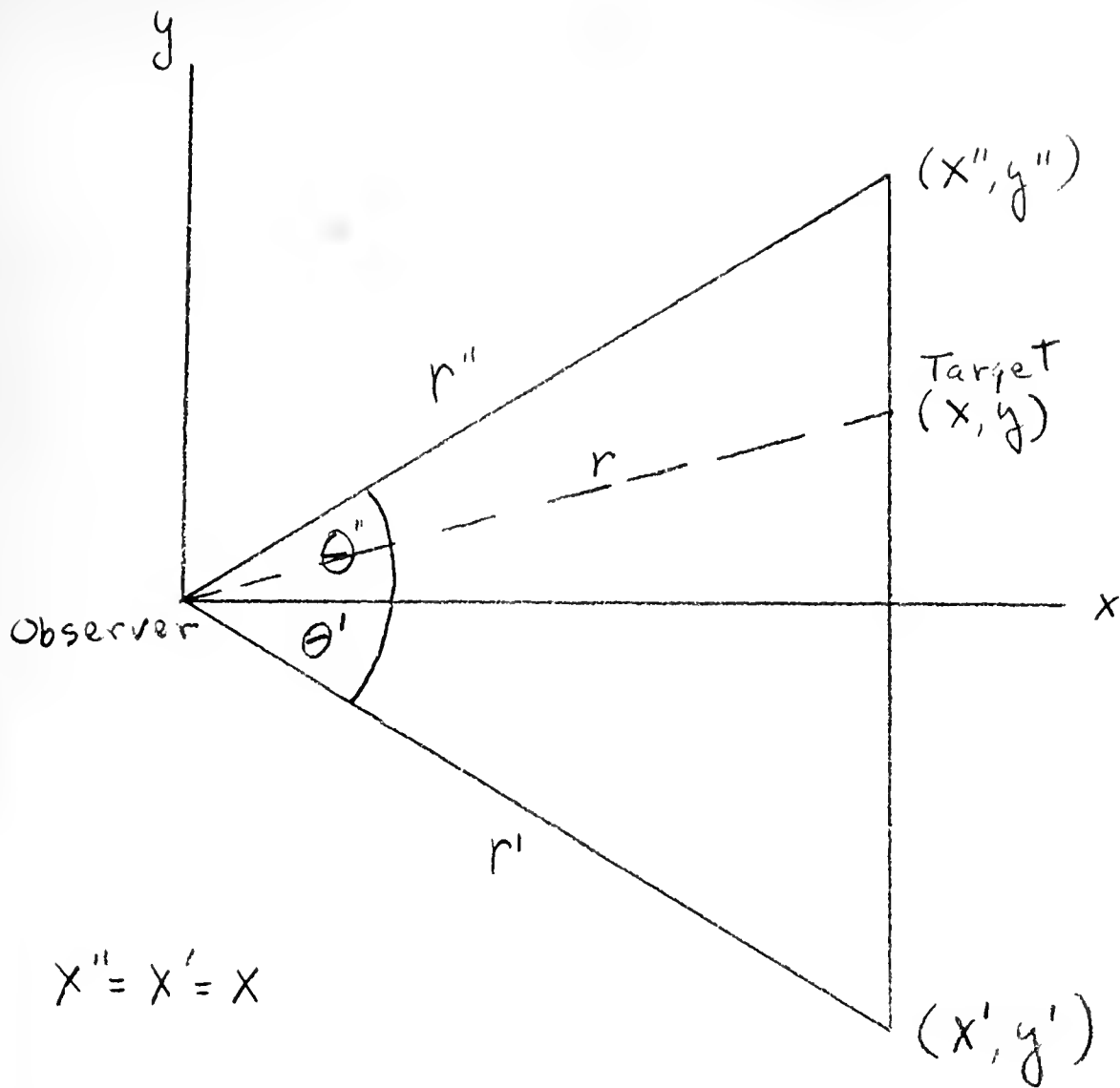


Fig. 10 Detection at fixed speed and course.

When the sweep is "relatively" infinite  $\theta' = \theta'' = 90^\circ$  and -

$$(3) \quad F[C] = F[X] = \frac{k h}{\omega x^2} (1+1) = \frac{2 k h}{\omega x^2}$$

When the observer and the target are on straight courses at constant speeds for a long time before and after their closest point of approach, the probability of detection is a function of the lateral range  $X$ .

$$p(x) = 1 - \exp[-F(x)]$$

## 2. Parallel sweeps -

A target is presumed to be at rest on the ocean in an unknown position, all equal areas having the same chance of containing it. A search is made along a large ("infinite") number of parallel lines a



common distance apart. This distance is referred to as Sweep Spacing ( $s$ ) and the problem is to determine the probability of detection of a target,  $P(s)$ , by this configuration. Other questions concerning probability of detection, if target speed and course are known or have a distribution of their own, can follow in development.

Consider the lateral ranges of the target from various sweeps

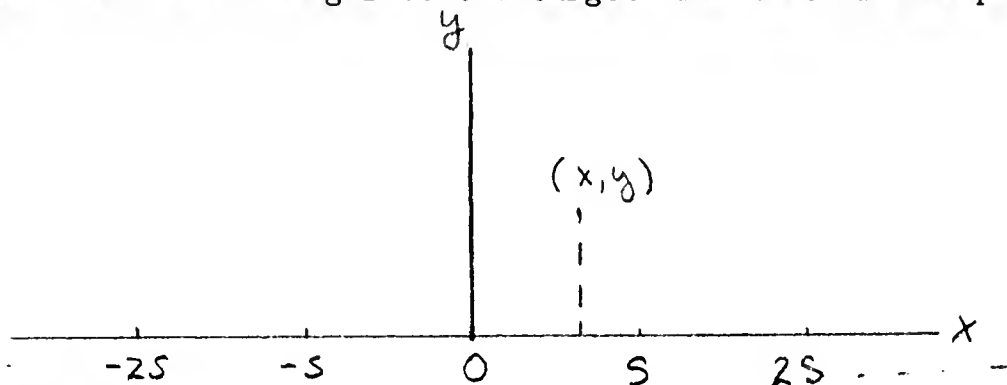


Fig. 11 Parallel sweeps.

For paths to the left the distances are  $X, X + s, X + 2s \dots$  and for those to the right  $s - X, 2s - X, 3s - X \dots$ . Both cases can be combined in the absolute expression

$$\text{lateral range} = |X - ns| \quad \text{where} \quad 0 \leq X \leq s$$

$$n = 0, \pm 1, \pm 2, \pm 3, \dots$$

The probability of detection by the  $n^{\text{th}}$  lateral sweep when the target is at  $(X, y)$  is:

$$p_n(x) = 1 - \exp[-F(|X - ns|)]$$

The probability of no detection by the  $n^{\text{th}}$  sweep is  $1 - p_n$ ; and no detection by any sweep is the infinite product  $\prod (1 - p_n)$  for all values of  $n$ . The probability that at least one sweep detects a target at  $(X, y)$  is

$$(4) \quad p(x, s) = 1 - \prod_{n=-\infty}^{\infty} \exp[-F(|X - ns|)] = 1 - \exp[-\phi(x, s)]$$

$$(5) \quad \text{where} \quad \phi(x, s) = \sum_{n=-\infty}^{\infty} F(|X - ns|); \quad 0 \leq X \leq s$$



Consider the lateral distance of the target  $X$  as having a uniform distribution between 0 and  $s$ .  $P(s)$  is the average of  $P(X, s)$  over all values of  $X$  in the interval. The expected or average value of the probability of detection for a given  $s$  can be expressed as a function of  $s$ .

$$(6) \quad P(s) = \int_0^s P(X, s) \frac{1}{s} dx = \frac{1}{s} \int_0^s (1 - \exp[-\phi(X, s)]) dx$$

This is the solution to the problem but it remains to express it more quantitatively.

The effective visibility ( $E$ ) is defined as half that sweep spacing for which the probability of detection by parallel sweeps is  $\frac{1}{2}$ ; i.e.  $P(2E) = \frac{1}{2}$ .

In the definite range law detection occurs if and only if, the target happens to be within the definite range  $R$  of either of two adjacent sweeps. The chance for this is  $\frac{2R}{s} = \frac{W}{s}$  when  $s > 2R = W$ , and unity when  $s \leq W$ . From this it follows that  $E = W$  (-since  $\frac{W}{s} = .5$ ;  $\frac{W}{2E} = .5$ ;  $W = E$ ).

For the inverse cube law when  $h \ll r$  we get from equation (3):

$$F(X) = \frac{2 h k}{W X^2}; \text{ and from equation (5): } \phi(X, s) = \frac{2 h k}{W}$$

This can be restated as  $\phi(X, s) = \frac{2 k h}{W} \frac{\pi^2}{s^2} \csc^2 \frac{2\pi X}{s}$  because of the

following development:

- a. The infinite product expression for  $\sin z$  is

$$\sin z = z \prod_{n=1}^{\infty} \left(1 - \frac{z^2}{n^2 \pi^2}\right)$$

- b. Take  $\ln$  of each side -

$$\ln \sin z = \ln z + \sum_{n=1}^{\infty} \ln \left(1 - \frac{z^2}{n^2 \pi^2}\right)$$





c. Differentiate both sides -

$$\frac{\cos z}{\sin z} = \frac{1}{z} + \sum_{n=1}^{\infty} \left(1 - \frac{z^2}{n^2 \pi^2}\right)^{-1} \left(-\frac{2z}{n^2 \pi^2}\right)$$

d. Which may be rewritten:

$$\cot z = \frac{1}{z} - \sum_{n=1}^{\infty} \frac{2z}{(n^2 \pi^2 - z^2)}$$

Note: This is the Fourier expression for  $\cot z$  and could have been used as the starting point of this development.

e. Break up d. and solve for A and B by partial fractions:

$$\cot z = \frac{1}{z} - \sum_{n=1}^{\infty} \left( \frac{A}{n\pi - z} + \frac{B}{n\pi + z} \right)$$

From partial fractions =

$$A(n\pi + z) + B(n\pi - z) = 2z$$

$$Az - Bz = 2z$$

$$A = 2 + B$$

$$An\pi + Bn\pi = 0$$

$$2 + B + B = 0$$

$$\therefore \begin{aligned} B &= -1 \\ A &= 2 + B = 1 \end{aligned}$$

$$(7) \cot z = \frac{1}{z} - \sum_{n=1}^{\infty} \left( \frac{1}{n\pi - z} - \frac{1}{n\pi + z} \right)$$

$$(8) \cot z = \frac{1}{z} + \sum_{\substack{n=-\infty \\ n \neq 0}}^{\infty} \frac{1}{z - n\pi}$$

$$(9) \cot z = \sum_{n=-\infty}^{\infty} \frac{1}{z - n\pi}$$

The only way to see the above steps is to substitute values for  $n$  in (7) and see that you get two terms for each  $n$  which can be represented by the expanded limits of the expression in (8). Note also that when  $n = 0$  in (8) the missing term is  $\frac{1}{z}$  which has thoughtfully been provided.

f. Differentiate (9):



$$(10) \quad \csc^2 z = \sum_{n=-\infty}^{\infty} \frac{1}{(z - n\pi)^2}$$

g. Let  $z = \frac{\pi x}{s}$  and rearrange (10)

$$\frac{\pi^2}{s^2} \csc^2 z = \sum_{n=-\infty}^{\infty} \frac{1}{(x - ns)^2}$$

$$(11) \text{ Then } \phi(x, s) = \frac{2\hbar k}{\omega} \sum_{n=-\infty}^{\infty} \frac{1}{(x - ns)^2} = \frac{2\hbar k}{\omega} \frac{\pi^2}{s^2} \csc^2 \frac{\pi x}{s}$$

Inserting this in (6):

$$P(s) = \frac{1}{s} \int_0^s \left[ 1 - \exp\left(-\frac{2\hbar k}{\omega} \frac{\pi^2}{s^2} \csc^2 \frac{\pi x}{s}\right) \right] dx$$

There is one more bit of wizardry which Koopman applies:

$$\text{Let } B = \frac{2\hbar k \pi^2}{\omega s^2}; \quad \theta = \frac{\pi x}{s}; \quad d\theta = \frac{\pi}{s} dx$$

$$\phi(B) = P(s) = \frac{1}{s} 2 \int_0^{\frac{\pi}{2}} \left[ 1 - \exp(-B \csc^2 \theta) \right] \frac{s}{\pi} d\theta$$

Differentiate with respect to B

$$\begin{aligned} \phi'(B) &= \frac{2}{\pi} \int_0^{\frac{\pi}{2}} \csc^2 \theta \exp(-B \csc^2 \theta) d\theta \\ &= \frac{2}{\pi} \int_{-\infty}^0 \exp(-B) \exp(-B \cot^2 \theta) \csc^2 \theta d\theta \end{aligned}$$

$$\csc^2 \theta d\theta = -d(\cot \theta)$$

$$\text{when } \theta = 0, \cot \theta = \infty$$

$$\theta = \frac{\pi}{2}, \cot \theta = 0$$

$$\text{Let } \cot^2 \theta = x^2$$

$$d \cot \theta = dx$$

$$\begin{aligned} \phi'(B) &= -\frac{2}{\pi} \exp(-B) \int_{-\infty}^0 \exp(-B x^2) dx \\ &= \frac{2}{\pi} \exp(-B) \frac{1}{2} \left( \frac{\pi}{B} \right)^{1/2} = \frac{\exp(-B)}{(B\pi)^{1/2}} \end{aligned}$$

Integrate  $\phi'(B)$  with respect to (B) from 0 to  $B^1$  (a particular value of B)



$$\text{Let } X^2 = B$$

$$2 X dx = dB$$

$$X = B^{\frac{1}{2}}$$

$$\text{when } B = 0 \quad X = 0;$$

$$\text{when } B = B^1, \quad X = (B^1)^{\frac{1}{2}}$$

$$\phi(B) = \int_0^{B^1} \frac{\exp(-B)}{(B\pi)^{\frac{1}{2}}} dB = \frac{1}{(\pi)^{\frac{1}{2}}} \int_0^{(B^1)^{\frac{1}{2}}} \frac{\exp(-x^2)}{x} \cdot 2x dx$$

$$(12) \quad \phi(B) = \frac{2}{(\pi)^{\frac{1}{2}}} \int_0^X \exp(-x^2) dx$$

$$(B^1)^{\frac{1}{2}} = X^1 = \text{a particular value of } X.$$

By definition (12) is the error function (erf) based on the normal distribution.

$$\text{Hence } P(S) = \phi(B) = \text{erf } (B)^{\frac{1}{2}} = \text{erf } \frac{\pi}{s} \left( \frac{2kh}{W} \right)^{\frac{1}{2}}$$

$$\text{For the inverse cube law the effective sweep width } W = 2 \left( \frac{2kh}{W} \right)^{\frac{1}{2}}$$

$$(13) \quad P(s) = \text{erf } \frac{W}{s} \left( \frac{\pi}{2} \right)^{\frac{1}{2}}$$

$$P(2E) = \frac{1}{2} = \text{erf } \frac{(\pi)^{\frac{1}{2}} W}{4E}$$

$$\text{Since } \text{erf } 0.477 = 0.5, \text{ then } \frac{(\pi)^{\frac{1}{2}} W}{4E} = .477$$

$$\text{and } W = 1.076E, \quad \frac{hk}{W} = .046E^2$$

Substituting this in (13)

$$P(s) = \text{erf } \left( 0.954 \frac{E}{s} \right)$$

It is of particular interest at this time to note that the probability of detection is not particularly sensitive to the law by which the spacing (s) is determined - particularly at lower probabilities.



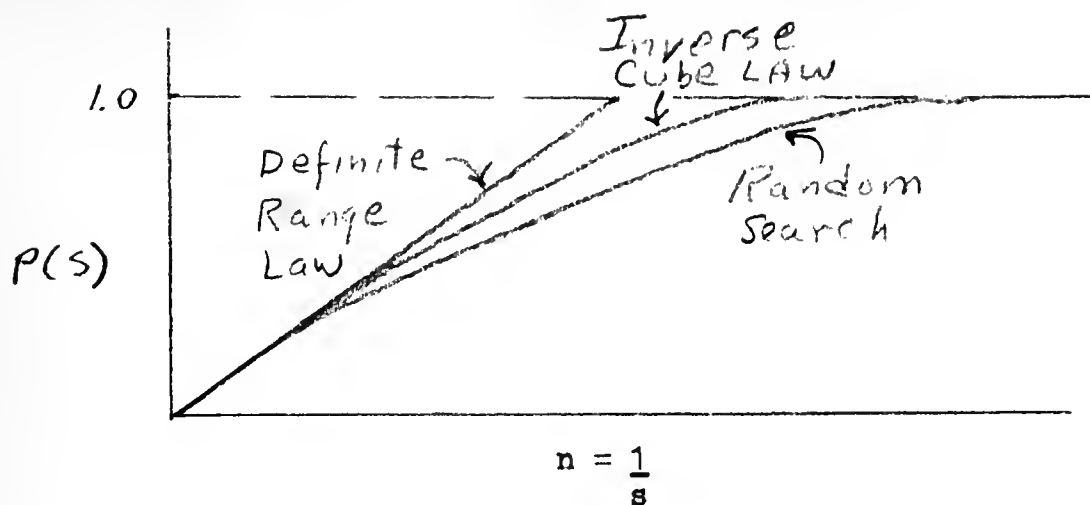


Fig. 12 Probabilities with parallel sweeps.

Recall the following equations:

$p(X) = 1 - \exp[-F(X)]$  for lateral range distribution;

$$(14) \quad p(X) = 1 - \exp\left[-\frac{2hk}{W^2 X^2}\right] \text{ for inverse cube law;}$$

$W = 1.076E$  from the error function development;

$$(15) \quad \frac{hk}{W^2} = 0.046E^2 \text{ from the error function development}$$

Substituting (15) into (14):

$$P(X) = 1 - \exp\left[-0.092\left(\frac{E}{X}\right)^2\right]$$

Which is equation (1), the immediate object of the above expansions.

Before proceeding, let us review the principal assumptions upon which the "error function" development is based.

a. Target at rest in an unknown position with lateral distribution UNIFORM between sweeps.

b. Observer is on a straight course at a constant speed for a "long" time before and after the closest point of approach to the target. (Sweep is "relatively infinite").

c. Inverse cube law of sighting applies and  $h \ll r$ . ("h" is the vertical height of the observer and "r" is the horizontal distance from





observer to center of the target.)

d. Sweeps are independent.

B. SPACING (S).

Consider the SQUARE OF UNIFORM COVERAGE search pattern (section 7.3.2 of reference 2).

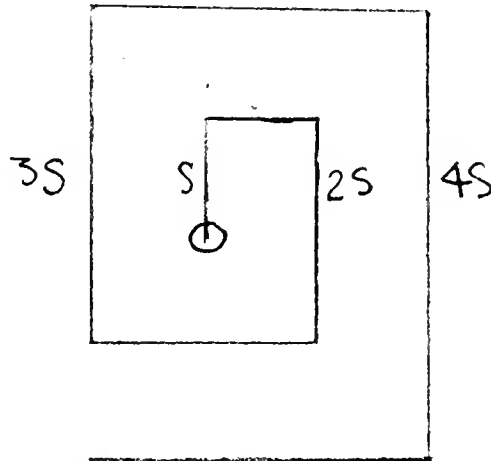


Fig. 13 Square of Uniform Coverage.

Let the normal density function

$$(16) f(x, y) = f(r) = \frac{1}{2\pi\sigma^2} \exp\left(-\frac{r^2}{2\sigma^2}\right)$$

represent the probability that the target at the time of the fix be in the small region  $dx dy$  at the point  $(x, y)$ , a distance of  $r$  from the origin and where  $\sigma$  is the standard deviation of fix accuracy. The first problem is to find a spacing so that on the initial square, the probability of detection per unit time shall be a maximum.

As was indicated before, the spacing is not sensitive to the law of detection, and the inverse cube law development will be followed so that the probability of detection of a target of lateral range  $x$  from a straight aircraft track is

$$(17) p(x) = 1 - \exp\left[-0.092\left(\frac{E}{x}\right)^2\right]$$



Reflect for a moment on our problem and the assumptions of the previous section. The same error function result is being used.

1. The lateral distribution is certainly no longer uniform between sweeps; however when the standard deviation is large compared to the spacing the approximation of uniformity between sweeps is not very inaccurate.

2. The sweeps are not "infinite" in any one given direction, but except in the center the length of sweep is relatively large, and again the practical approximation is acceptable.

3. The inverse cube law is assumed in the development with  $h \ll r$ . First of all, as already stated, the spacing is not sensitive to the law. Caution must be used in proceeding, however, because although the distance to the center of the detected configuration can normally be expected to be greater than the height of the aircraft, in the case of an extremely weak source approaching the minimum detection capability of the meter - when directly over the pool - the range to the center would be less than the height and the probability of detection would be overestimated. The instantaneous probability (s) would equal  $\frac{k h}{(h^2 + r^2)^{3/2}}$  vice  $\frac{k h}{r^3}$  and the error would increase as the ratio of height to horizontal distance increased.

4. Sweeps are still considered independent.

The probability of the target lying on the strip parallel to the y axis between x and x + dx is found by integrating equation (16) over all values of y and obtaining the marginal:

$$(18) \quad dx \int_{-\infty}^{\infty} f(x, y) dy = \frac{1}{\sigma(2\pi)^{1/2}} \exp\left(-\frac{x^2}{2\sigma^2}\right) dx$$

The peak of the distribution is located at the center. If an



indefinite straight flight is made along the y axis and has failed to detect the target the distribution is altered and the differential coefficient of (18) no longer represents the lateral density of the targets. By Bayes theorem the "a posteriori" probability considers the "a priori" probability of (18) above and the "productive" probability of not detecting the target on a sweep through the center:

$$1 - p(x) = \exp \left[ -0.092 \left( \frac{E}{x} \right)^2 \right] \quad (\text{See equation (17)})$$

Bayes Theorem states:

Let the union of events  $B_1$  be the sample space where  $B_1$  ( $i = 1, 2, \dots, k$ ) are mutually exclusive and exhaustive.

Let event C also be defined on the same sample space

$$P(B_j|C) = \frac{P(C|B_j) P(B_j)}{\sum_{i=1}^k P(C|B_i) P(B_i)}$$

In our problem let:

C = not detecting target

$B_j$  = target located in strip  $(x, x+dx)$

The denominator of Bayes theorem can be expressed in the continuous case as

$$\int_{-\infty}^{\infty} P(C|y) f(y) dy \quad \text{where } y \text{ represents any strip.}$$

This integral is just a number, say K, which actually normalizes the numerator so that instead of speaking of the probability of the event  $B_j$  given event C we speak of the density function

$$f_2(x) = g(B_j|C) = \frac{P(C|B_j) f(B_j)}{K}$$

- so that the new density function is proportional to  $P(C|B_j)f(B_j)$  and this translates to



$$(19) \quad \frac{[1 - P(x)]}{K} f(x) = k' \exp \left[ -\frac{x^2}{2\sigma^2} - 0.072 \left( \frac{E}{x} \right)^2 \right]$$

In words - the probability of not detecting the target given that it is in a strip  $(x, x+dx)$  times the probability that it is in a strip  $(x, x+dx)$  is proportional to the new density of the probability that the target is in a strip  $(x, x+dx)$  given that it was not located on the first sweep.

To find the maximum of the new distribution differentiate (19) and solve for the  $x$  which makes the expression zero.

$$-\frac{2x}{2\sigma^2} + \frac{2(0.072)E^2}{x^3} = 0$$

$$x = \pm 0.655 (E\sigma)^{1/2}$$

So the maximum probability target position is no longer humped at zero. Double peaks now occur with a depression at the origin. However the distribution is skewed, and the distance between the first and second tracks,  $D$ , should be slightly greater than  $.65(E\sigma)^{1/2}$  to cover a larger volume of probability on the second sweep.

The probability of not detecting on the second sweep given that the target is in a strip  $(x, x+dx)$  times the probability that it is in a strip  $(x, x+dx)$  is proportional to the new density of the probability that the target is in a strip  $(x, x+dx)$  given that it was not located on the second sweep. This follows from the same reasoning used in equation (19)

$$f_2(x) dx \approx \exp \left[ -\frac{x^2}{2\sigma^2} - 0.072 \frac{E^2}{x^2} - \frac{0.072 E^2}{(x-D)^2} \right] dx$$

Integrating this function for all  $x$  and solving for a  $D$  which would minimize the remaining function we would be maximizing the probability of detection on the second pass. Koopman presents the solution, arrived at by numerical integration, in section 7.3.2 of SEARCH AND SCREENING /2/





as  $0.75(E\sigma)^{\frac{1}{2}}$ . This spacing is then used for searching about a point of fix.

### C. Search Patterns

1. Square search for a stationary target ("Square of Uniform Coverage").

The details of the theory are described very explicitly in SEARCH AND SCREENING /2/. This search assumes a circular distribution of target position as a result of a probabilistic fix. This pattern attempts to give a high probability of detection per unit time at the beginning of the search when covering the area where the target is most likely to be.

2. Retiring square search for a moving target (Section 7.3.3 of SEARCH AND SCREENING /2/).

In this development it is assumed that the direction of movement is not known but uniformly distributed (i.e., equally likely in any direction), while the speed of movement is reasonably well established.

The theory is to search the peak of the distribution at the time of arrival. It has moved outward from the fix a radius of  $Ut$  where  $U$  is the speed of target movement and  $t$  is time late. During the search the target continues to move and the pattern is to search the peak, then outside, then inside, then outside, ... etc. This will give the maximum probability of detection per unit time of search effort.

It is recognized that both of these patterns present operational problems in implementing. Expanding searches are always frowned upon because of the navigational difficulty in making legs precise. This is particularly true when spacing is small - less than 5 miles.



## APPENDIX III

### SEARCH WIDTH

USNRDL Technical Report 525 /1/ envisions an airborne detection instrument capable of sensing radioactive surface activity on the sea when the intensity at the meter is 0.2 microroentgens/hr. At a search height of 500 feet the intensity of a broad source at the surface would have to be 0.74 microroentgens per hour. The meter envisioned would be collimated about a central angle of  $150^\circ$  to reduce cosmic interference.

A. For determination of the effective search width consider the following model:

1. Physical parameters:

- a. Search height - 500 feet.
- b. Meter described above (i.e., shielded around arc of  $150^\circ$ , and capable of detecting 0.2 micror/hr).
- c. Minimum surface intensity present - 0.74 micror/hr.
- d. Meter system time constant about 2 seconds. (The technical report anticipates 0.2 sec for the meter and it is presumed that a recorder, alarm and other auxiliary equipment would make system time constant an order of magnitude greater).

2. Assumptions:

- a. Surface pool of radiation is circular and of uniform intensity.
- b. The radiation on the surface ends abruptly at a definite boundary.
- c. Definite Range Law of detection obtains ( $W = E$ ).

Due to the geometry the meter will see a circular area about 0.613 miles in diameter (See Fig. 14).



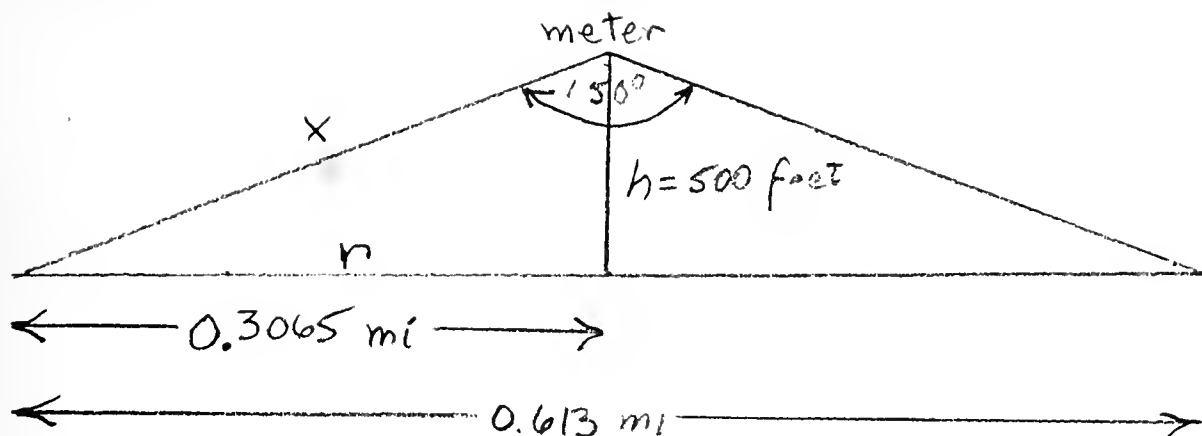


Fig. 14 Meter geometry (side view).

If a circular area of 0.74 micro-r/hr intensity and 0.613 miles diameter were present in the search area, the effective visibility ( $E$ ) would be zero since the plane would have to fly directly over the center in order to detect it.

If the pool were larger, the search width could be considered as the diameter of the pool minus the meter visibility (0.613 miles).

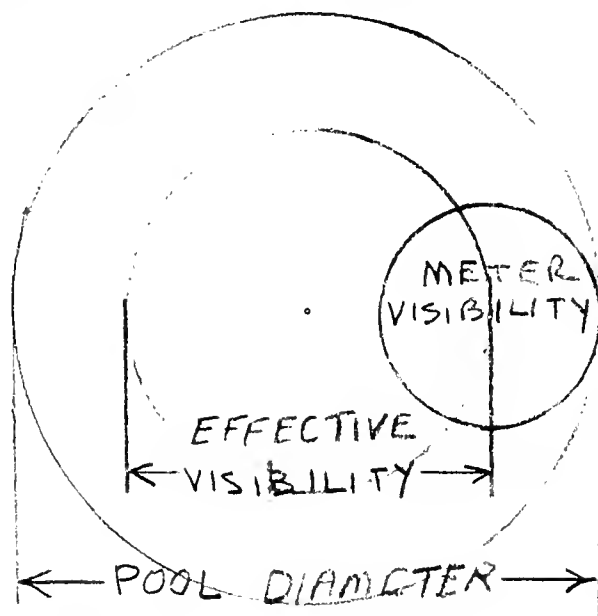


Fig. 15 Surface geometry.

Another consideration in determining the effective visibility ( $E$ ) is the meter system response time. In the USNRDL report /1/ the following standard formula is provided.



$$(1) \quad S = S_0(1 - \exp[-t/T])$$

where S = meter indication

$S_o$  = source strength

t = time over source

$T$  = system time constant

Neglecting attenuation and build-up, if the meter were over the source for ten seconds the meter would indicate over 99% of the source strength.

For an aircraft traveling at 180 knots the meter would have to be over the source for 0.5 miles. This cuts down the effective diameter another 0.1 miles for a pool of two miles diameter and a lesser amount for larger pools.

$$OB = (\overline{OA}^2 - \overline{AB}^2)^{\frac{1}{2}}$$

$$OB = 0.646 \text{ mi}$$

$$EB = 1.292$$

$$OF = 1 \text{ mi}$$

$$AC = 0.5 \text{ m}$$

$$AF = 0.3065 \text{ mi}$$

$$OA = 0.6935 \text{ mi}$$

C = First meter indication

A = Last meter indication

CA = Time meter registers  
over pool (10 sec =  $\frac{1}{2}$  mi)

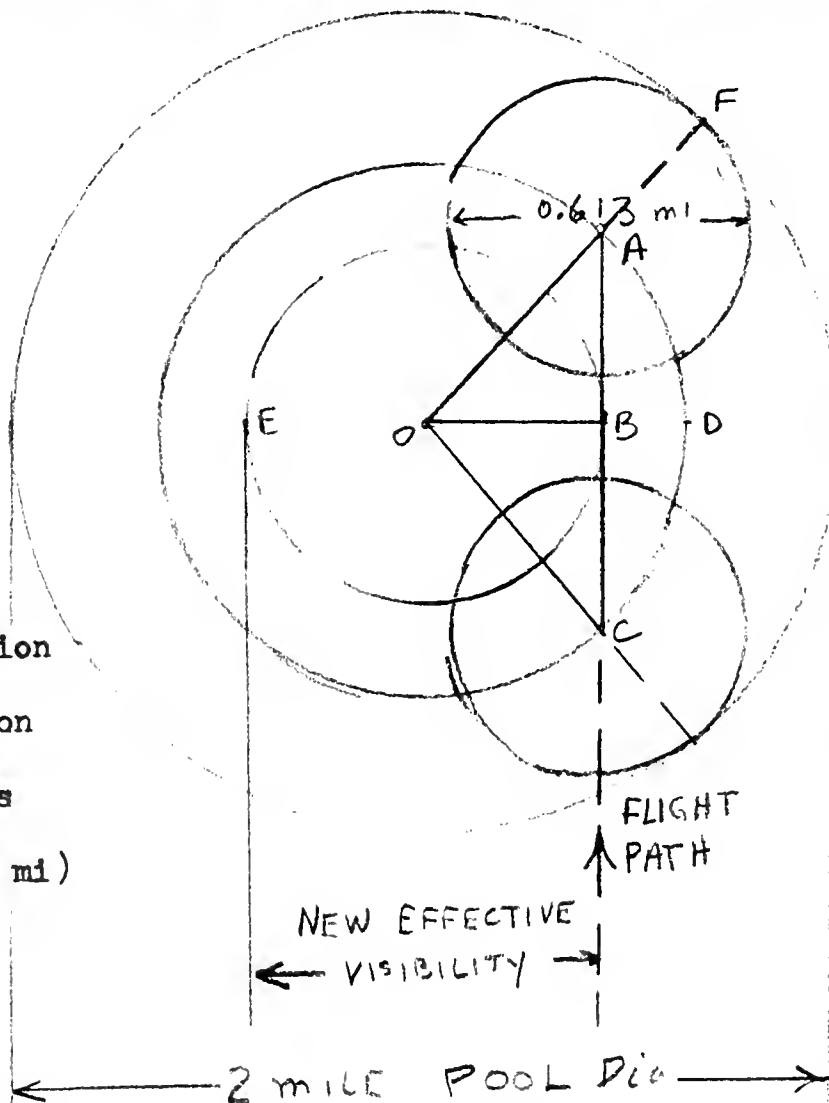


Fig. 16 System time constant effect.





For this problem a correction of -0.7 miles is made to pool diameter to obtain effective visibility.

Since the size of the pool is an unknown in the search several sizes will be looked at to determine sensitivity.

For a search of a stationary object using a Square of Uniform Coverage pattern assume a fix error (2 standard deviations) to be 50 miles and an error in navigation of 10 miles in locating point of fix. The total deviation would be 25.5 miles. For simplicity we will adopt the following expression for the probability of detection:

$$(2) \quad p = 1 - \left(1 + \frac{nW}{S}\right) \exp \left[ -\frac{nW}{S} \right] \quad (\text{See Koopman /2/ pg 113 and 114})$$

$n$  = # passes over area;  $W$  = search width =  $E$ ;  $S$  = spacing.

(miles) Pool Dia	$E=W$ Effect. Visibility(mi)	$3/4(E \text{ StdDev})^{1/2} =$ Spacing (miles)	$\frac{W}{S}$	Prob. of detection		
				n=1	n=2	n=3
2	1.3	4.31	.302	.024	.121	.23
4	3.3	6.86	.481	.085	.25	.42
6	5.3	8.7	.609	.125	.344	.545
8	7.3	10.2	.715	.14	.416	.632
10	9.3	11.5	.809	.193	.479	.698
20	19.3	16.6	1.16	.321	.673	.857
30	29.3	20.4	1.435	.42	.752	.928

TABLE 4. Uniform square coverage probabilities.

Since it is unlikely that data are available for such small intensities (0.74 micro r/hr), it is desirable to consider intensities that are more likely to be recorded and scale effects from available search data.

Consider a circular pool of higher intensity, say 0.05 r/hr. If the attenuating distance of two configurations were equal, then for each to



induce the same intensity at the meter, the product of each area and surface intensity must equal the same product of the others.

$$(3) \quad I_1 A_1 = I_2 A_2$$

$$0.74 \times 10^{-6} \pi (0.3065)^2 = .05 A_2$$

$$A_2 = 4.375 \times 10^{-6} \text{ sq mi}$$

$I_1$  = Minimum detectable surface  
intensity when spread  
uniformly over  $A_1$

$I_2$  = Uniform intensity of new  
configuration

$A_2$  = Area of new configuration

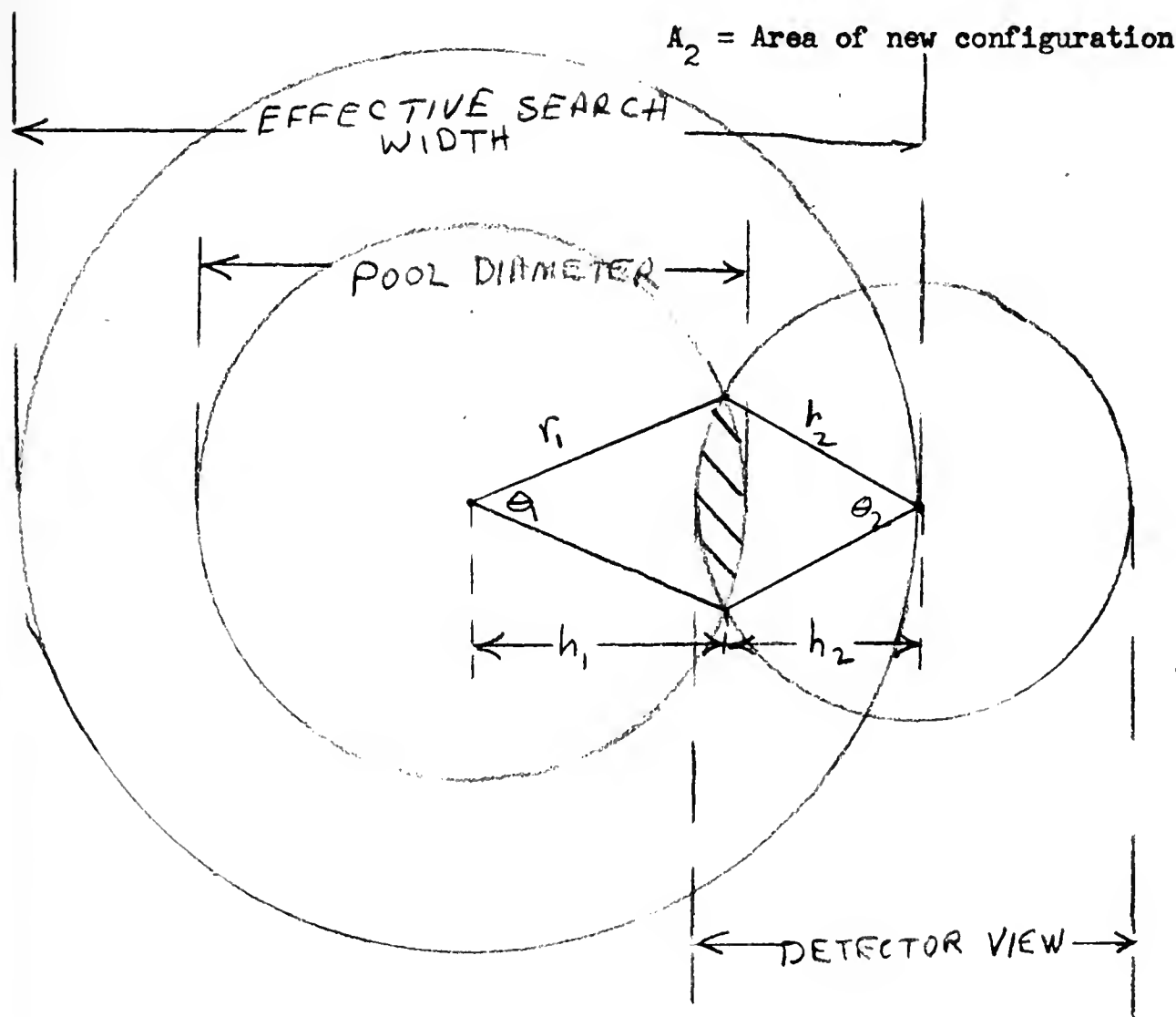
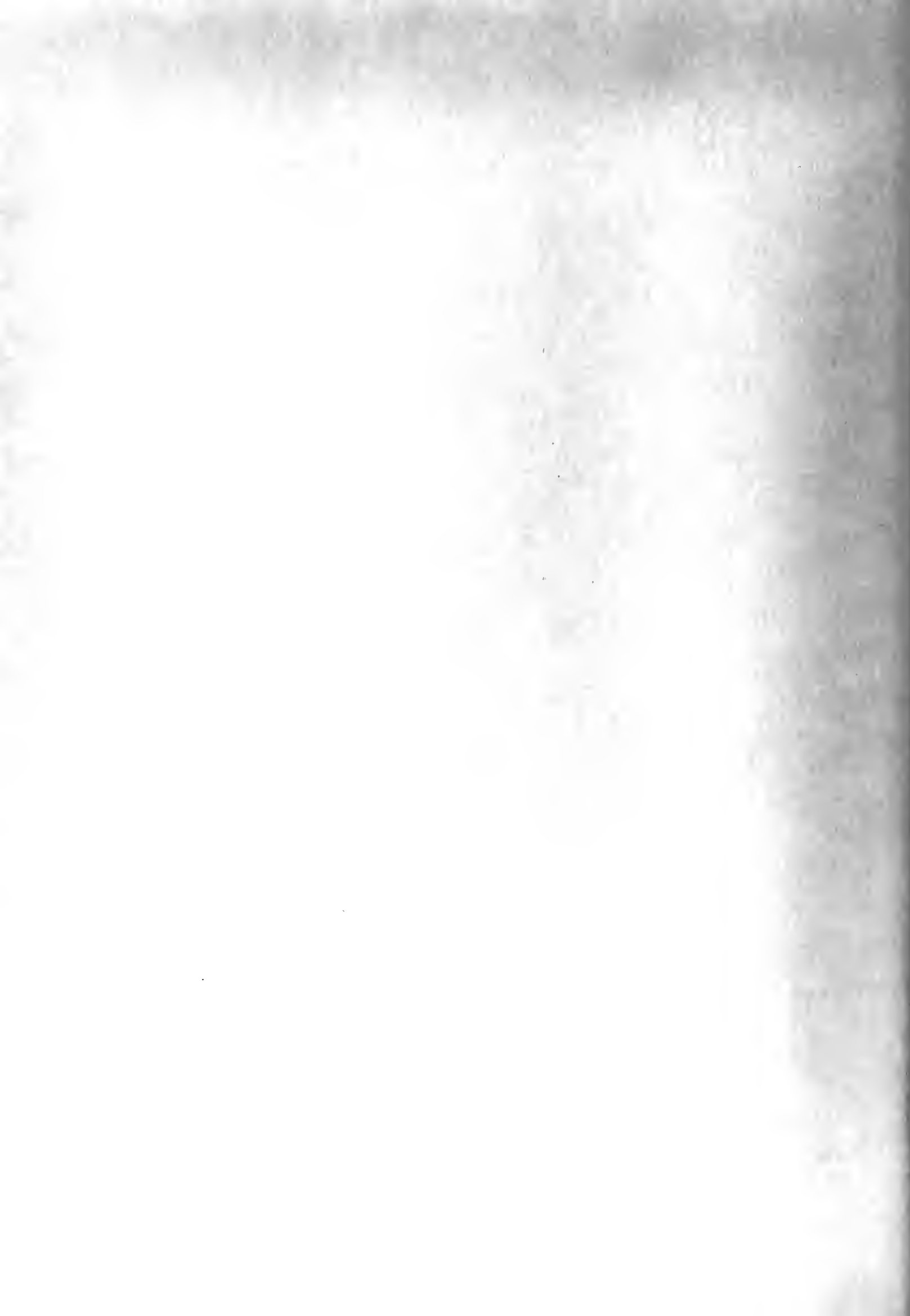


Fig. 17 Geometry of detector view of high intensities.

Area of radiation in view of detector is the sum of the segments:

$$(4) \quad A = \frac{1}{2} r_1^2 (\theta_1 - \sin \theta_1) + \frac{1}{2} r_2^2 (\theta_2 - \sin \theta_2)$$



(5) Common chord yields:  $\frac{r_1}{r_2} = \frac{\sin \frac{\theta_2}{2}}{\sin \frac{\theta_1}{2}}$

The effective search width =  $2(r_1 + h_2 - (r_1 - h_1))$   
 $= 2(h_1 + h_2)$

$h_1 = r_1 \cos \frac{\theta_1}{2} ; h_2 = r_2 \cos \frac{\theta_2}{2}$

(6)  $W = E = 2(r_1 \cos \frac{\theta_1}{2} + r_2 \cos \frac{\theta_2}{2})$

From (4):

(7)  $\frac{2A}{r_2^2} - \frac{r_1^2}{r_2^2} (\theta_1 - \sin \theta_1) = (\theta_2 - \sin \theta_2)$

From (5):  $\frac{r_1}{r_2} \sin \frac{\theta_1}{2} = \sin \frac{\theta_2}{2}$

(8)  $\frac{r_1^2}{r_2^2} (1 - \cos \theta_1) = (1 - \cos \theta_2)$

Equations (7) and (8) are transcendental and can be solved graphically.

miles Pool radius	From equation (7) radians		From equation (8) radians	
	$\theta_1$	$\theta_2$	$\theta_1$	$\theta_2$
ALL	0	.082	0	0
.5			.005	.008
1				.016
2				.033
3				.049
4	.005	.081		.065
5	.005	.080		.081
10	.005	.075		.163
.5			.01	.015
1			.01	.032
2	.01	.08	.01	.066
3	.01	.077	.01	.097
4	.01	.073	.01	.130
5	.01	.066	.01	.162
10	.01	0	.01	.327
.5				
1				
2	.015	.0745		
3	.015	.062		
4	.015	0		
5				
10				

(Cont'd next page)



Pool radius	From equation (7)		From equation (8)	
	$\theta_1$	$\theta_2$	$\theta_1$	$\theta_2$
2	.02	.06		
3	.02	0		
2	.025	0		
.5	.03	.079		
1	.03	.065		
.5	.035	.076		
1	.035	.047		
.5	.04	.072		
1	.04	0		
.5	.05	.06		
.5	.06	0		

TABLE 5. Data for graphical solution to transcendental equations.

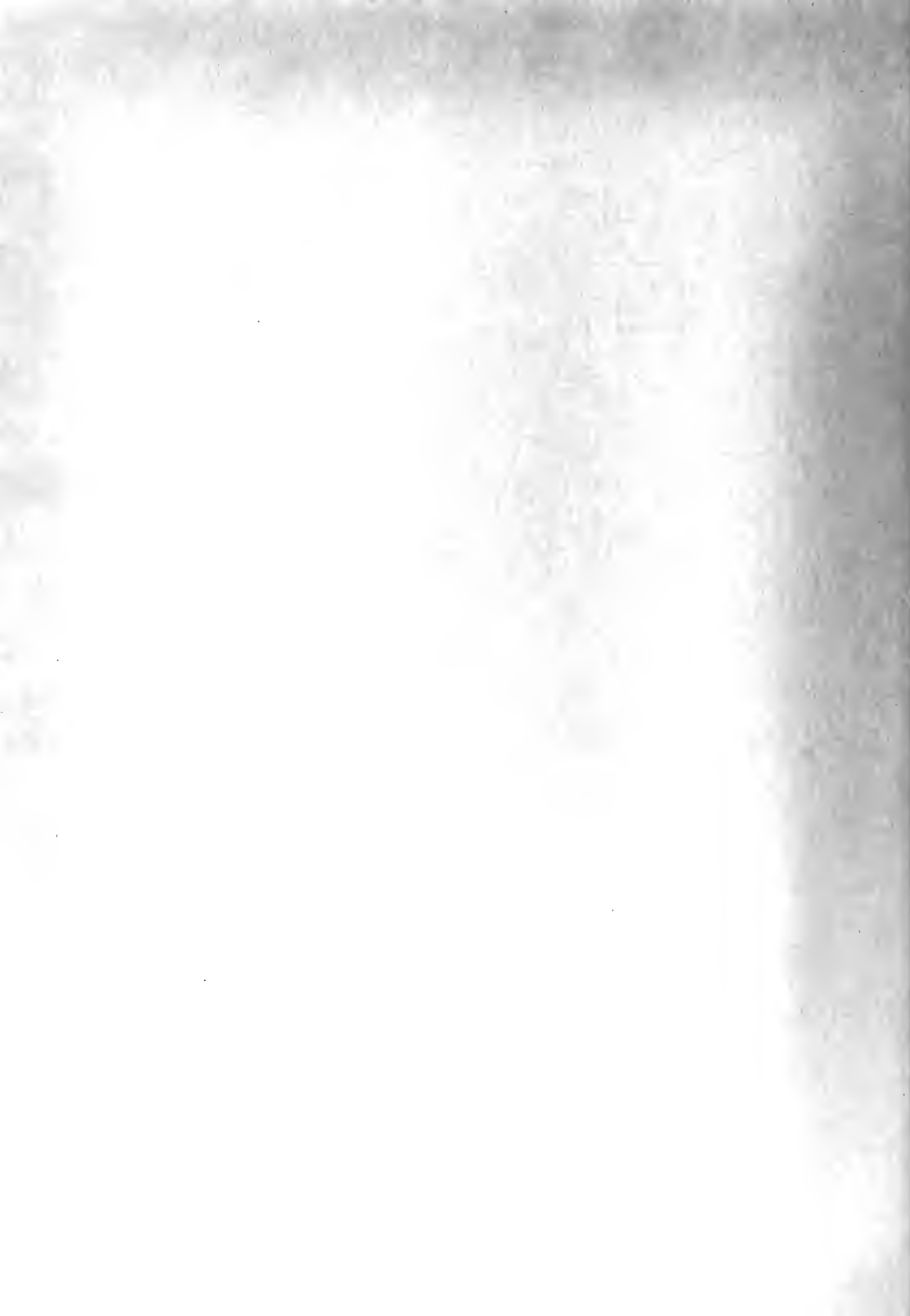




Fig. 18. GRAPHIC SOLUTIONS FOR EQUATIONS (7) AND (8)

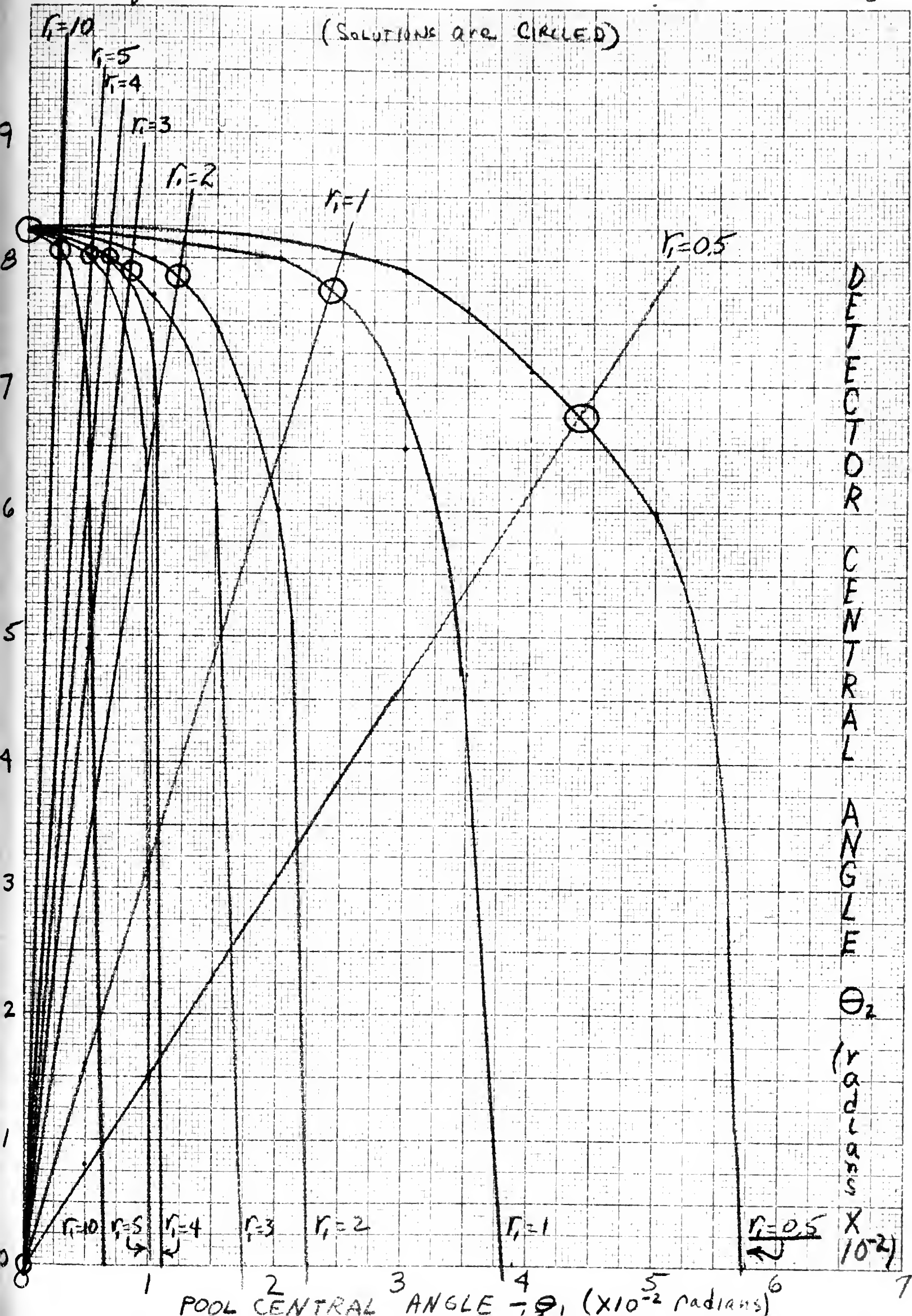




Fig. 18 is a plot of these curves. The points of intersection yield the solution for  $\theta_1$ ,  $\theta_2$  for various pool sizes.

Note the limiting case in which the pool is so large that the arc approaches the chord of the detector's circle. In this situation all of the area is described by the segment of the detector's circle.

$$A = \frac{1}{2} r_2^2 (\theta_2 - \sin \theta_2)$$

$$\theta_2 = 0.082 \text{ radians.}$$

The solutions for  $\theta_2$  range from .0675 radians ( $3^{\circ}51'$ ) for  $\frac{1}{2}$  mile radius pool to 0.082 radians ( $4^{\circ}42'$ ) for an infinite pool. With these figures and for the pools under consideration the effective search width varies from

2(pool radius + .306 mi) for large pools to

2(0.5 + .306) for the half mile radius pool.

Therefore the search width is increased by the diameter of the detector "look" at the surface (approximately) regardless of pool size.

Remember that a specific example of a pool of 0.05 r/hr with the detector at 500 feet altitude is the case under consideration.

There is one very unrealistic assumption in the above discussion.

The intensity at the meter is not just proportional to the area. The distance of the meter from the source is of principal concern when considering attenuation. Ignoring the build-up factor the interrelationship is as follows:

$$\int_{A_1} \frac{I_1 A_m h \exp[-ux] r dr d\theta}{4\pi x^3} = \int_{A_2} \frac{I_2 A_m h \exp[-ux] r dr d\theta}{4\pi x^3}$$

$A_m = \text{area of meter}$

$$(9) \quad .2 \text{ micro r/hr} = \int_{A_2} \frac{.05 h \exp(-ux) r dr d\theta}{4\pi x^3}$$



(The effect of the Barometer equation is considered negligible - see Appendix I)

Equation (9) would be solved numerically for  $A_2$  or more meaningfully for the  $I_2$  required in the pool to register at the meter.

A rough approximation for the effect of the different distances of the source from the meter can be obtained by comparing the intensity of a particle at the average distance of each configuration.

The average distance to the particle in the case of the circle of minimum intensity is

$$\frac{\int_0^{0.3065} \int_0^{2\pi} x r dr d\theta}{\iint r dr d\theta} = \frac{\int_0^{0.3065} \int_0^{2\pi} (r^2 + h^2)^{1/2} r dr d\theta}{\pi r^2}$$

(For circle)  $\bar{X}_1 = 0.223$

In the case of the segment the average distance is:

$$\bar{X}_2 = .3178$$

Let  $I_1$  = meter intensity for circle of minimum intensity

$I_2$  = meter intensity for segment

$I_{10}$  = surface intensity for circle

$I_{20}$  = surface intensity for segment

$$I = \frac{I_0 A h \exp(-u x)}{4\pi x^3} \text{ for point source.}$$

$$\frac{I_1}{I_2} = \frac{I_{10} A_m h \exp(-u \bar{X}_1) 4\pi \bar{X}_2^3}{I_{20} A_m h \exp(-u \bar{X}_2) 4\pi \bar{X}_1^3} = \frac{I_{10} 0.032 \exp(-12.8(-.0942))}{I_{20} 0.0111}$$

For

$$I_1 = I_2$$

$$0.347(0.27) = \frac{I_{10}}{I_{20}} ; I_{20} = 10.65 I_{10}$$

In order for the meter intensity to be the threshold intensity in the case of both patterns, the surface intensity of the segment would have to be 10.65 the intensity of the circular configuration to compensate for the different mean distances.



In the previous scaling discussion the characteristics deduced would pertain to a surface intensity of 0.5 r/hr vice 0.05 r/hr.

The following table will assist in scaling:

Altitude = 500 ft;  $\bar{X}_1 = .223$ ;  $u = 13.788/\text{mi}$ .

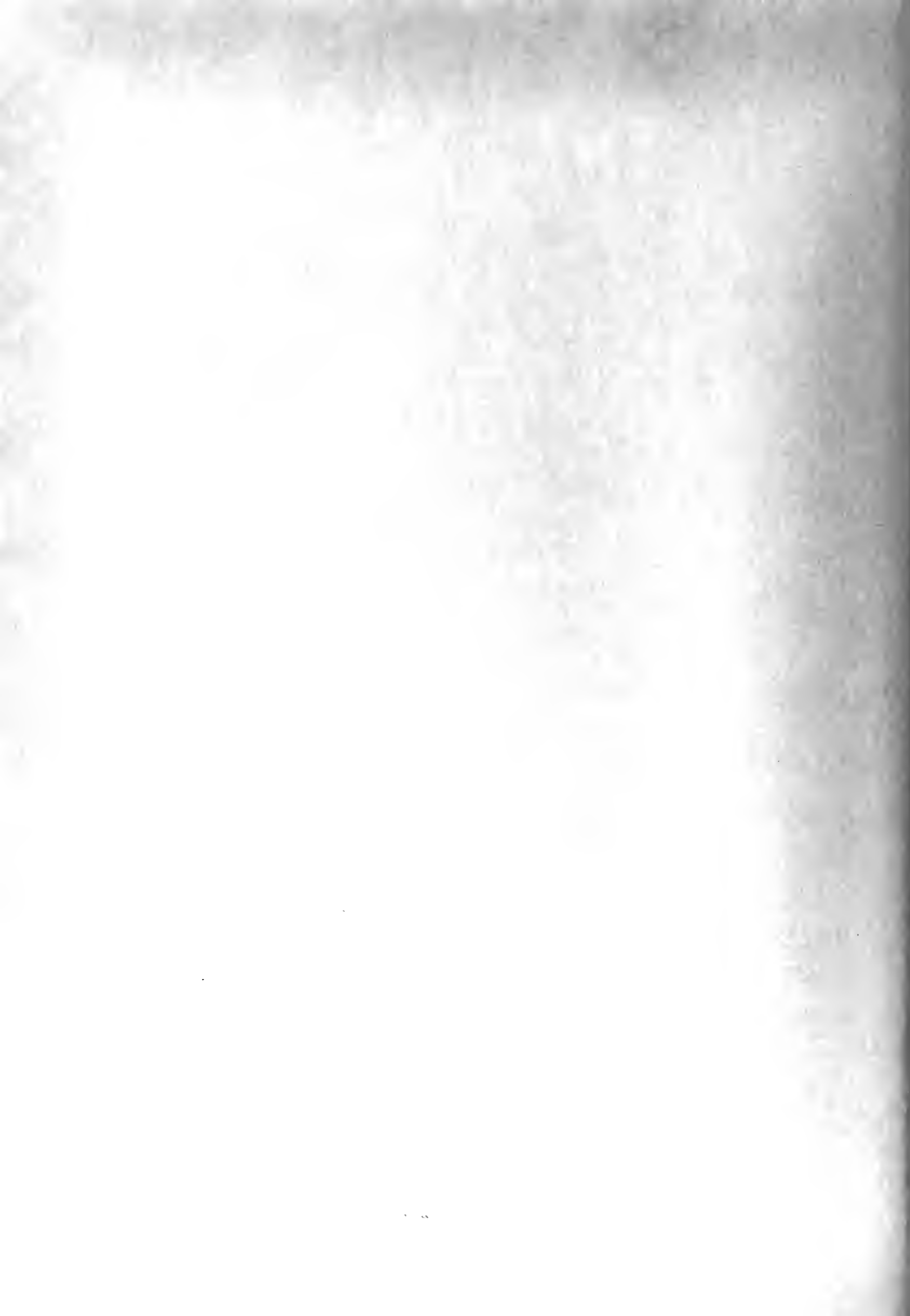
$I_{10}(\text{r/hr})$	$A_2(\text{mi}^2)$	Limiting $\theta_2^\circ$	$h_2(\text{mi})$	$\bar{X}_2(\text{mi})$	$I_{20}/I_{10}$	$I_{20}$	$W(\text{mi}) =$ Pool Size plus $(h_2+r_2)$
.5	$4.375 \times 10^{-7}$	2.18	.3064	.3175	10.6	5	.6129
.05	$4.375 \times 10^{-6}$	4.7	.3063	.3175	10.6	.5	.6128
.005	$4.375 \times 10^{-5}$	10.14	.3057	.3167	10.4	.05	.6122
.0005	$4.375 \times 10^{-4}$	21.94	.3015	.314	9.8	.005	.608
.00005	$4.375 \times 10^{-3}$	47.73	.2805	.311	9.1	.0005	.587
.000005	$4.375 \times 10^{-2}$	107.72	.1809	.235	1.4	.00005	.487

If search altitude is 1000 feet the following table can be used:

$$\bar{X}_1 = .446$$

$I_{10}(\text{r/hr})$	$A_2(\text{mi}^2)$	Limiting $\theta_2^\circ$	$h_2(\text{mi})$	$\bar{X}_2(\text{mi})$	$I_{20}/I_{10}$	$I_{20}$	$W(\text{mi}) =$ Pool +
.05	$1.003 \times 10^{-3}$	10.5	.6101	.635	39	1.95	1.22
.005	$1.003 \times 10^{-2}$	22.5	.6001	.628	34.6	.173	1.21
.0005	$1.003 \times 10^{-1}$	48.9	.559	.599	19.9	.00995	1.17
.00005	1.003	111.2	.346	.565	10.45	.0005225	0.96

TABLE 6. Search widths for various intensities.





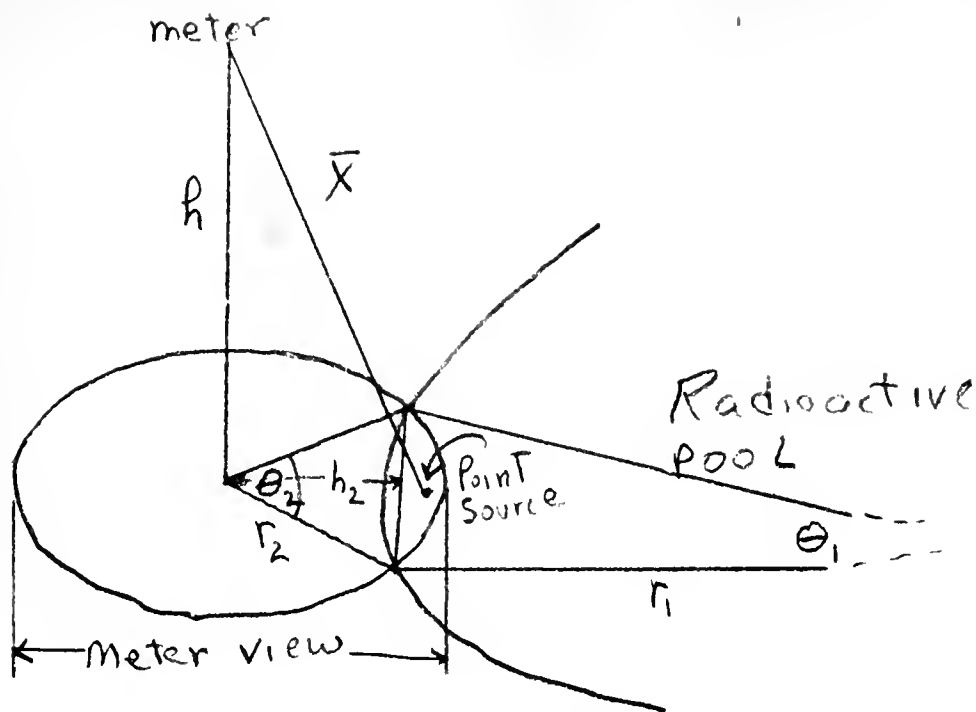


Fig. 19 Identification of symbols for previous tables.

Interpretation of above tables:

For scaling purposes use column  $I_{20}$  as the surface intensity which is known and from which it is desired to scale.

For example, if the contour of a pool of intensity .05 r/hr is known and it is desired to determine the search width, enter column  $I_{20}$  and find .05 r/hr. The search width would be the pool size plus .6122 miles when searching at 500 feet altitude or plus 1.18 miles (interpolating) for a search height of 1000 feet.

### Conclusion

The diameter of the detector view can be added to the pool diameter to obtain search width when scaling from surface radiation more than one order of magnitude larger than the minimum circular surface intensity.



## APPENDIX IV

### EFFECT OF OCEAN CURRENTS

#### A. General.

There are many contributing causes of currents, both external and internal to the water. In the deep open ocean wind is a prominent influence. Persistent winds interact with surface water, imparting up to two percent of the wind velocity to water movement. The direction of the movement is complicated, with the resultant of the "coriolis force" and layer friction balancing the actual wind imparted force.

P. H. Kuener in MARINE GEOLOGY /5/, page 29, is quoted in part:

Flow in deep water far from the coast driven by a constant wind (i.e., drift currents) at a constant speed, the motion at the surface is directed  $45^\circ$  to the right (in the northern hemisphere) of the wind. Below the surface the direction gradually diverges farther and farther to the right of the wind and concomitantly the velocity decreases. At a depth called the friction depth, which varies with the latitude and force of the wind and does not exceed 200 m, the current is directly opposite to the surface current and has fallen to 4% of the surface velocity. If bottom friction is left out of account the average movement is at right angles to the direction of the wind. The frictional force exerted by the wind and the coriolis force at right angles to the movement are then equal and exactly opposed in direction. This state is closely attained in nature. Yet there is some slight friction, and the resulting force plus the "coriolis force" is equal and opposite to the force exerted by the wind.....

When the wind just begins to blow the first movement of the water will be in the same direction as the wind, but as soon as motion of the water sets in the rotation of the earth makes itself felt. In shallow water, where the friction with the bottom is considerable, the current will be less deflected by the coriolis force than in the ideal case. In regions like the North Sea and the Baltic, where the winds are variable, where the water is shallow, and where the surrounding coasts are at no great distance wind driven currents will generally follow the direction of the motive force fairly closely.

Internal characteristics and variants create an isobaric gradient between waters. Salinity, temperature, pressure, level, etc. all have a bearing on currents; however, considering all open ocean currents, none



are stronger than the GULF STREAM which has a velocity of up to 3 knots. Most open water movements run between 0.3 and 0.7 knots, but it is very difficult to predict the direction of flow at any given location at any given time.

Bowditch /4/ states:

Current arrows on nautical charts represent average conditions and should not be considered reliable predictions of the conditions to be encountered at any given time.

## B. Analysis of Currents in Sample Ocean Areas.

### 1. Set.

Enclosed are data on current direction and speed. The first eight (8) pages (figures 20 - 27) are plots of the frequency of current directions (set) for the specified areas for the months indicated. Data were collected by the Hydrographic Office from ship reports. The number of observations upon which the graphs are based is indicated inside each curve. This figure is followed by a single number representing the percent of observations which reported no current (no set or drift). The area represented, broken into  $5^{\circ} \times 5^{\circ}$  quadrangles, is a ten degree strip of latitude ( $25^{\circ}\text{N}$  to  $35^{\circ}\text{N}$ ) across the Pacific from  $150^{\circ}\text{E}$  to  $170^{\circ}\text{W}$  longitude (about  $1\frac{1}{2}$  million square miles). Choice of the area was influenced by the large number of observations available over such a large expanse of open ocean. The months plotted were chosen arbitrarily to provide a three month period to observe gradual changes (January, February, and March) and other samples during the year to show overall variation (June and September). The source of the information is the ATLAS OF SURFACE CURRENTS /5/.

Such random behavior lends itself to a probabilistic formulation rather than a deterministic approach. However the metamorphosis of the



frequency plots precludes any distribution other than UNIFORM. This assumption is the safest one to make when generalizing for large areas and over the whole year.

A bar chart of current persistency derived from Hydrographic records and compiled by Mrs. Martha Olson of USNRDL, San Francisco, Calif. is enclosed as figure 28. This chart shows the frequency in large ocean areas that the most frequent set in smaller  $5^{\circ} \times 5^{\circ}$  quadrangles occurs for three categories of persistency. For example: In 55% of the  $5^{\circ} \times 5^{\circ}$  sub areas of the Northwestern Pacific the most frequent direction of the set occurs in less than 25% of the observations. In 45% of the sub areas the most frequent direction of the set occurred in 25% to 50% of the observations. Table 7 lists the data from which the bar chart was derived.

## 2. Drift.

Figure 29 was compiled by Mrs. Olson from 1961 Hydrographic Office information not yet published. It depicts the frequency of drift for various mean speeds of the "most frequent current." It shows that in over 80% of the areas the drift of the most frequent current is between 0.4 and 0.8 knots. This graph refers only to the North Atlantic.

Table 8 that follows lists the mean speed and deviation for various sectors at various times of the year. In general the deviation is no more than 0.2 knots, and the mean is less than the mean of the speed in the most frequent direction (because when the set is in other than the most frequent direction there is a tendency for the movement to be less defined.

## C. Conclusions.

1. SET is an unpredictable variable at any given time. The safest and broadest assumption that can be made is that the direction of current





at any given time and at any given place is UNIFORMLY distributed.

2. The strip considered in figures 20 through 27 was sampled for the month of January to determine the percent of area under the curve within the semicircle centered at the prevailing set. Two thirds of the total area is included under this half of the curve.

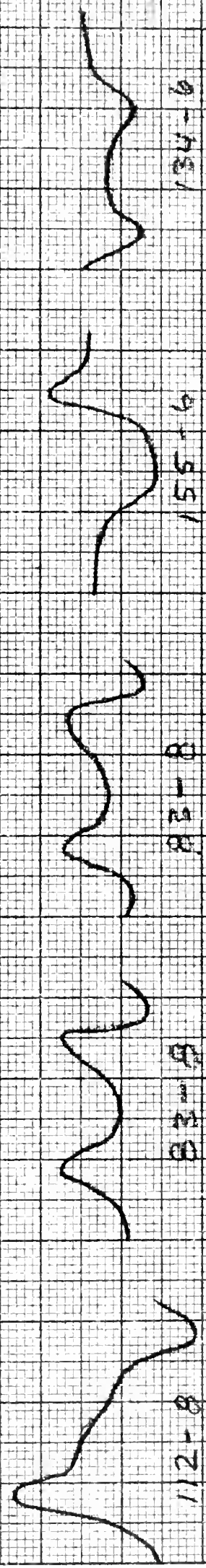
3. No matter what the direction of the set is, the drift is reasonably predictable. The variance of the drift is small and in view of the time late involved in the problem, the solution is not sensitive to such small variances.



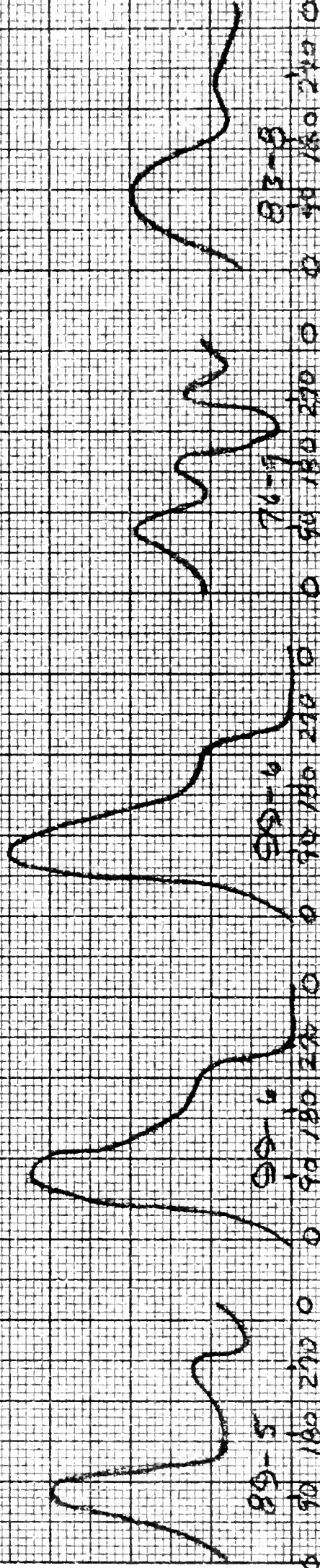
JANUARY FEBRUARY MARCH JUNE SEPTEMBER

LONGITUDE 175° W to 170° W

LATITUDE 25° N to 30° N



LATITUDE 30° N to 35° N



DIRECTION OF CURRENT (degrees)

Fig 20

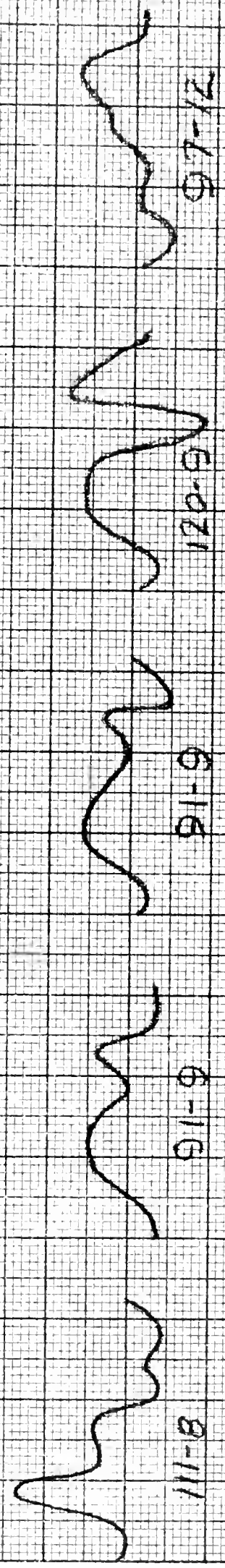




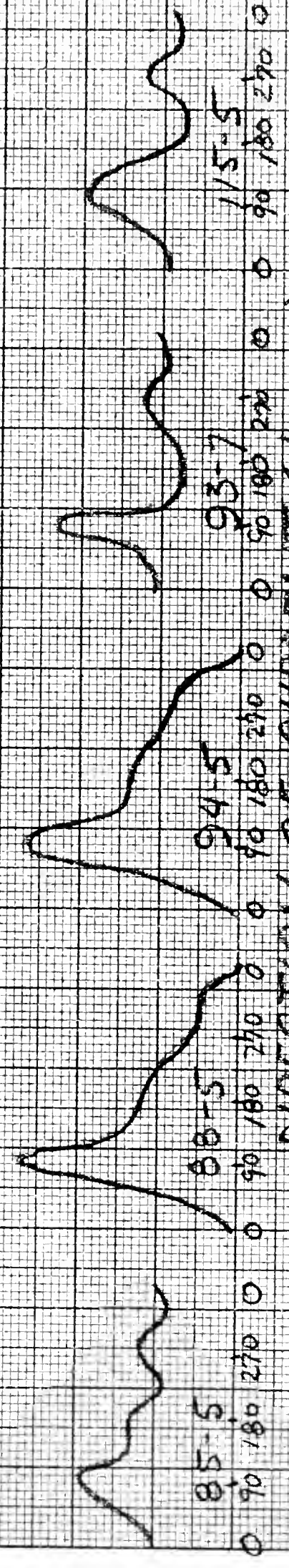
JANUARY    FEBRUARY    MARCH    JUNE    SEPTEMBER

LONGITUDE 180° TO 175°W

LATITUDE 25°N TO 30°N



LATITUDE 30°N TO 35°N



DIRECTION OF CURRENT (degrees)

Fig 21



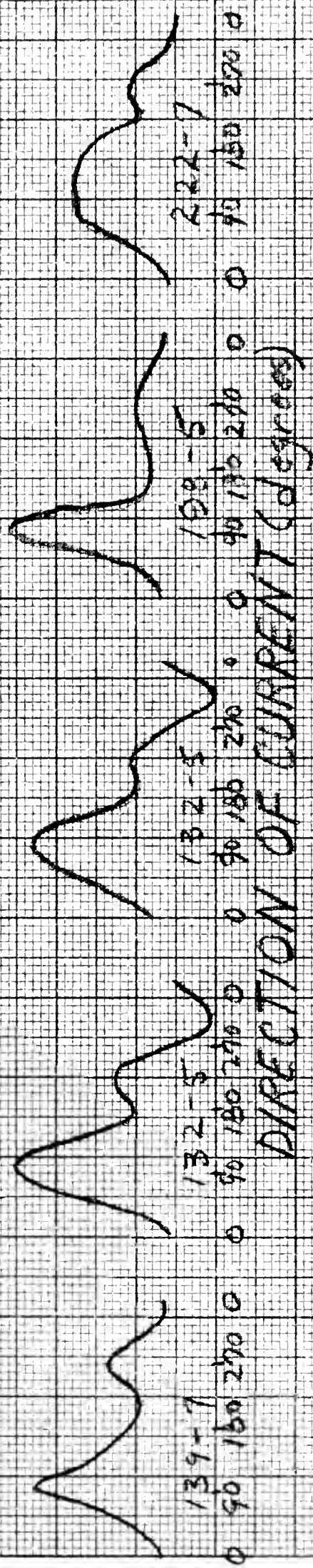
JANUARY      FEBRUARY      MARCH      JUNE      SEPTEMBER

LONGITUDE 175°E to 180°

LATITUDE 25°N to 30°N



LATITUDE 30°N to 35°N



DIRECTION OF CURRENT (degrees)

Fig 22



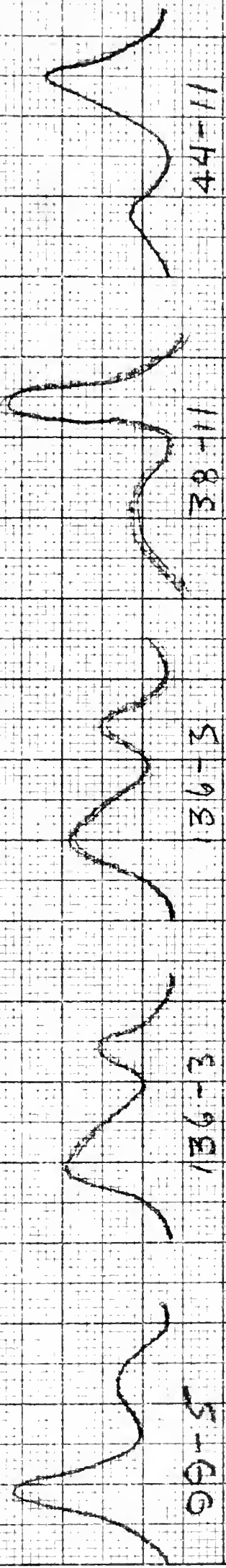


200-12571500 04 000 412321-021

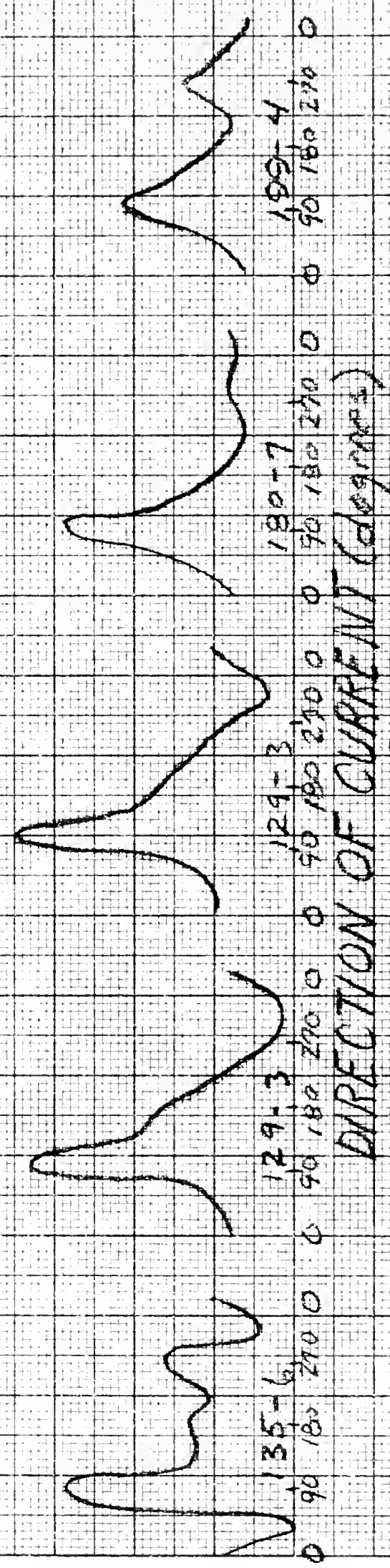
JANUARY FEBRUARY MARCH JUNE SEPTEMBER

LONGITUDE 170°E to 175°E

LATITUDE 25°N to 30°N

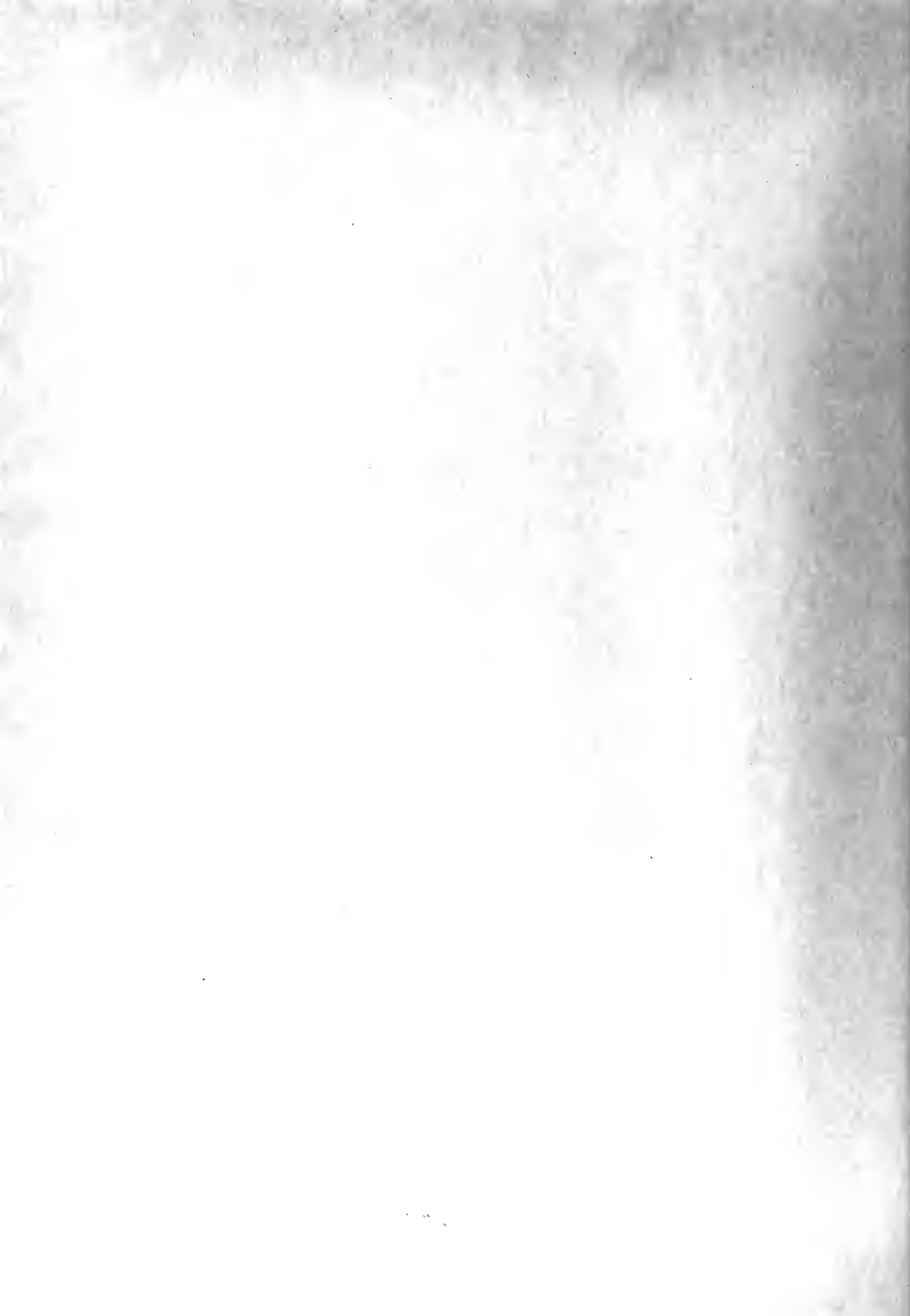


LATITUDE 30°N to 35°N



DIRECTION OF CURRENT (degrees)

Fig 23

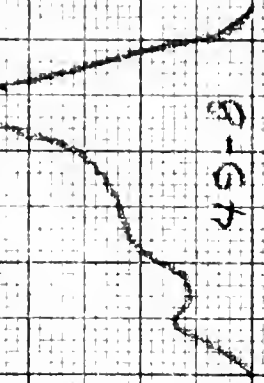
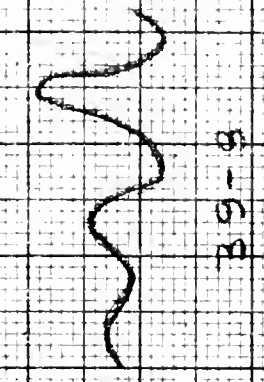
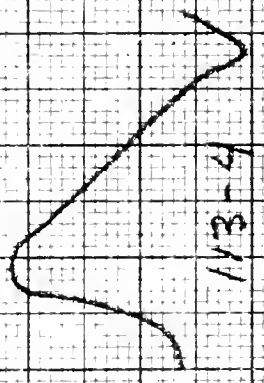


RECEIVED - 04 OCTOBER 1965

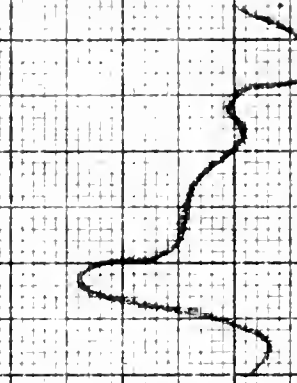
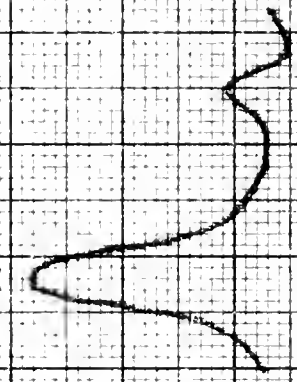
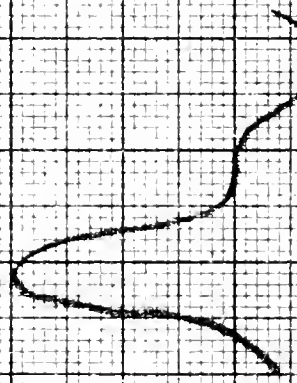
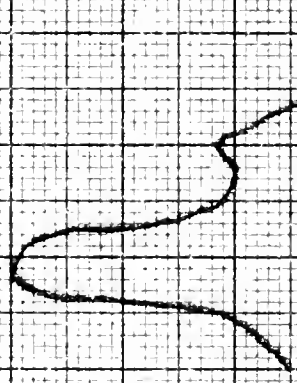
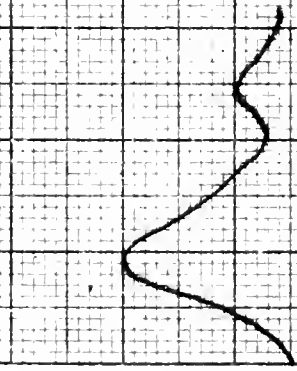
JANUARY      FEBRUARY      MARCH      JUNE      SEPTEMBER

LONGITUDE 165°E to 170°E

LATITUDE 25°N to 30°N

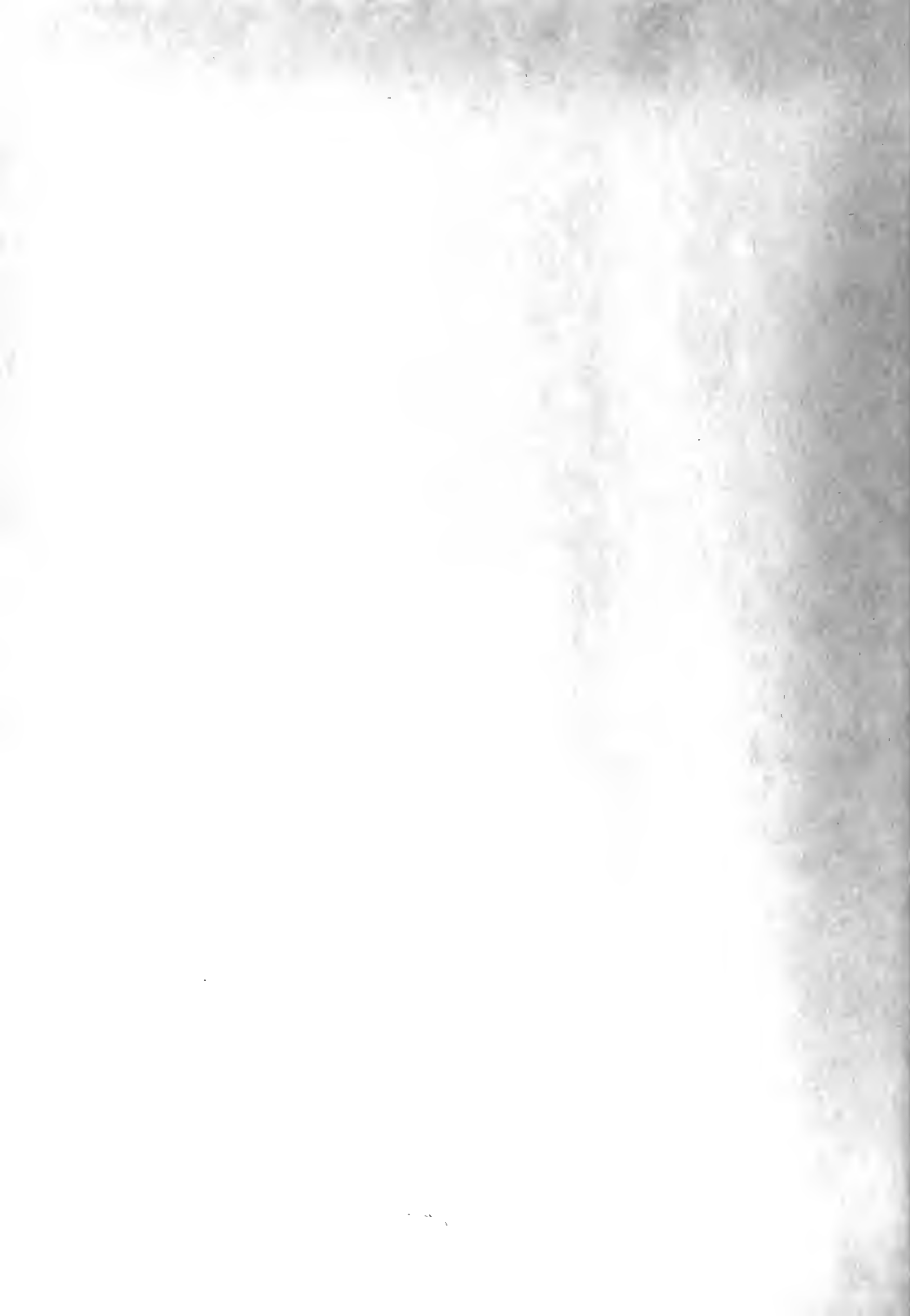


LATITUDE 30°N to 35°N



DIRECTION OF CURRENT (degrees)

Fig 24

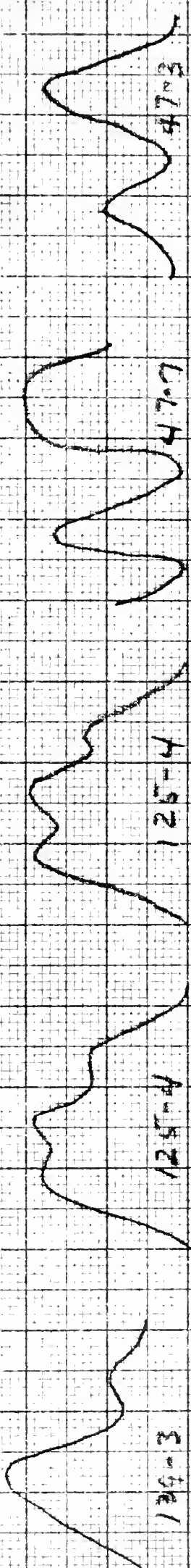




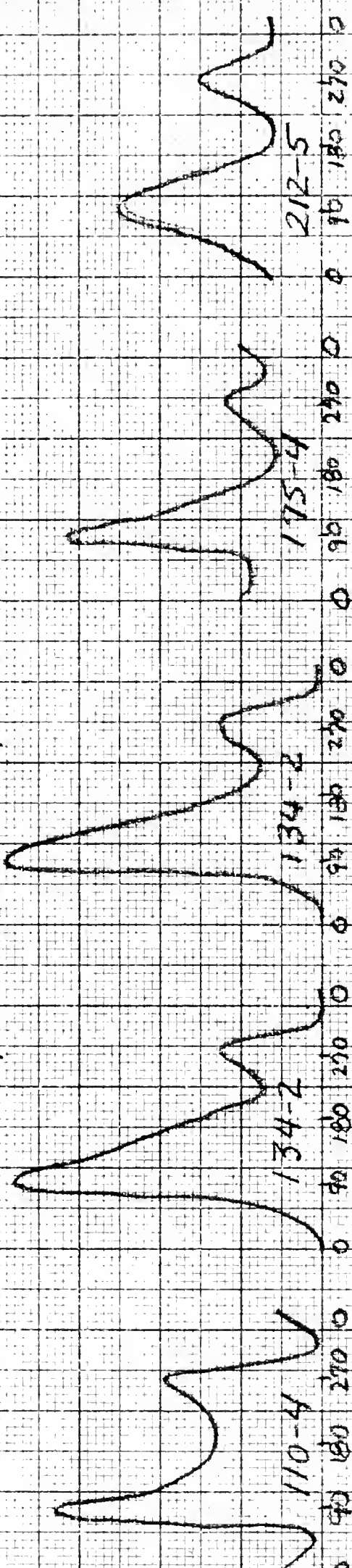
JANUARY FEBRUARY MARCH JUNE SEPTEMBER

LONGITUDE 160°E TO 165°E

LATITUDE 25°N TO 30°N



LATITUDE 30°N TO 35°N



DIRECTION OF CURRENT (degrees)

Fig 25

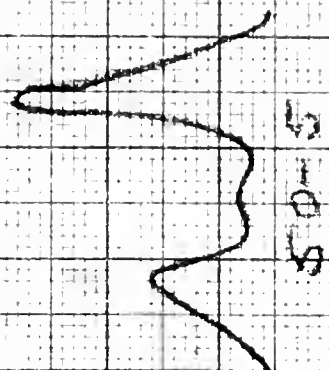
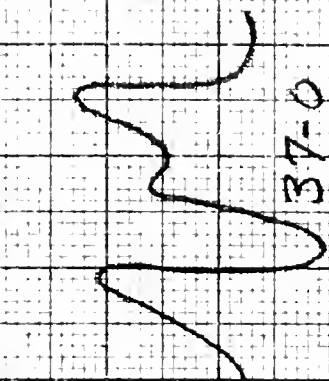


JANUARY FEBRUARY MARCH

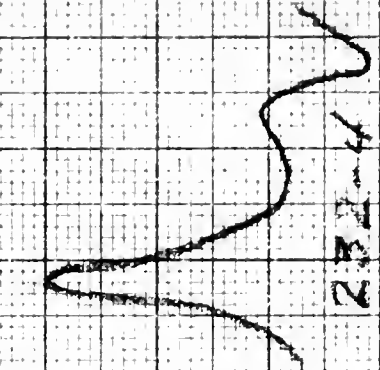
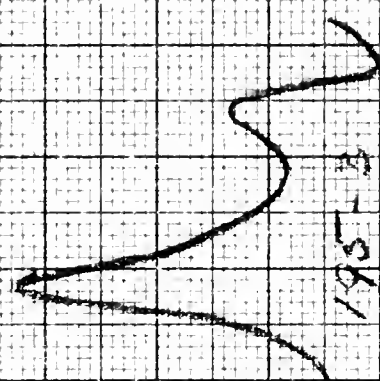
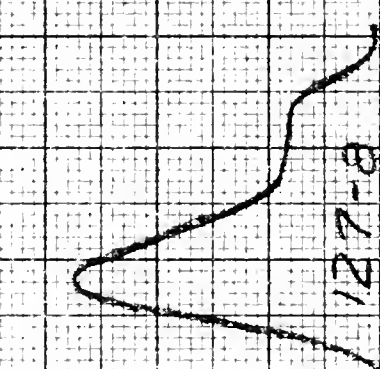
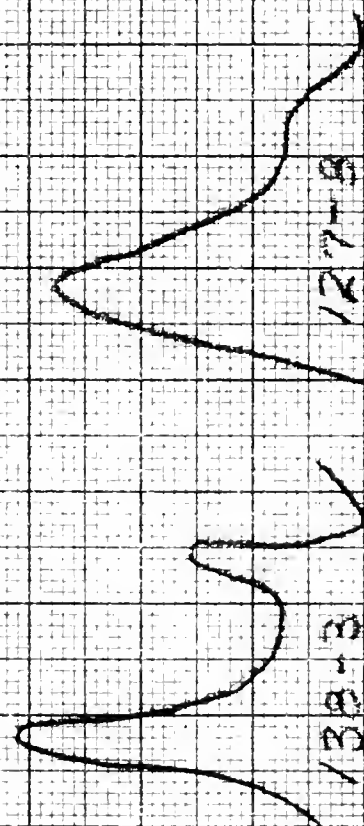
JUNE

WILLIAMS

LONGITUDE 155° 16' W

LATITUDE  $25^{\circ}\text{N}$  to  $30^{\circ}\text{N}$ 

WTTT 30° 16' 35" N



# DICTIONARY OF CURRENT (6-1989)

Fr 26

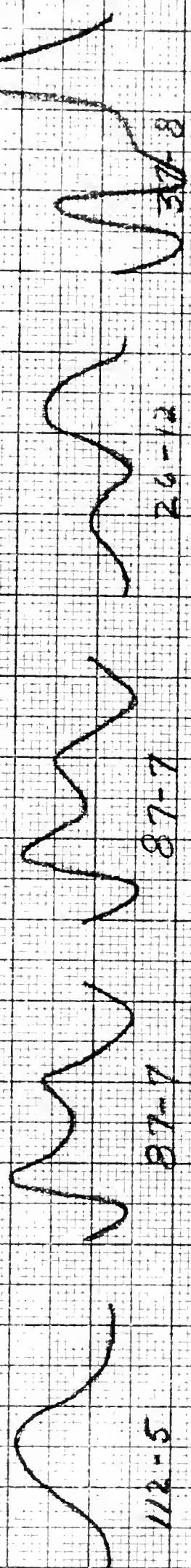




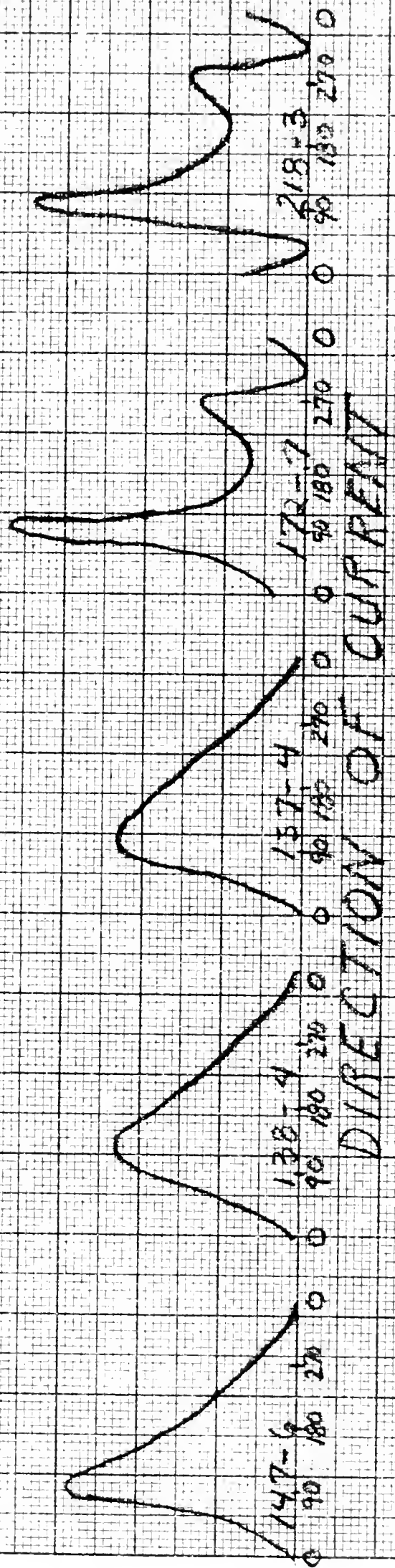
JANUARY FEBRUARY MARCH JUNE SEPTEMBER

LONGITUDE 150°E to 155°E

LATITUDE 25°N to 30°N



LATITUDE 30°N to 35°N

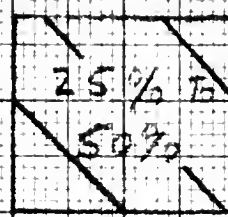
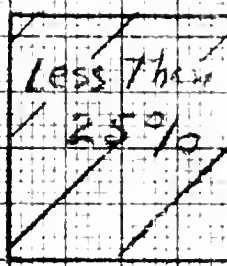


DIRECTION OF CURRENT

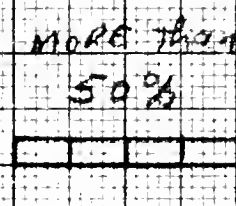
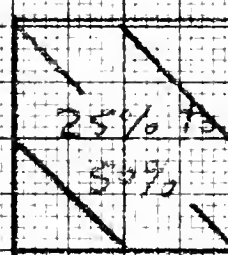
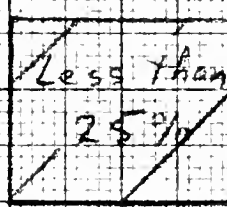
(degrees) Fig 27



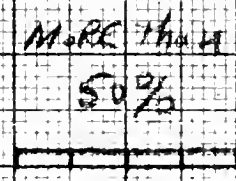
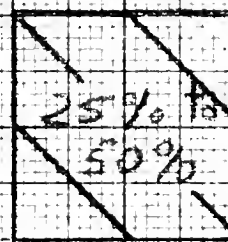
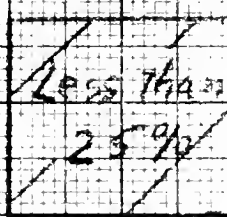
# NORTHWESTERN PACIFIC



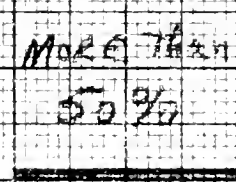
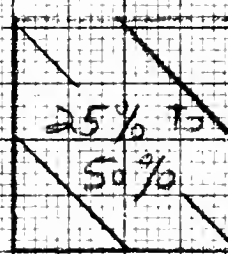
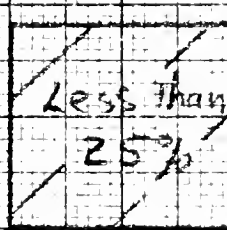
# NORTHEASTERN PACIFIC



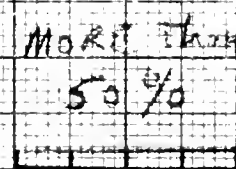
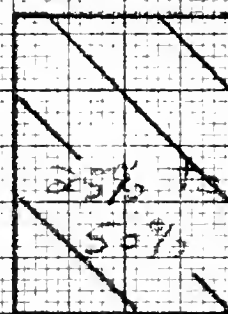
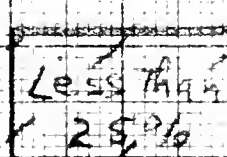
# NORTH ATLANTIC



# WEST INDIAN



# NORTHWESTERN INDIAN



% of QUADRANGLES IN SAMPLE FOR WHICH MOST FREQUENT DIRECTION OCCURRED  
IN THE INDICATED % OF OBSERVATIONS

% of observations in which most frequent direction occurred



TABLE 7

## A MEASURE OF CURRENT PERSISTENCY IN FIVE SELECTED AREAS

## PART 1

REGION	Number of Quadrangle- Months	Number of Observations	Number of Quadrangle-Months in Which Most Frequent Di- rection is Observed the Indicated % of Observations		
			25%	25%-50%	50%
A. Northwestern Pacific Ocean	80	9,512	45	35	0
B. Northeastern Pacific Ocean	150	12,595	62	78	10
C. North Atlantic Ocean	253	184,760	90	149	14
D. East Indian Ocean	59	1,092	27	31	1
E. Northwestern Indian Ocean	96	10,236	28	64	4
TOTAL	638	218,195	252	357	29

## PART 2

REGION	% of Quadrangle-Months in Which Most Frequent Direc- tion is Observed the Indicated % of Observations		
	25%	25%-50%	50%
A. Northwestern Pacific Ocean	56%	44%	0%
B. Northeastern Pacific Ocean	41%	52%	7%
C. North Atlantic Ocean	35%	59%	6%
D. East Indian Ocean	66%	29%	5%
E. Northwestern Indian Ocean	29%	67%	4%
TOTAL	39%	56%	5%

\*Additional information on the following page.

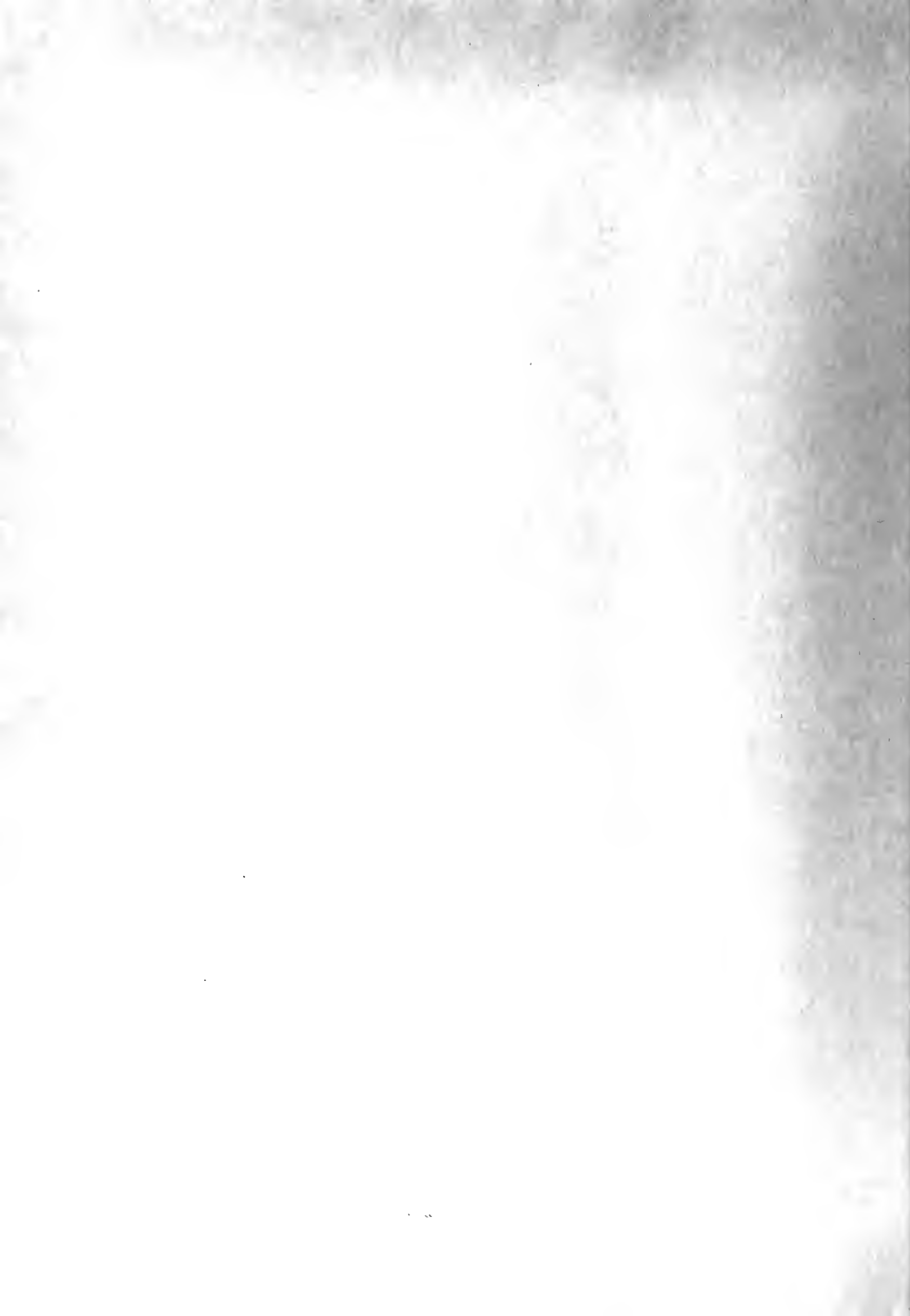


TABLE 7 - Cont'd.

Quadrangle-Month: Grouping of data from all observations over the years taken during the indicated calendar month and in the same quadrangle of approximately  $5^{\circ} \times 5^{\circ}$ .

Source of Data: Measurement of lengths and widths of spokes of current roses in HO Publications, Atlas of Surface Currents.

Courtesy of Mrs. Martha Olson,  
USNRDL, San Francisco, Calif.





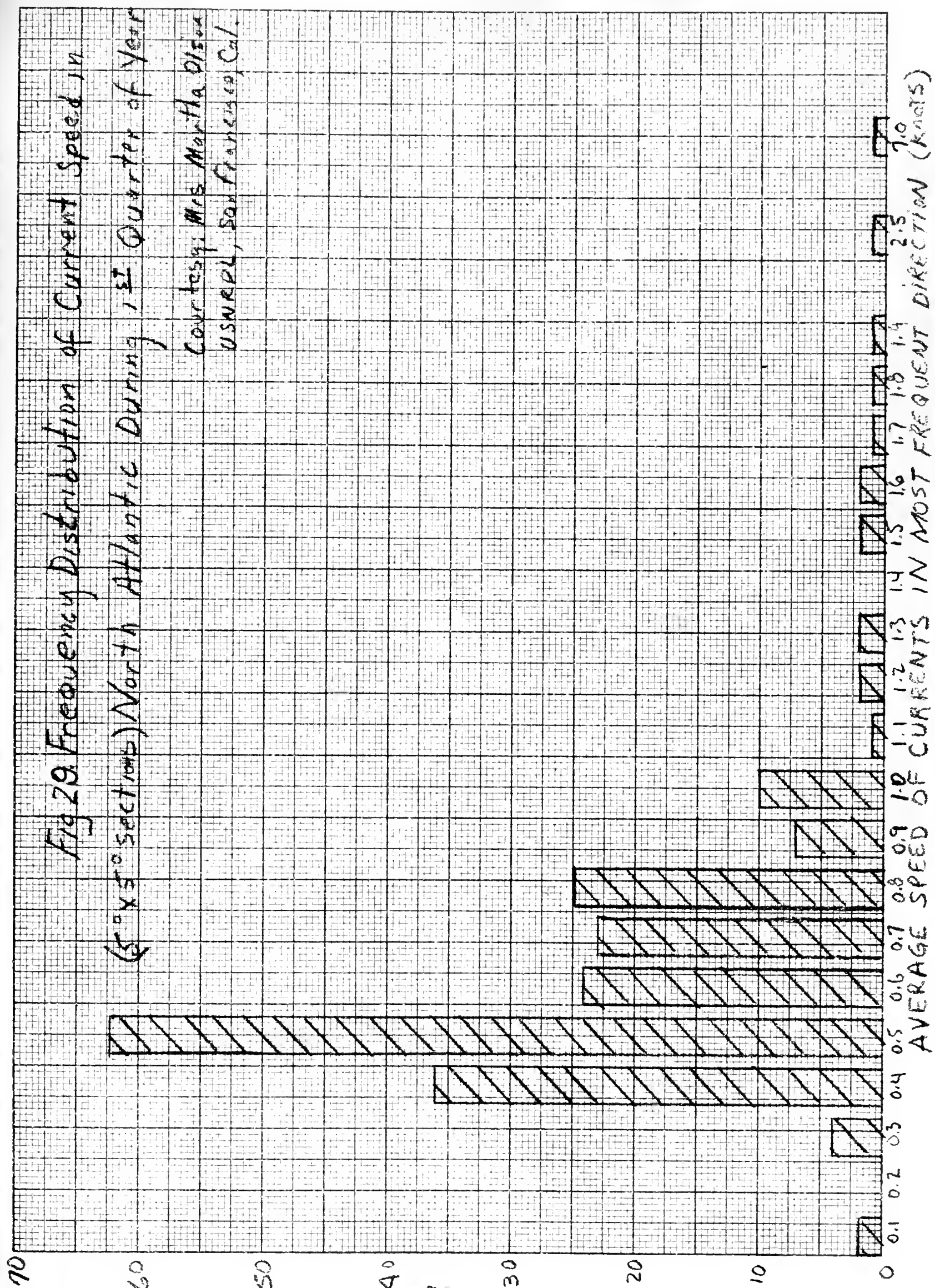




TABLE 8

MEANS AND STANDARD DEVIATIONS OF CURRENT SPEED IN SELECTED QUADRANGLES

A. NORTHWESTERN PACIFIC OCEAN

Month	Lat. 25°-30°N Long. 150°-155°E	Lat. 30°-35°N Long. 165°-170°E	Lat. 25°-30°N Long. 180°-175°W						
	Mean	Std.Dev.	"0"	Mean	Std.Dev.	"0"	Mean	Std.Dev.	"0"
January	0.2	0.1	5	0.3	0.2	7	0.2	0.2	8
February	0.2	0.1	7	0.3	0.2	2	0.2	0.1	9
March	0.2	0.2	9	0.2	0.2	5	0.2	0.1	8
June	0.3	0.2	12	0.2	0.1	4	0.2	0.1	9
September	0.3	0.2	8	0.2	0.2	5	0.1	0.1	12

Mean: Average in 5°X5° quadrangles of the average of each 1°X1° sub area for which observations were available.

Standard Deviation: Estimated standard deviation of average current speeds of 1°X1° rectangles.

Mean and Standard Deviation are in knots.

"0" gives the percent of total observations made in the quadrangle during the given month having no appreciable current observed.

Courtesy of Mrs. Martha Olson  
USNRDL, San Francisco, Calif.



TABLE 8

## MEANS AND STANDARD DEVIATIONS OF CURRENT SPEED IN SELECTED QUADRANGLES

## B. NORTHEASTERN PACIFIC OCEAN

Month	Lat. 16°-20°N Long. 150°-155°W	Lat. 36°-40°N Long. 150°-155°W	Lat. 4°-8°N Long. 140°-145°W
	Mean      Std.Dev.      "0"	Mean      Std.Dev.      "0"	Mean      Std.Dev.      "0"
January	0.4      0.3      3	0.2      0.1      14	0.5      0.3      7
February	0.3      0.2      0	0.2      0.1      7	0.5      0.4      0
March	0.3      0.2      5	0.2      0.1      10	0.4      0.3      6
June	0.4      0.1      4	0.3      0.3      6	0.6      0.3      0
September	0.3      0.1      4	0.3      0.2      3	1.0      0.2      4

Month	Lat. 24°-28°N Long. 140°-145°W
	Mean      Std.Dev.      "0"
January	0.1      0.1      13
February	0.1      0.1      7
March	0.1      0.1      17
June	0.2      0.1      9
September	0.2      0.1      13



TABLE 8

MEANS AND STANDARD DEVIATIONS OF CURRENT SPEED IN SELECTED QUADRANGLES

C. NORTH ATLANTIC OCEAN

Month	Lat. 37°-40°N Long. 65°-60°W			Lat. 34°-38°N Long. 60°-55°W			Lat. 35°-39°N Long. 30°-25°W		
	Std.Dev.		"0"	Std.Dev.		"0"	Std.Dev.		"0"
	Mean	$\sigma$		Mean	$\sigma$		Mean	$\sigma$	
January	0.7	0.2	4	0.1	0.1	7	0.1	0.1	7
February	0.6	0.2	4	0.1	0.1	7	0.1	0.1	6
March	0.5	0.2	4	0.2	0.1	6	0.2	0.0	7
April	0.6	0.2	4	0.2	0.1	6	0.2	0.1	7
May	0.6	0.2	4	0.1	0.1	9	0.1	0.0	6
June	0.6	0.1	5	0.1	0.1	5	0.1	0.1	8

MEANS AND STANDARD DEVIATIONS OF CURRENT SPEED IN SELECTED QUADRANGLES

D. EAST INDIAN OCEAN

Month	Lat. 30°-35°S Long. 85°-95°E			Lat. 20°-25°S Long. 95°-105°E			Lat. 35°-40°S Long. 95°-105°E		
	Std.Dev. σ		"0"	Std.Dev. σ		"0"	Std.Dev. σ		"0"
	Mean			Mean			Mean		
January	0.3	0.2	8	0.5	0.2	6	0.3	0.2	6
February	0.5	0.3	9	0.4	0.2	3	0.4	0.1	4
March	0.3	0.2	9	0.4	0.2	0	0.3	0.2	4
June	0.3	0.2	11	0.5	0.4	0	0.7	0.1	20
September	0.3	0.1	8	0.4	0.2	11	0.4	0.1	0

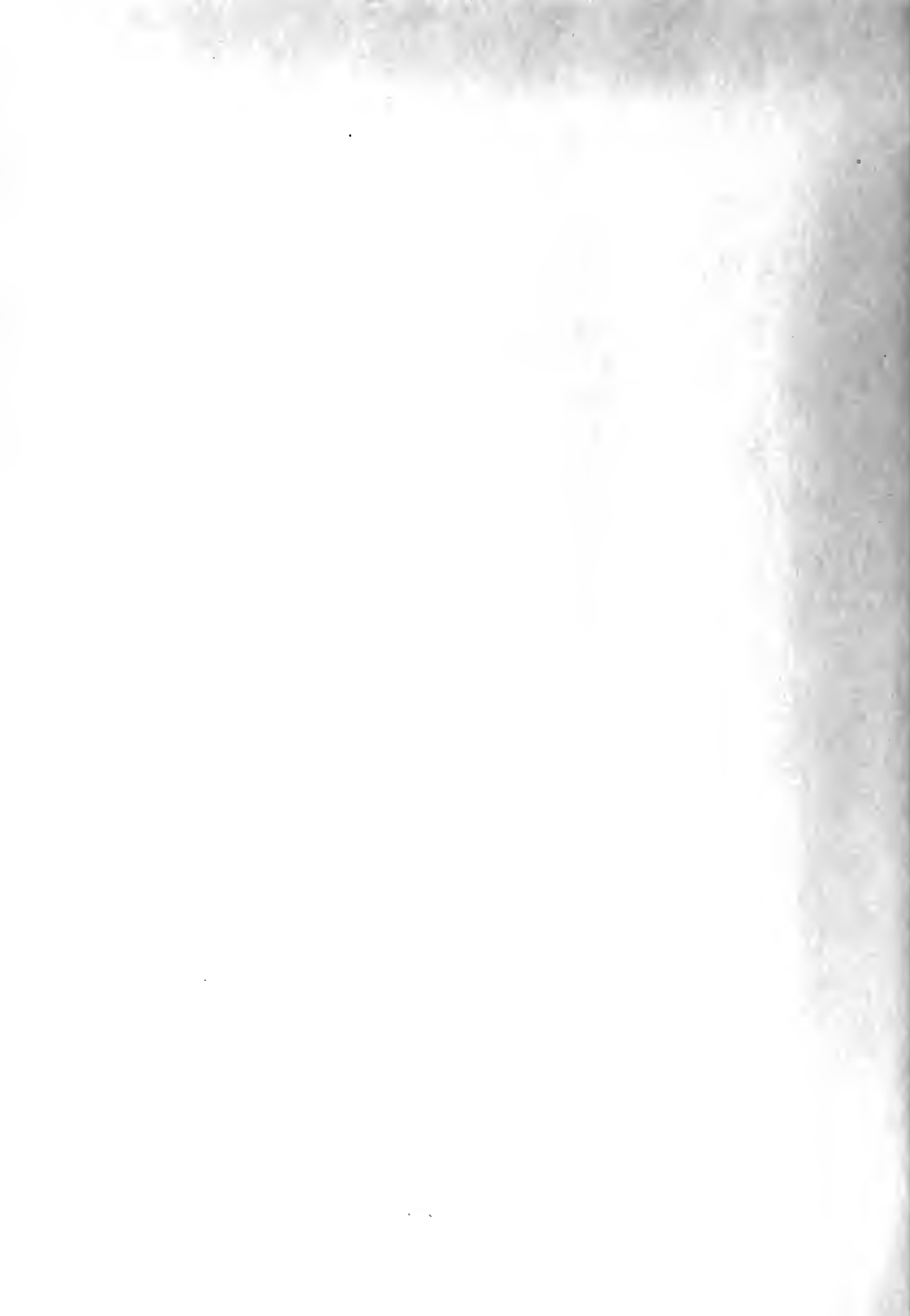




TABLE 8

MEANS AND STANDARD DEVIATIONS OF CURRENT SPEED IN SELECTED QUADRANGLES

E. NORTHWESTERN INDIAN OCEAN

Month	Lat. 15°-10°N Long. 51°-56°E			Lat. 0-5°S Long. 55°-61°E			Lat. 15°-10°N Long. 56°-61°E		
	Mean	Std.Dev.	"0"	Mean	Std.Dev.	"0"	Mean	Std.Dev.	"0"
January	0.3	0.1	5	0.9	0.6	0	0.3	0.2	4
February	0.2	0.1	5	0.8	0.5	5	0.2	0.1	4
March	0.3	0.1	5	0.8	0.5	5	0.2	0.1	4
June	0.6	0.3	2	0.6	0.3	6	0.6	0.2	3
September	0.8	0.3	2	0.5	0.3	8	0.6	0.1	2

Month	Lat. 5°-10°S	Long. 61°-67°E	Lat. 15°-10°N	Long. 61°-67°E
	Mean	Std.Dev.	Mean	Std.Dev.
January	0.7	0.3	0.2	0.1
February	0.5	0.3	0.2	0.1
March	0.6	0.3	0.2	0.1
June	0.4	0.2	0.7	0.3
September	0.4	0.3	0.3	0.1



## APPENDIX V

### SEARCH PLAN FOR SMALL FIX DEVIATION

Two other errors in location are considered besides the fix error.

a. Navigational errors of an aircraft in finding the exact location to which dispatched are characterized by a normal distribution. In this model it is assumed that the error due to navigation is normally distributed with a standard deviation of five miles. The variances of the fix error and navigation error are additive with a resulting standard deviation of 5.6 miles ( $\sqrt{(2.5)^2 + (5)^2}$ ).

b. Current flow is assumed to be equally likely in direction at a given location and time. The drift is dependable enough as published for the area of interest.

The first pass of the area should conform to the pattern shown in figure 31. The search is designed to investigate the peak of the distribution at the time of arrival and follow up with loops outside and then inside. This will maximize the probability of detection per time of search effort. Koopman /2/ discusses this plan in detail.

$u$  = drift

$v$  = aircraft velocity

$T$  = time elapsed since initial detection

The time to go from A to B in Figure 30 is  $\frac{r_1 + r_2}{r}$



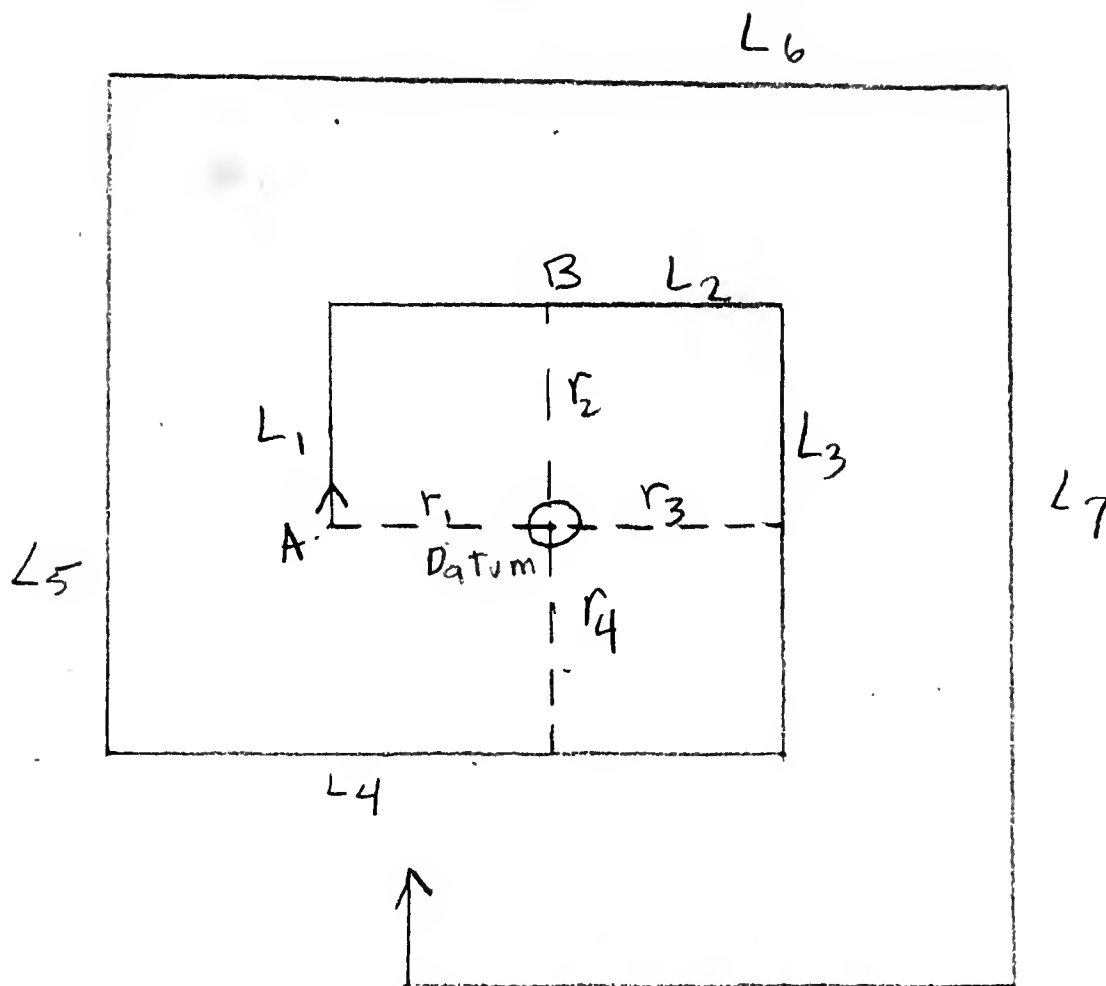


Fig. 30 Pattern for retiring search.

The time for the object of the search to move from circle  $r_1$  to circle  $r_2 = \frac{r_2 - r_1}{u}$

To make this equal to search vehicle's time to go from A to B,  $r_2 = mr_1$ , where  $m = \frac{v+u}{v-u}$ . Similarly  $r_3 = mr_2$ ;  $r_4 = mr_3$ ; etc....

To prevent overlap and expand or contract about the loop  $r_5 \neq mr_4$ . To make this leg be S miles outside the first leg determine  $r_5$  such that  $\frac{r_5 + r_4}{v} = \frac{r_5 - r_4}{u} - S$ , from which  $r_5 = mr_4 + a$  where  $a = \frac{vS}{v-u}$

The distance  $r_1$  should equal  $uT$ . However since in practice the expanding square is used to approximate a spiral, a mean  $r_1$  is selected so



that  $r_1 = 0.9ut$ . To further allow for the fact that any change in course of the pool, at the same speed will reduce the outward component,  $r_1$ , is selected as  $0.8ut$ .

$$L_1 = mr_1$$

$$L_2 = mL_1 + r_1$$

$$L_3 = mL_2$$

$$L_4 = mL_3 + a \quad (\text{outside})$$

$$L_5 = mL_4$$

$$L_6 = mL_5 + a$$

$$L_7 = mL_6$$

$$L_8 = mL_7 - 2a \quad (\text{inside})$$

$$L_9 = mL_8$$

$$L_{10} = mL_9 - 2a$$

$$L_{11} = mL_{10}$$

$$L_{12} = mL_{11} + 3a \quad (\text{outside})$$

etc..

.

.

.

A sample search is worked out for the following situation:

Height of aircraft = 500 feet

Spacing (S) = 9.61 miles

Drift (u) = 0.5 knots

Speed of aircraft (v) = 180 knots

Time late (T) = 24 hours





$$r_1 = .8(.5)(24) = 9.6 \text{ miles}$$

$$a = \frac{v_s}{v-u} = \frac{180(9.61)}{179.5} = 9.65$$

$$m = \frac{v+u}{v-u} = \frac{180.5}{179.5} = 1.0056$$

$$L_1 = 9.65$$

Total mileage for this pattern 460 mi.

$$L_2 = 19.3$$

Time for pattern - 2 hrs 35 min.

$$L_3 = 19.4$$

If this plane only has 3 hrs on station

$$L_4 = 29.2$$

available it should spend the last 25

$$L_5 = 29.4$$

minutes sweeping the lower left corner.

$$L_6 = 39.3$$

Another aircraft will have to make the

$$L_7 = 39.5$$

parallel sweep.second pass which re-

$$L_8 = 20.4$$

quires 1 hr 40 min (300 miles).

$$L_9 = 20.5$$

$$L_{10} = 1.3$$

$$L_{11} = 1331$$

$$L_{12} = 30.3$$

$$L_{13} = 30.5$$

$$L_{14} = 59.7$$

$$L_{15} = 60$$

$$L_{16} (\text{end}) = 60$$

The plan leaves a holiday in the lower left corner of the pattern.

In order to take advantage of the best information the upper right corner should be oriented in the direction of the prevailing current so that the starting leg is  $45^\circ$  to the left of the most frequent current.

Note that the center may be adequately covered before outside areas are searched - depending on the balance of the time late and standard



deviation of location. In case this happens the pattern should be continued with outside expansion only. In the example cited above the center search is just a narrow turn of  $270^{\circ}$  to right.

After this search is completed proceed with a parallel sweep as explained in paragraph 11b of the main body of this study.



1 Small square =  
 $\frac{1}{2}$  mile  $\times$   $\frac{1}{2}$  mile

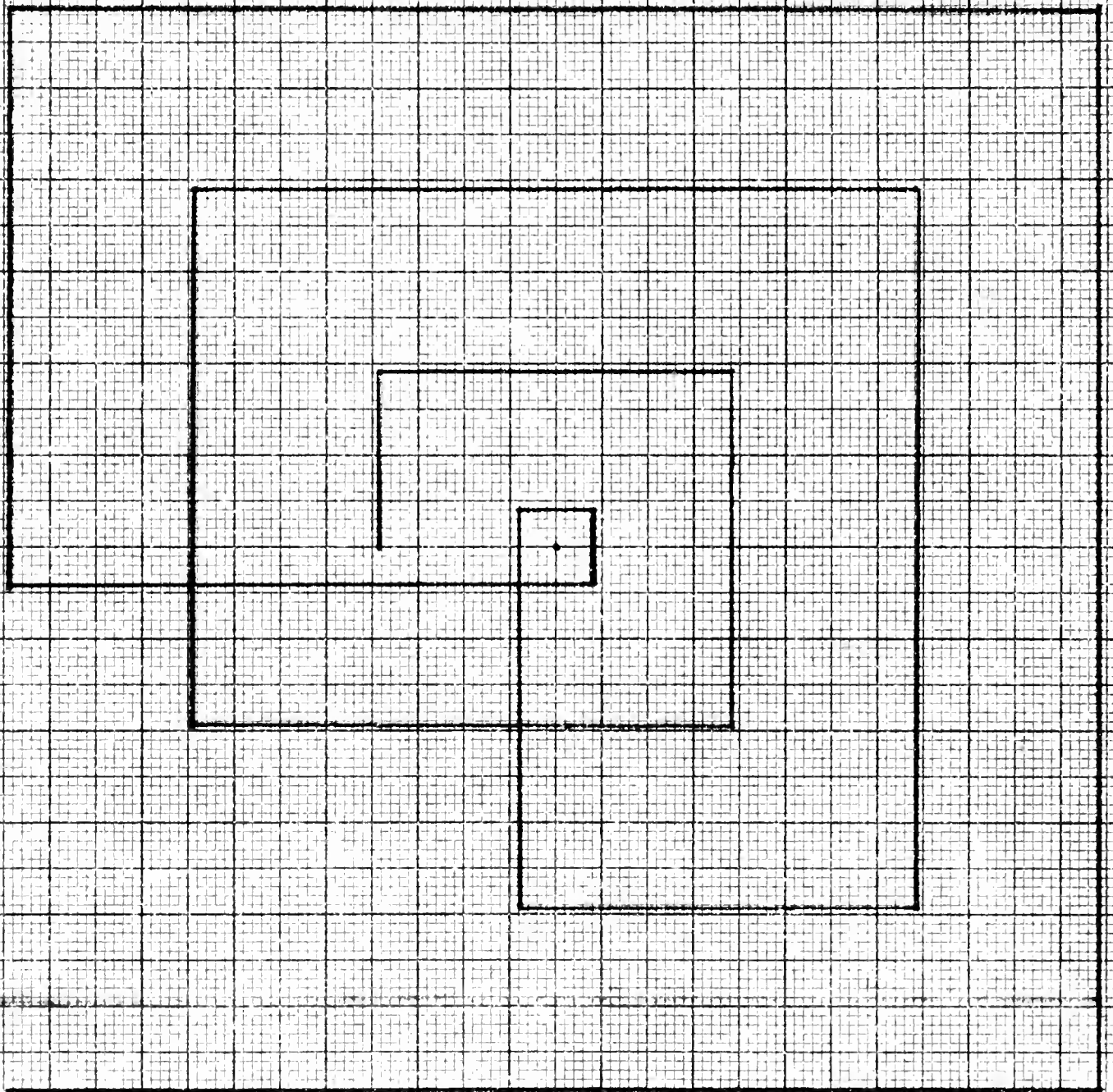


Fig 31. Search pattern for small deviation.



## APPENDIX VI

### SEARCH PLAN FOR LARGE FIX DEVIATION

For the case where the fix is not any more certain than within a standard deviation of 25 miles or more, the errors in navigation and current movement can be ignored. A set of expanding squares - squares of uniform coverage - are superimposed in the square pattern. Koopman /2/ covers the subject in detail.

The altitude of the aircraft should be as low as operationally acceptable and for an example 500 feet will be used.

Figure 32 is a drawing of the pattern for the following problem:

Aircraft speed = 180 kts.

Endurance on station  $\geq 540$  miles

Spacing = 11.0 miles

Average search width ( $W=E$ ) = 8.44 miles

Coverage factor  $\phi = WL = 4558$  square miles

Maximum search radius =  $a = (43.7 \text{ miles}) = \left( \frac{45^2 \phi}{\pi} \right)^{\frac{1}{4}}$

Half length of  $K^{\text{th}}$  square ( $S_k$ ) =  $\left[ \frac{\pi}{4} \frac{W^2}{S} (2k-1) \right]^{\frac{1}{2}}$

Number of passes  $n = \frac{a^2 S}{2\phi^2 W} = 2$

$$S_1 = 19.5$$

$$S_2 = 33.8$$

Length of a side of  $K^{\text{th}}$  square =  $2S_k$

$$L_1 = 39$$

$$L_2 = 67.6$$





Number of circuits within  $k^{\text{th}}$  major square ( $N_k$ ) =  $\frac{L_k}{2S}$

$$N_1 = 2$$

$$N_2 = 3$$

The second uniform square is tilted  $45^\circ$  to the first. This pattern is plotted in figure 32.

The average probability of detection is:

$$P = 1 - \left(1 + \frac{nW}{S}\right) \exp\left[-\frac{nW}{S}\right] = .434$$

If the search aircraft has more endurance than considered above (3 hours at 180 kts - assuming the search area up to 1000 miles from base) the plan should be appropriately recomputed.

For instance if search area were only 500 miles from base

Station Endurance 1500

Coverage Factor  $\phi = WL = 12660$

Maximum search area radius  $a = 55.4$

Number of passes  $n = 3$

$$S_1 = 19.5 \qquad L_1 = 39 \qquad N_1 = 2$$

$$S_2 = 33.8 \qquad L_2 = 67.6 \qquad N_2 = 3$$

$$S_3 = 43.6 \qquad L_3 = 87.2 \qquad N_3 = 4$$

The average probability in this case would be:

$$P = 1 - \left(1 + \frac{3W}{S}\right) \exp\left[-\frac{3W}{S}\right] = 0.67$$



1 small square =  
 $\frac{1}{2}$  mile  $\times$   $\frac{1}{2}$  mile

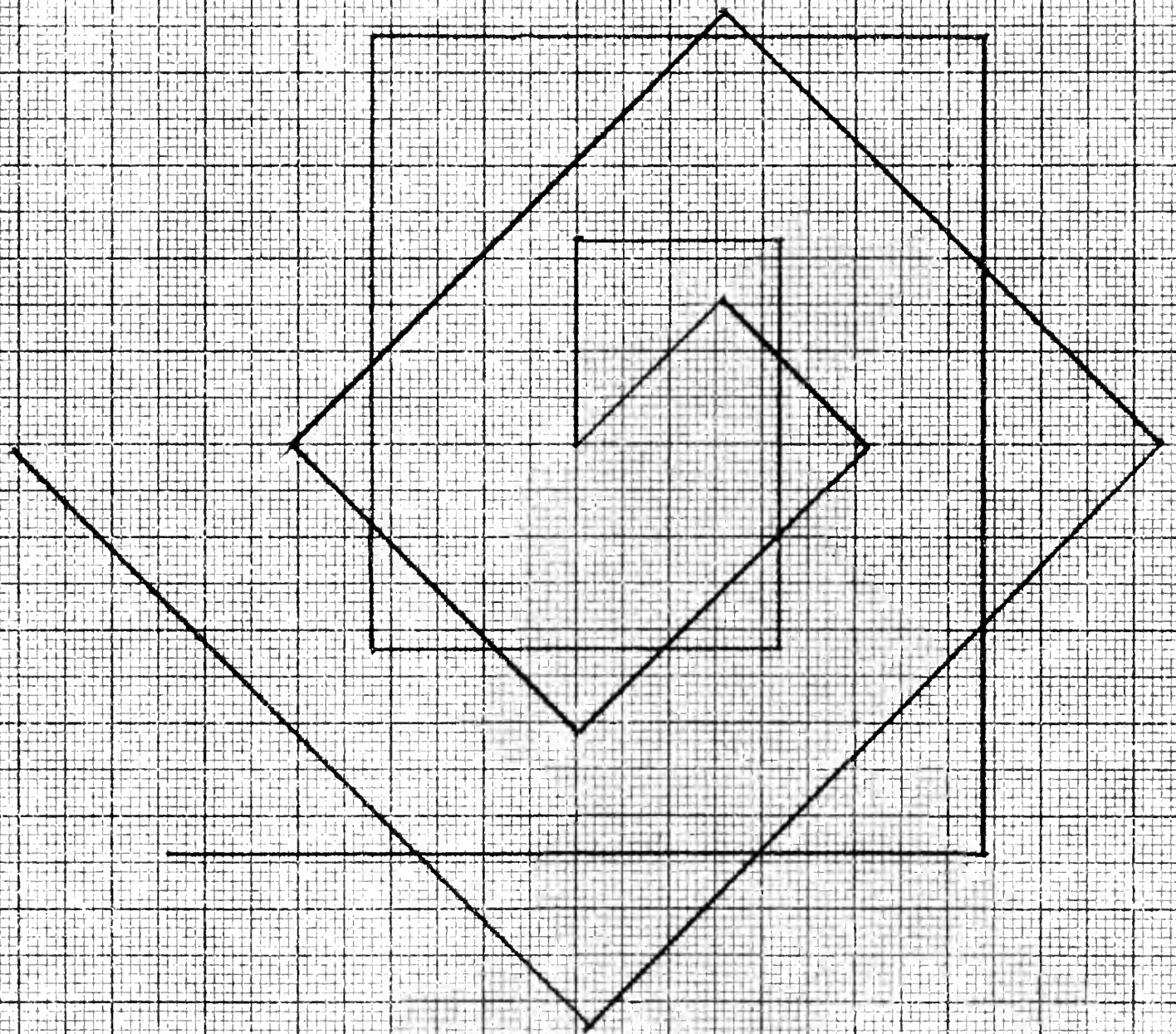


Fig 32 Search pattern for large deviation.













62  
12285  
14874

BINDERY  
12285  
14874

Thesis

H86

Hughes

57059

Locating an under-  
water site of a nuclear  
explosion detected by a  
hydroacoustic network.

BINDERY

MY 10 63

12285

20 JAN 65

14874

Thesis

H86

Fughes

57059

Locating an under-  
water site of a nuclear  
explosion detected by a  
hydroacoustic network.

Locating an underwater site of a nuclear



3 2768 001 03563 7

DUDLEY KNOX LIBRARY